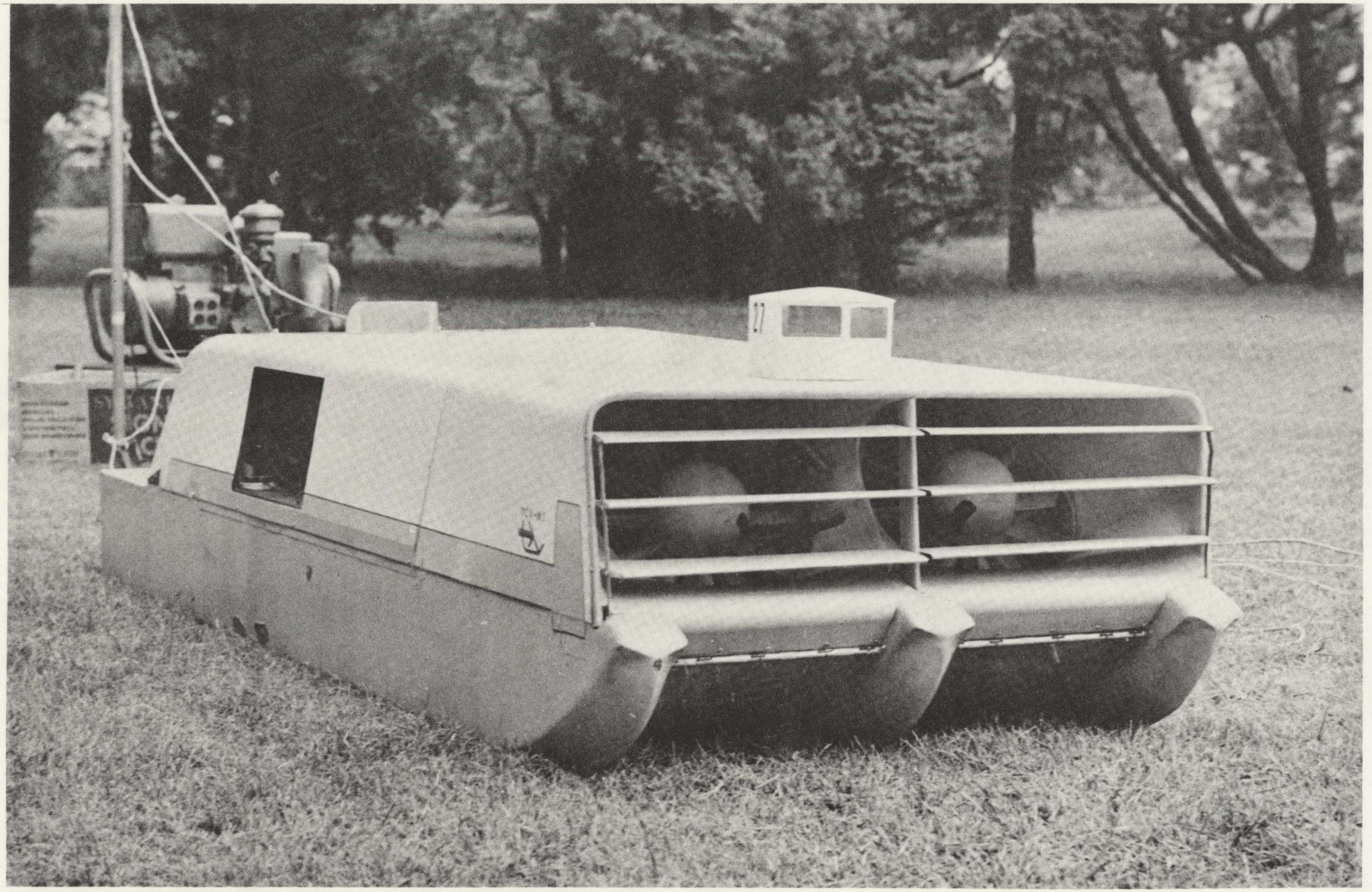

THRUST-CUSHION VEHICLES

THRUST-CUSHION VEHICLES

A PRELIMINARY ANALYSIS

By

GRAHAM GEORGE COCKSEDGE, B.Sc.F.

A Thesis

Submitted to the School of Graduate Studies

in Partial Fulfilment of the Requirements

for the Degree

Master of Engineering

McMaster University

September 1969

MASTER OF DESIGN (1972) McMASTER UNIVERSITY
(Mechanical Engineering) Hamilton, Ontario

TITLE: THRUST-CUSHION VEHICLES, A PRELIMINARY ANALYSIS

AUTHOR: Graham George Cocksedge, B.Sc.F. (University of New Brunswick)

SUPERVISOR: Professor W. R. Newcombe

NUMBER OF PAGES: xi, 128

SYNOPSIS:

Air-cushion vehicles (ACV) are defined as surface vehicles that utilize air pressure for partial or total support over the operational surface. An outline of the history of the five widely known ACV concepts and an analysis of the mode of operation of each is given, with their advantages and disadvantages.

A sixth type, called the thrust-cushion vehicle (TCV), is a promising but unknown concept which, as yet, has not received much study or recognition. A preliminary theoretical analysis for design purposes is made, and the test results of a static model and a model running on a radial tether are given to establish a research and design basis for future work.

ACKNOWLEDGEMENTS

The author is deeply indebted to Professor Newcombe for his guidance and concern which was often called upon and was always generously given.

Considerable motivation, though indirect, for this project was provided by George Cocksedge, the author's father. The experience has illuminated some of his extensive design skills and I am thankful for that. His direct motivation and support played a large part in the culmination of this thesis.

The support and assistance of my wife, Patricia, was complete and quite appreciated.

TABLE OF CONTENTS

LIST OF ILLUSTRATIONS

NOMENCLATURE

A	area
b	width of cushion
d	depth of cushion
h	daylight clearance
l	length of cushion
P	pressure
Q	flow
s	stern plate setting
t	thickness
V	velocity
ρ	mass density of air
ρ_w	mass density of water
β, γ, θ	angles

Subscripts

c	cushion
d	duct
f	fan
s	stern plate
v	vehicle

INTRODUCTION

Air cushion vehicles, hereafter abbreviated to ACV, are defined as surface vehicles that utilize air pressure for control or total support over the operational surface.

Currently, there are five widely known ACV concepts. These are: the ram wing, the open plenum chamber, the sidewall craft, the edge-jet (or peripheral-jet), and the tracked ACV.

Extensive research and development has taken place on at least two of these types: the edge-jet, as a potential all-terrain and amphibious vehicle, and the tracked ACV, as a potential high-speed or urban transport vehicle. As yet, this desired and expected potential has not been realized. The vehicle's low earning capacities have been a major deterent. Also, it seems clear that hovercraft, which is the name now generally applied to the edge-jet concept, will not make efficient all-terrain vehicles because of limited ability to clear obstacles and negotiate slopes. They do have potential for travel over water, reasonably smooth and level snow and ice, and on roughly prepared roads.

A sixth concept, the thrust-cushion vehicle (TCV), was patented by its Canadian inventor in 1961. This type of vehicle has the potential of overcoming the economic, stability, and control problems for operation on water or

roughly prepared tracks on land, ice or snow.

Very little research has been done on the thrust-cushion concept, and the aims of this thesis are as follow:

(1) To carry out a general survey of progress made on air cushion vehicle designs.

(2) To describe the thrust-cushion vehicle concept, and present an approximate analysis of the principles involved so that prototype vehicles may be designed.

(3) To carry out an experimental program on one-twelfth scale models in both the fixed and tethered running condition to determine pressure and flow patterns, and the relationship between thrust, daylight clearance, and input power.

CHAPTER I

A BRIEF HISTORY OF AIR CUSHION VEHICLE DEVELOPMENT AND DESIGN PHILOSOPHY

I.1 Development Prior to 1960

First Concepts. The first ground effect machine appears to have been conceived and modeled by a Swedish scientist in 1716 [1]. To provide the cushion flow, this craft had "air oars" which seem to have been designed to provide an action similar to feathers operating in a bird's wing. The off-centre shaft of the oar's vanes would open on an upstroke, and close on the downstroke to create resistance. The inventor realized that development would have to await a suitable power plant.

Antifriction Hulls. At the beginning of the century, one of the New York ferry boats, referred to as the "Flatiron", operated for several years (Fig. 1). The ferry had a conventional plan shape, but its lower surface was flat (hence its name), and was dotted with openings from a compressed air system. The craft was designed as an antifriction hull, and in operation, a film of air bubbles was released under the vehicle to effectively reduce the hull's viscous drag. Unfortunately, because

the propulsive power saved was used by the air system, and no net power reduction resulted, the project was eventually abandoned.

Ground Effect Wings and Ram Wings. The increased lift/drag ratios achieved by early aircraft flying near the surface instigated some wing-in-ground-effect (WIG) experiments which may have been responsible for the development of the ram wing.

The WIG was basically a wing brought into close proximity to the surface where the pressure increase below the wing would increase beyond that which was possible away from the surface. When large endplates were used to contain the increased pressure region, the WIG was referred to as a Channel Wing. When the trailing edge of the wing was sufficiently close to the surface so that the air flow below the wing effectively stagnated, then the configuration was referred to as a True Ram Wing. The ram wing may or may not have a lifting upper surface. The true ram wing could become fully airborne faster than the WIG or channel wing, was more stable over surface irregularities, and could carry the heaviest loads at a given speed. The WIG had the least drag and best potential for high speed service (above 100 knots). In operation, a thrust system, aero or marine, pushed the vehicle over the surface until the "unstick" speed was attained and the craft became fully airborne. Normally, it would not have

sufficient power to lift out of ground effect. Obstacle clearance was effected by suitable clearance between the leading edges and the surface. Endplates and trailing edges were subject to collisions and abrasion, but design care could reduce the wear factors.

WIG or ram wing operations are subject to instabilities which are not yet clearly understood. If a vehicle in ground effect climbs out of ground effect, or has the surface fall away below it, the vehicle will fall to the surface without ground effect being reestablished.

It is interesting to note the design and operation of present day "hydroplane" racers. They seem to have developed into a form of channel wing ACV, and at speed do, in fact, become fully airborne to minimize drag.

Open Plenum Chambers. The lifting ability of open plenum chambers has been utilized from the 1880's, and examples appeared in Paris and London in the 1890's [1]. In operation, a fan supplied a flow of air to the plenum chamber against a static pressure equal to the vehicle weight divided by the effective cushion area. The craft would then lift clear of the surface until the flow of air exiting under the chamber edge was equal to the intake flow. The vehicle could hover clear of the surface and be fully airborne, independent of vehicle speed. Any reasonably clear and level surface could now be negotiated. The need for continual replacement of

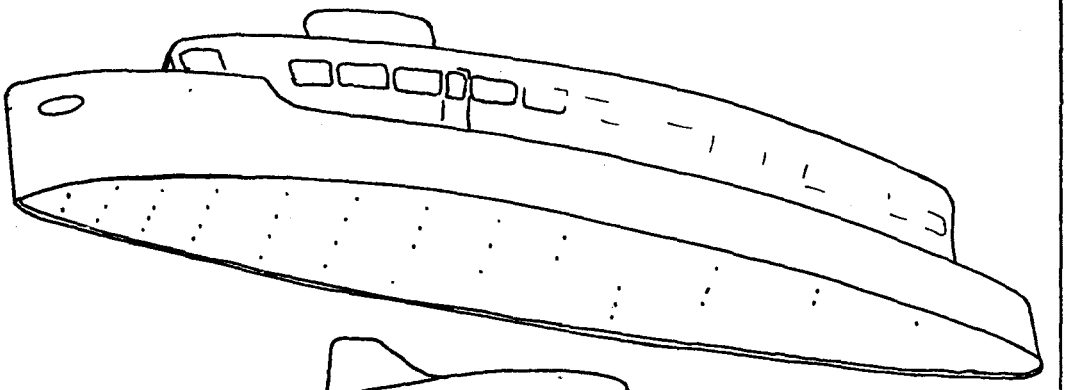

The "Flatiron" 1890
An anti-friction hull designed to reduce or eliminate water viscous drag.

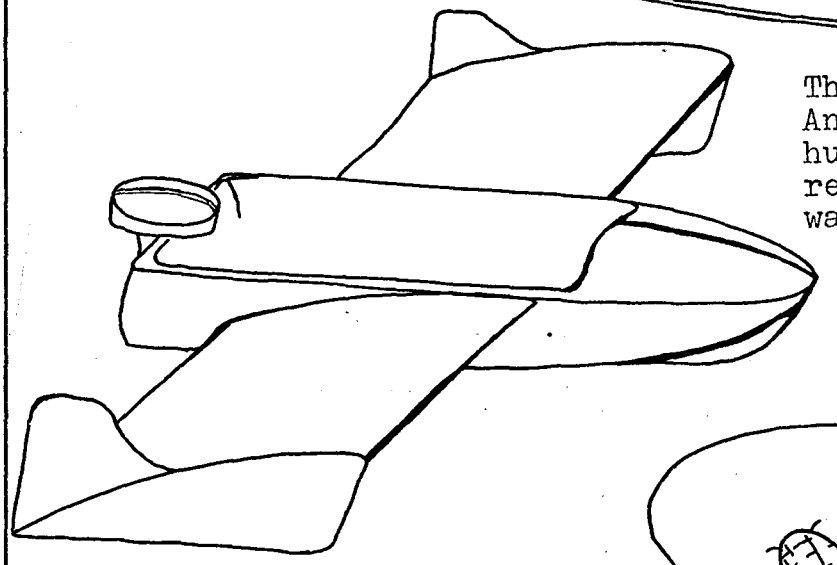

Lockheed winged hull
50% increase in speed
A ram (or channel) wing designed to eliminate all hull water drags at speed.

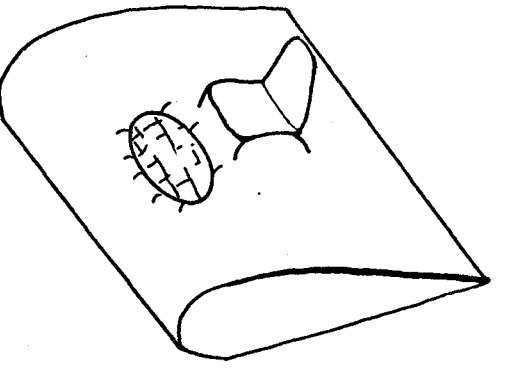

A Finnish open plenum chamber with top surface designed for lift -- 1930

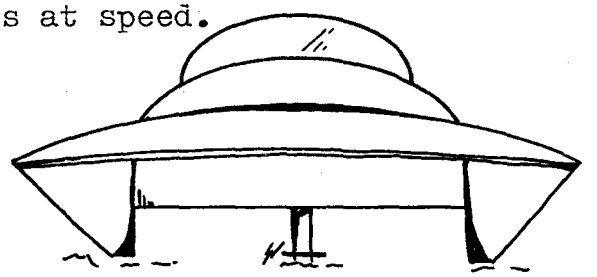

Hydroplane racer,
a channel wing

PRE-1950 AIR CUSHION VEHICLES

FIG. (1)

air limited the vehicle to a few inches of daylight clearance with reasonable power. Design concentrated on obtaining the maximum daylight clearance to allow operation over a greater variety of surfaces.

The United States had operational open plenum chamber vehicles in 1959. The Curtis-Wright Air Car was 8' x 21', and had two 180 horse power engines to carry four people. It achieved eight inches of daylight clearance. However, because the lower surface of the plenum chamber caused harsh drag forces on surface contact, and because lift power requirements rapidly became unreasonable with increasing daylight clearance, the vehicle was not produced.

Hydrokeels and Sidewall Vehicles. The hydrokeels and the sidewall ACV are a class which lie between the antifriction hull and the open plenum chamber configurations.

The hydrokeel attempted to reduce both the viscous and impact drags of a marine craft by forming a rather thin air cushion between the water and the craft's lower surface. The stern of the vehicle remained in the water. Sidewalls and a bowplate contained the air cushion. In 1959, the conversion of a U.S. Navy landing craft from a displacement hull to a hydrokeel led to a tripling of its top speed, from 16 knots to 45 knots (Fig. 2). The air system absorbed 15 horsepower.

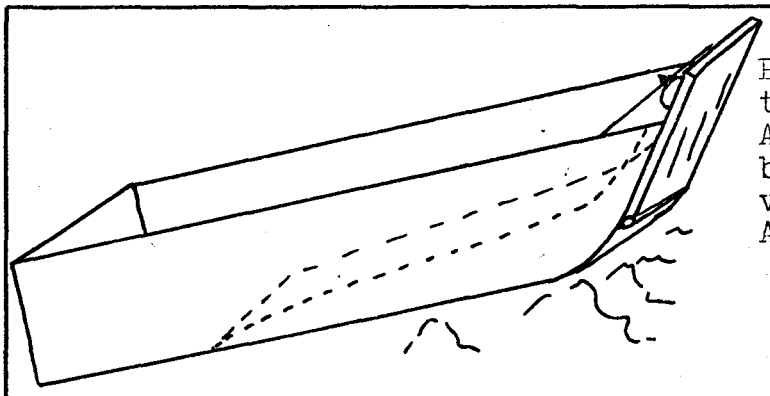

Priest modification to landing craft. A thin air cushion broke the water viscous drag. A hydrokeel, 1959

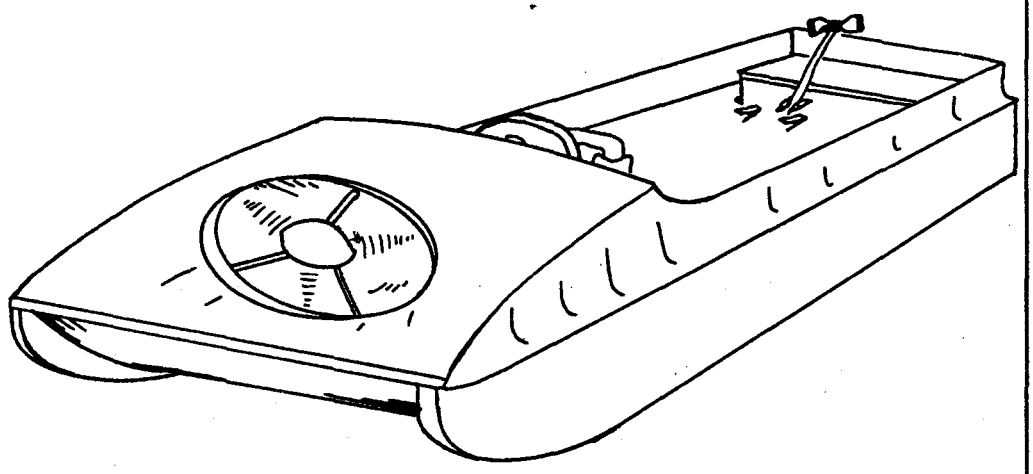

First thrust-cushion vehicle, 1959.
One duct, 7' X 14', VW 30 Hp. engine.
Marginal perfomance and skid control problèms but concept proven.

SRN-1, Saunders-Roe
circular, peripheral-jet
crossed English Channel,
July, 1959
450 hp., 9 in. clearance

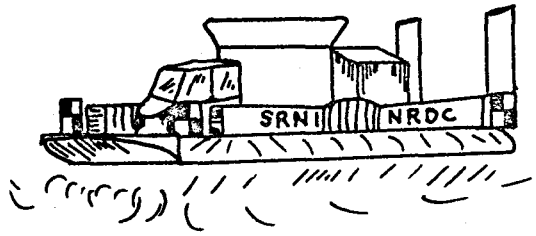

PRE-1960 AIR CUSHION VEHICLES

FIG.(2)

Amphibious and very shallow water operation was compromised for very low cushion air flows to minimize cushion power requirement.

The sidewall (or captured air bubble ACV as it is called in the United States) utilized submerged sidewalls, a bow, and a stern plate to completely contain the air cushion supplied by a lift fan [2]. The air cushion tended to be thick and complete over the hull bottom, in comparison to the hydrokeel cushion. Lift power was then minimized by the lack of an effective air flow, and very efficient operation resulted up to approximately 40 knots where drag forces on the submerged hulls became prohibitive. The bow and stern plates were not controllable, but were hinged to allow them to swing out of the way of obstacles. The true sidewall (CAB), while known and experimented with, was not commercially developed until the 1960's (Fig. 4).

Edge-Jet Vehicles. In 1958, Sir Christopher Cockerell invented and patented the edge-jet or peripheral-jet configuration. By directing the intake air into a duct system to form a high speed curtain of air around the periphery of the vehicle, the air within the cushion could be better contained. Daylight clearance was increased by approximately 75% over what was possible with an open plenum chamber. Further, if the air curtain was directed inward at some angle, then the cushion pressure could be

held by the momentum energy change of the air jet as it was forced to bend outward by the cushion pressure (Sec. II.4.1).

The advent of the edge-jet seemed to solve the daylight clearance dilemma of the open plenum chamber, and the British Government was encouraged enough to subsidize extensive research and development of these craft. In fact, the edge-jet became so popular that it, alone, was implied when the word "hovercraft" was used. In 1959, the SRN-1 (Fig. 2) was driven across the English Channel and a new hovercraft industry was predicted. The SRN-1 was circular in plan shape, used a 450 horsepower piston engine and achieved nine inches of daylight clearance. Thrust and control air was ducted from the high speed cushion intake air.

Thrust-Cushion Vehicles. Also in 1959, George T. Cocksedge, of Niagara Falls, Ontario, constructed his first man-carrying ACV based on some promising model studies conducted in 1958. This ACV was referred to as a thrust-cushion vehicle (TCV), as a single fan assembly ingested air to provide both lift and thrust (Fig. 2). That is, it rode on the air mass which was to provide the thrust.

Unlike any of the other ACV, the thrust-cushion vehicle had positive control over daylight clearance at any speed, and the amount of air cushion support; that is,

control over its mode of cushion support as described below. With the stern plate open, the vehicle was operated as a catamaran boat with air propulsion; on snow, it was an air-powered sled. On water, at low speed, with partial air support, it operated as a CAB; at higher speeds it operated like a channel wing with an enclosed cushion. On land, at slow speed, operation was similar to that of the open plenum chamber, but because the cushion air exited primarily in the rearward direction, a true hover required special trimming.

The original design aim was to simply reduce viscous and pressure drag on marine hulls. Experimental results, however, directed the design toward a vehicle having variable modes of travel and superior handling. Further, the concept of travelling "just at the surface" to minimize both cushion power and contact drags was unique to the TCV at that time. The sidewalls were true hulls designed to pierce wavetops so that water contact was not disastrous at speed.

The air was ingested at the very front of the vehicle, and was turned downward to run into a single large duct beneath the floor of the craft. The cushion was contained by hinged bow and stern plates. The bow plate could swing out of an obstacle's way, but was not controllable. The stern plate was manipulated by the driver to obtain control of daylight clearance. Yaw

control was provided by air rudders in the high speed air exiting at the stern plate. The sidewalls were 8 in. thick to provide all the required flotation for the vehicle, and the basic hull shape was that of the dynamically stable catamaran boat. The vehicle was 7 ft. X 14 ft., weighed 800 lb. empty, and was powered by a VW 30 hp engine. In operation, very marginal air flow was available for thrust once lift was achieved, and control problems were evident. The vehicle would slide down the slightest incline and would tend to drift with the wind unless a component of thrust was established to hold it; but, then, the vehicle proceeded in an undesirable crabwise fashion. Of course, this was true for all ACV at that time.

I.2 1960 and Beyond

The year of 1960 saw the widespread development of ACV, and the establishment of an ACV industry in England. The promise of ACV concepts for military and commercial exploitation caused extensive research and development in France, United States, Canada, Japan, and Russia. The world waited for production of an ACV which would fill a large gap in the spectrum of vehicles between displacement ships and aircraft. The ACV required only a relatively clear pathway on moderate slopes, and, therefore, was potentially ideal for high speed transport on all the

waterways of the world, winter and summer.

The design philosophy of the industry at the time of the SRN-1 crossing is illustrated by the following statement on the crossing by W. A. Crago, Chief Research Engineer, B.H.C. [3]

> "Whilst the exercise undoubtedly demonstrated the basic principles of hovercraft in a practical manner and constituted a successful experiment, it was realized that unless the clearance of the structure above the water could be radically improved then hovercraft would have little or no future, since they would not be able to operate over waves or reasonably rough ground."

The advent of skirts for hovercraft, in 1961, provided the "radically improved" clearance without the power input penalty of non-skirted vehicles. The flexible skirts, several feet high, could deform over surface irregularities. Higher waves called for higher skirts or larger vehicles. Unfortunately, if a hovercraft, designed to operate with four feet of clearance, struck a four and one-half foot wave, severe deceleration resulted as the basic hull was incompatible with the water at speed.

While skirts gave clearance, they aggravated the stability problems of ACV. The skirts had to have a certain rigidity to supply corrective forces to upsetting loadings.

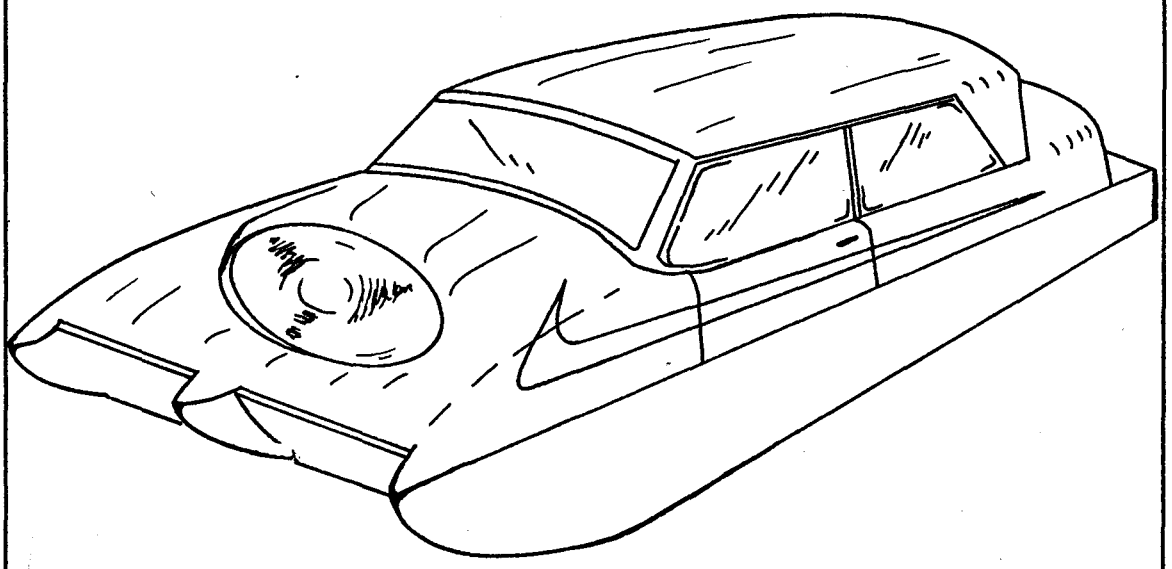

Second thrust-cushion vehicle.
4-passenger, 8' X 18';
positive roll control;
35 - 40 mph with 45 hp.
engine. Hovair, 1961

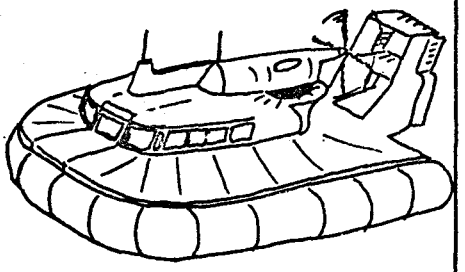

SRN-5 Saunders-Roe
skirted edge-jet;
14-passenger, 70 knot
vehicle; 1050 hp.
engine; 4 foot skirts,
1962

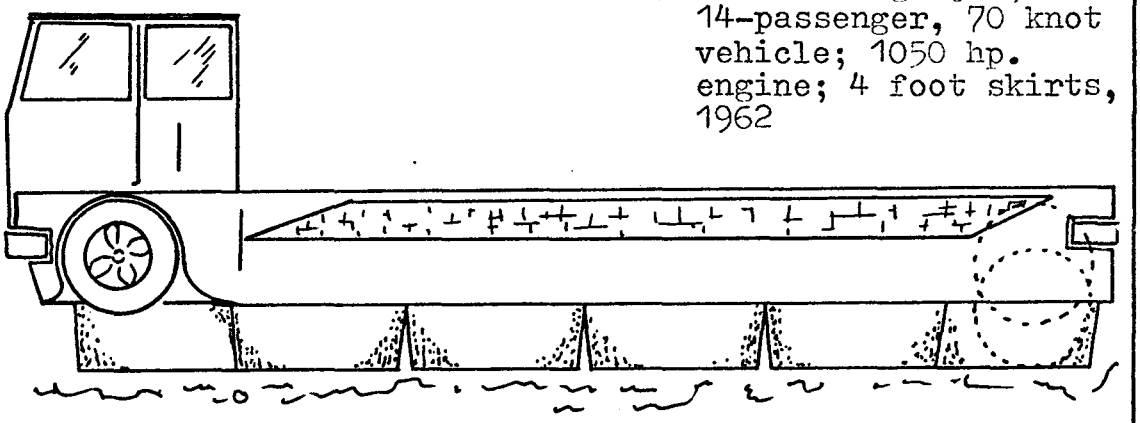

Sedam BC 7 terraplane. Bertin open plenum chamber cells (jupes) for ACV assisted off-road truck.

POST-1960 ACV

FIG.(3)

The skirts, when rigid enough to satisfy stability constraints, created substantial drag forces on surface contact. The large 165 ton SRN-4 hovercraft operating on the English Channel achieved a block speed of 40 knots in actual service after 80 knot speeds were predicted [4]. The unexpected discrepancy was attributed to underestimated skirt drag on the wave tops.

As operating experience built up on ACV, the power advantage of travelling with minimum daylight clearance became apparent, and this was incorporated into the design philosophy. The following statement by J. U. Kordenbrock, in 1969, is included in a description of design philosophy for hovercraft. [5]

> "The leakage of this (cushion) air from beneath the device must be kept to a minimum to reduce power losses... This clearance or "air-gap" must be adequate to prevent ground contact under normal operating conditions in order to take advantage of the low friction forces of the supporting layer of air..."

ACV are now operating with very low daylight clearances, but the problems of skirt wear, stability, and high contact drags remain. For these reasons, virtually all of the proposed very large ACV have resorted to sidewall configuration with the sidewalls above or in the

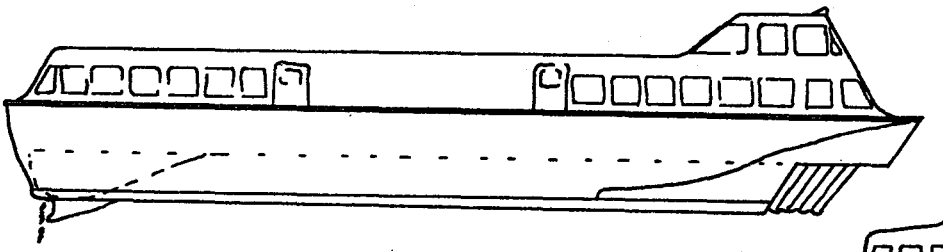

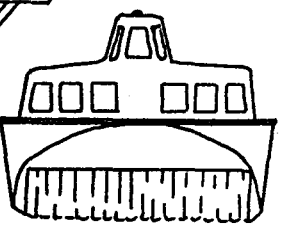

100-passenger, Hovermarine sidewall (or captured air bubble) ACV

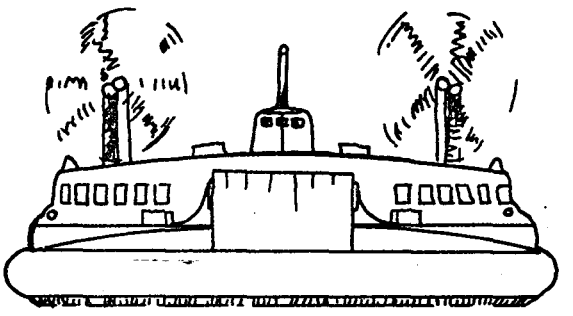

SRN-4

165 ton skirted edge-jet

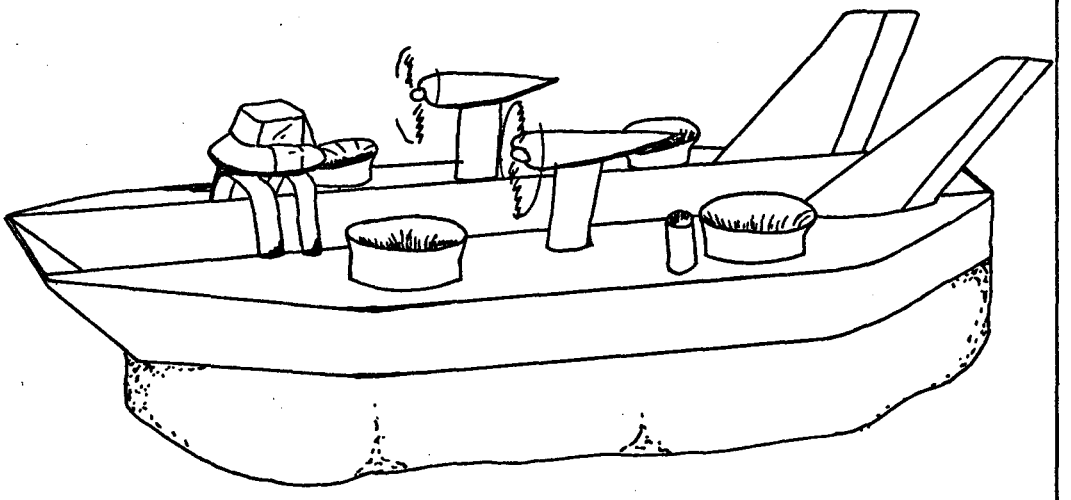

Sedam N300, multiple open plenum chambers

LARGER ACV FROM THE 1960's

FIG.(4)

surface (Fig. 5). Immersed sidewalls have approximately equal drag to that of skirts at about 40 knots, but lift power is reduced and stability is greatly enhanced.

Production did come on edge-jet and CAB vehicles (Fig. 4), but first costs and operating costs were in the order of helicopter costs, and they were simply not commercially viable. Even small, one and two place ACV have not become publicly acceptable due to control problems, cost, and undesirable exposed fans.

Also in the 1960's, ACV designed to operate on a guideway, (proposed and experimented with before 1900 in England), [1] were studied again. The French, through Bertin et Cie, developed tracked ACV earlier and more thoroughly than other countries, but both Britain and the United States are currently close to actual establishment of mass-transit, tracked ACV. The advent of the linear induction motor has made tracked ACV more appealing. One apparently highly feasible route is between Windsor, Ont., and Oshawa, where low land relief and high population densities could justify the 300 to 500 mph transit system.

In 1961, the second man-carrying thrust-cushion vehicle was built and tested (Fig. 3). It was 8 ft. X 17 ft., carried three passengers, and was powered by a 2-cycle engine which produced an erratic 45 hp. The vehicle contained a central third hull which ran the length of the vehicle. The ingested air passed into <u>two</u> lower

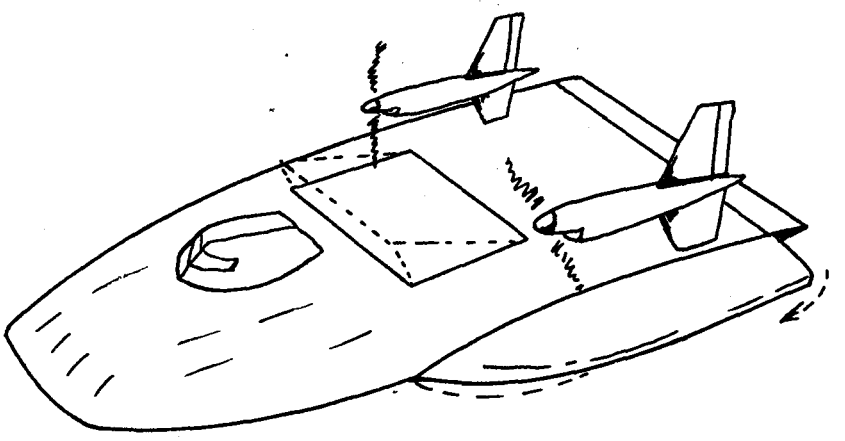

General Dynamics WIG with open plenum chamber components for low speed operation

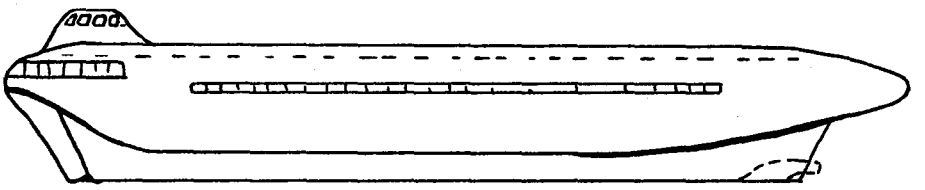

Hovermarine "Deep Cushion"

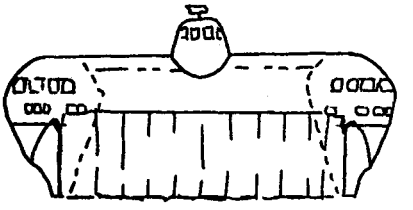

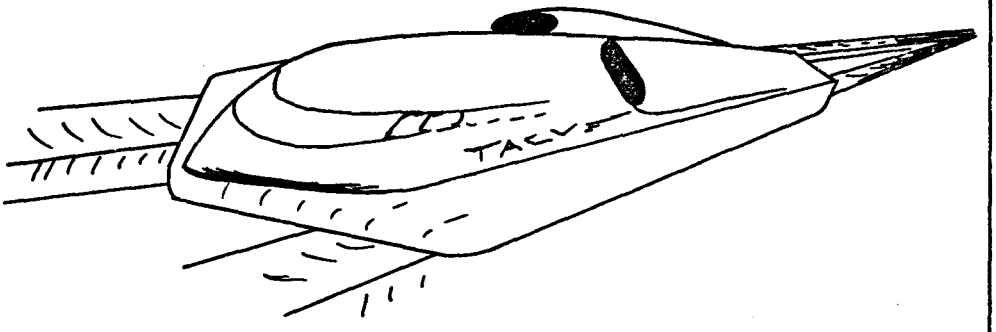

Large tracked ACV with jet thrust.

PROPOSED AIR CUSHION VEHICLES

FIG.(5)

ducts, and the daylight clearance and pressure could be differentially controlled in each. The thrust-cushion now had a positive roll control to couteract side forces to the vehicle. World-wide patents were applied for in 1959, 1960 and 1961, and the Hovair Company was formed in 1961. A 10 ft. X 28 ft., fourteen passenger vehicle is currently under construction.

CHAPTER II

ANALYSIS OF CURRENT AIR CUSHION VEHICLES

II.1 The Ram Wing

The ram wing is designed for fully air supported travel only after some critical speed. Below this critical speed, some other means of support is required. Lift is generated through body lift forces (L_b), and by the conversion of the freestream dynamic head to a static head beneath the craft. The pressure beneath the craft (or wing) is usually contained by large endplates, and the product of this cushion pressure (P_c) with the effective cushion area (A_c) gives rise to a cushion lift (L_c). Included in L_c is the usual pressure increase generated below any wing shape, especially near a surface. In a true ram wing, however, the air flow beneath the wing is fully stagnated as the trailing edge is located just at the surface. As indicated in Fig. 6a, the centre of lift for the cushion is behind the centre of lift for the body lift forces. If the ram wing achieved a sufficiently high speed, the body lift forces could become predominant while the vehicle was in a tail-heavy state, and an unstable pitching-up reaction would take place. The ram wing, therefore,

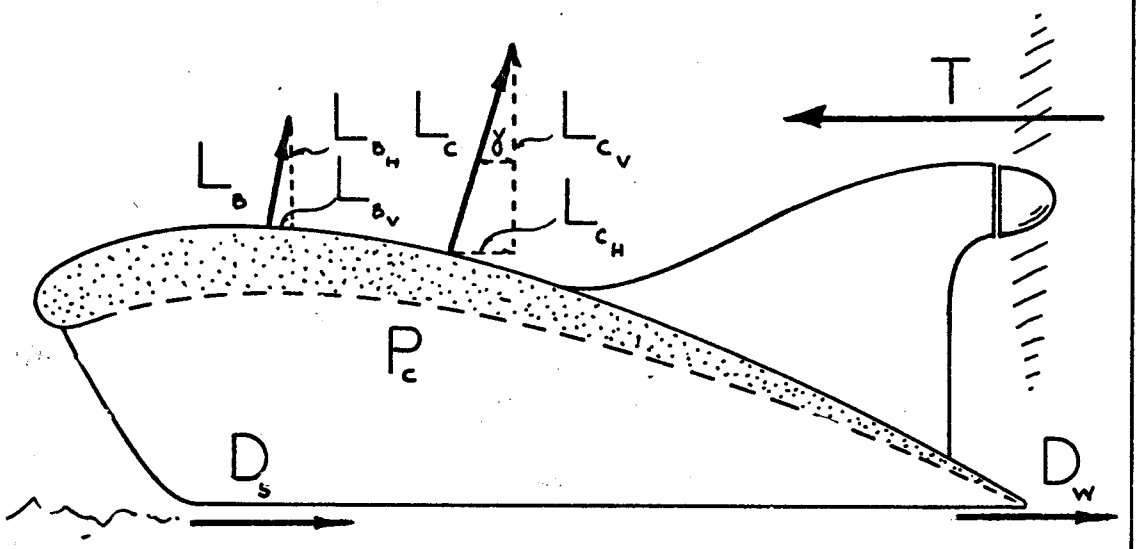

(a) TRUE RAM WING

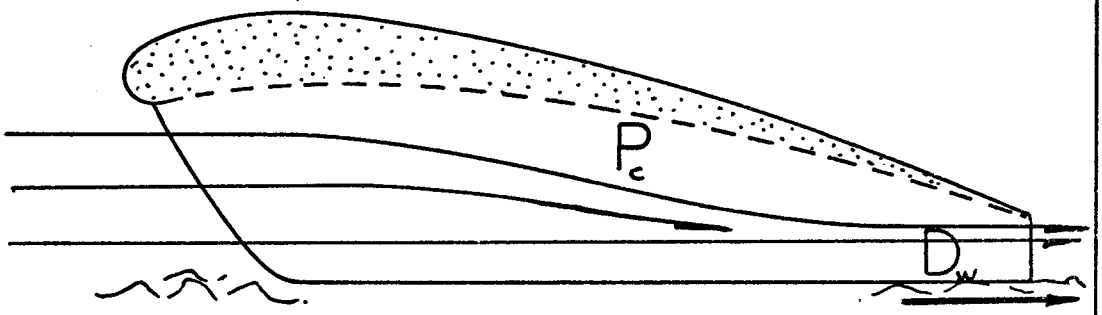

(b) CHANNEL WING

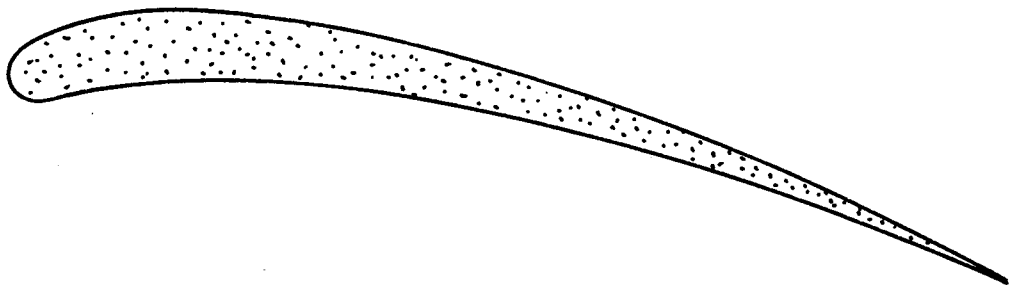

(c) WING-IN-GROUND-EFFECT

RAM WING VEHICLES

FIG.(6)

usually has an upper speed limitation.

A variant of the true ram wing is the channel wing, but the distinction is not always made. In the channel wing (Fig. 6b), there is air flow beneath the wing as the trailing edge is some distance above the surface. The air flow is restricted, however, and a pressure above atmospheric is generated below the wing.

The ram wing would suffer the usual drag forces associated with a lifting wing (L_{bh}), and those associated with any surface contact of the endplates and the trailing edge (D_e). Also, because there is a velocity differential between the cushion air and the surface, the true ram wing is subject to cushion shear drag (D_s, see Sec. III.3.3). Finally, there is the following drag associated with the necessary degree of incidence of the ram wing to the surface. L_c acts at some rearward angle (γ) to the vertical, and the horizontal component of L_c, that is, L_{ch}, acts against the vehicle motion. L_{ch} is a form of cushion trim drag (Sec. III.3.3).

$$L_{ch} = A_c P_c \sin \gamma \qquad (1)$$

where A_c = the cushion area

and P_c = the effective cushion pressure

The ram wing is simple in configuration, and lends itself to large sizes and high speed operations. Weights

per horsepower of 100 lbs. or more at 100 knots are predicted by the Columbia project [6], and by General Dynamics' large ram wing vehicles [7], however, instabilities arising from surface irregularities of wings in ground effect are not yet clearly understood.

II.2 The Open Plenum Chamber

The oldest form of ACV is the open plenum chamber which can be described as an open, inverted dish with an air supply [1]. A separate aero or marine system provides thrust. Air is forced into the chamber until the cushion pressure reaction on the chamber is sufficient to lift the vehicle clear of the surface. The vehicle will continue to lift until the intake flow equals the exit flow, and an equilibrium daylight clearance is established. Cushion pressure stabilizes to that pressure occurring at lift off.

Lift is contributed by the fan thrust (assuming a horizontal fan), the cushion lift, and any body forces generated at speed.

$$L = T_f + P_c A_c + L_b \qquad (2)$$

Daylight clearance is determined by the intake flow,

$$h = Q_f(KSV_1)^{-1} \qquad (3)$$

where h = the daylight clearance

Q_f = the flow through the fan

V_1 = the exit air velocity,

and S = the peripheral length of the cushion.

Note that $h \propto Q_f$ and $h \propto P_c^{-\frac{1}{2}}$. The factor K is the discharge coefficient for the exit flow. Coefficients for some typical cases are illustrated in Fig. 7. A polynomial approximation for experimental graphs, based on five points, is given as,

$$K = 0.500 + 0.400\theta \times 10^{-3} + 0.109\theta^2 \times 10^{-4} - 0.494\theta^3 \times 10^{-7} + 0.345\theta^4 \times 10^{-9} \qquad (4)$$

where θ, (Fig. 7), is in degrees [2]. A theoretical expression for K [2] is

$$K = \frac{1}{2}\left[1 + \frac{\sin\theta}{\left\{(\pi + 2)/(\pi - 2)\right\}\left\{1 + \cos\theta\right\} - \sin\theta\cos\theta}\right] \qquad (5)$$

Both give good correlation, but the theoretical K tends to be slightly low due to the neglected viscosity of air. The exit velocity (V_1) is dependent upon the cushion pressure, and, through the Bernoulli equation for energy inside and outside the cushion, is given, approximately, by

$$V_1 = \sqrt{\frac{2P_c}{\rho}} \qquad (6)$$

The air velocity within the cushion is assumed to be

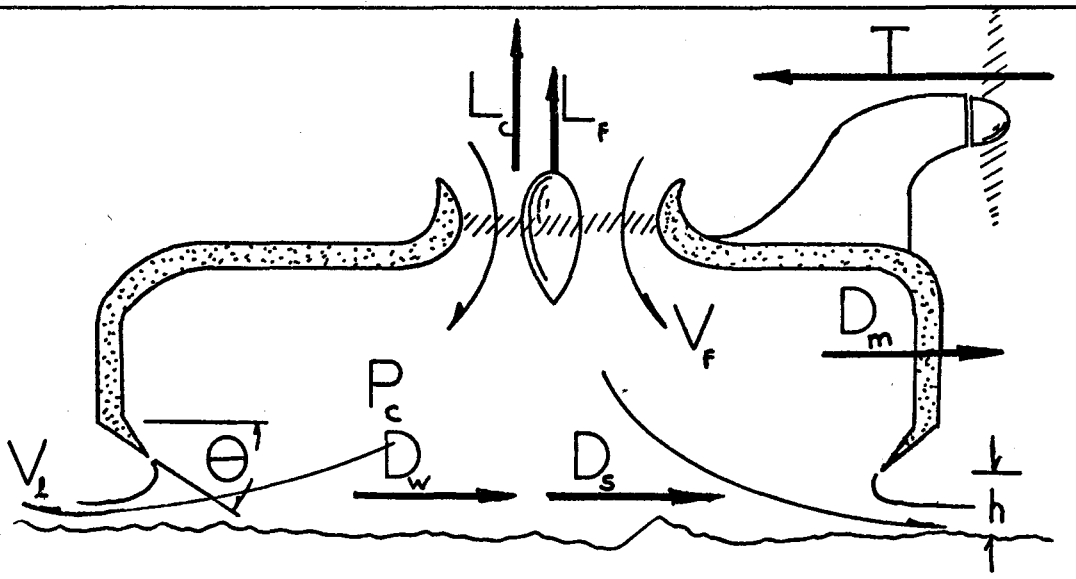

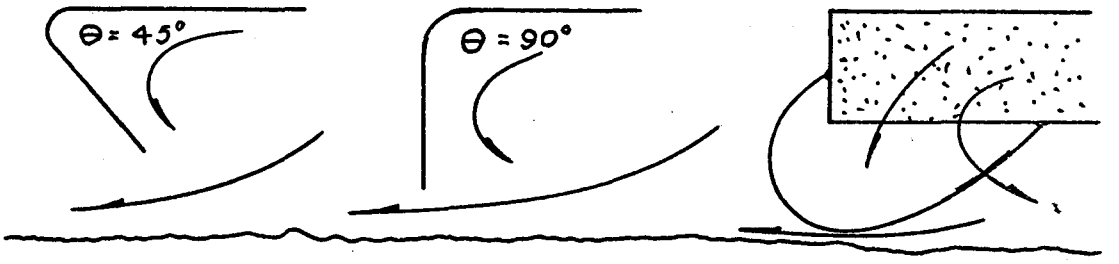

K = 0.58 K = 0.6 K = 0.95
Bag Skirt

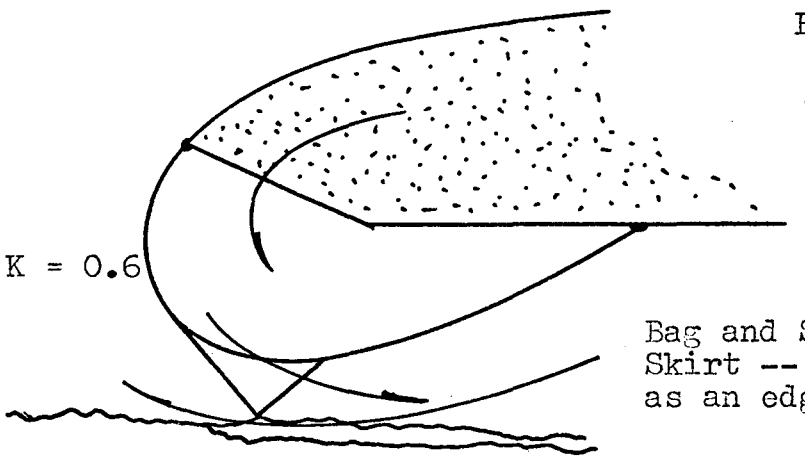

Bag and Segment Skirt -- considered as an edge-jet

THE OPEN PLENUM CHAMBER CONCEPT

FIG.(7)

negligible.

The fan thrust is determined by the velocity of the mass flow of the intake air, and is given by

$$T_f = \rho A_f V_f^2 \tag{7}$$

Through continuity of mass

$$V_f = \frac{A_1}{A_f} V_1 \tag{8}$$

where A_1 is the exit flow area.

Substituting equations (6) and (7) into (8),

$$T_f = \frac{2P_c A_1^2}{A_f} \tag{9}$$

Lift is now given by

$$L = \frac{2P_c A_1^2}{A_f} + A_c P_c + L_b \tag{10}$$

Statically, an expression for lift augmentation can now be formed by dividing equation (10) by T_f.

Therefore,
$$\frac{L}{T_f} = 1 + \frac{A_c A_f}{2A_1^2} \quad , \tag{10a}$$

and
$$\frac{L}{T_f} \propto \frac{1}{A_1^2}$$

One way of comparing ACV concepts is to compare nozzle powers (P_N) required to produce the same clearance height. The nozzle power for plenum chambers is

$$P_N = P_c Q_1 \tag{11}$$

But $$Q_1 = A_1 V_1$$

$$= \sqrt{\frac{2P_c}{\rho}}\, hSK$$

and $$P = P_c^{3/2}\, hSK \left[\frac{2}{\rho}\right]^{1/2} \tag{11a}$$

The open plenum chamber is subject to the following drag forces which are only briefly explained here, but are presented in more detail in Chapter III.

Momentum drag (D_m) forms as the ingested air is accelerated from rest to the vehicle's velocity. As air is continually ingested, a continual drag results. If more air is allowed to escape to the rearward, then a "momentum regain" of some percentage of the total is possible. Unfortunately, the likelihood of achieving any effective regain from a plenum chamber or edge-jet has been discounted as practical data increases. Momentum drag accounts for approximately one-third of the total drag of a plenum chamber or edge-jet at 60 knots[9].

Cushion shear drag (D_S) is the force resulting

from the velocity distribution which forms in the cushion as the vehicle is swept over the surface.

Wavemaking drag (D_W) is generated as a result of the cushion reaction on the water. Even though the craft is fully airborne, it still displaces its own weight in water. The vehicle must climb out of this depression as its velocity increases.

At speed, the open plenum chamber ACV does indeed substantially reduce thrust requirements as compared with displacement or planing craft. However, turning radii are very large causing control to be marginal due to poor course-changing abilities. Sideslopes and crosswinds are negotiated only in a "crabwise" form of travel; but perhaps the most serious drawback, at least to the author, is the rather poor specific power ratios (power per weight per velocity) of present vehicles [8].

II.3 Sidewall Vehicles

Sidewall ACV, or captured air bubble (CAB) vehicles, have relinquished amphibious qualities in an attempt to minimize cushion power requirements. The cushion is contained by longitudinal walls which penetrate some distance into the surface, usually about six inches to a foot. The cushion is contained at the front by a hinged bow plate or a flexible skirt, but some earlier CAB vehicles utilized a jet curtain. The rear of the cushion is usually contained

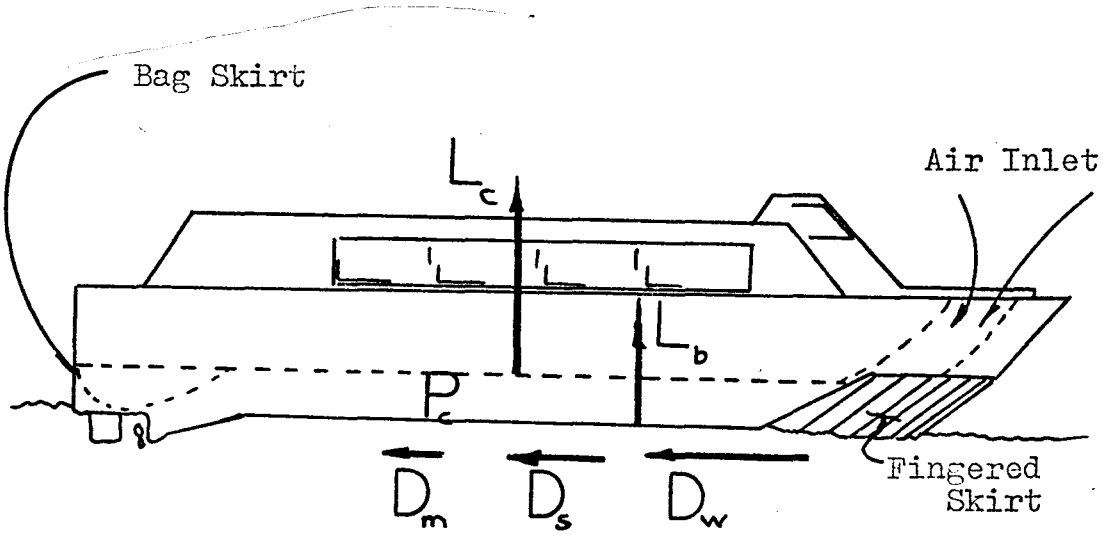

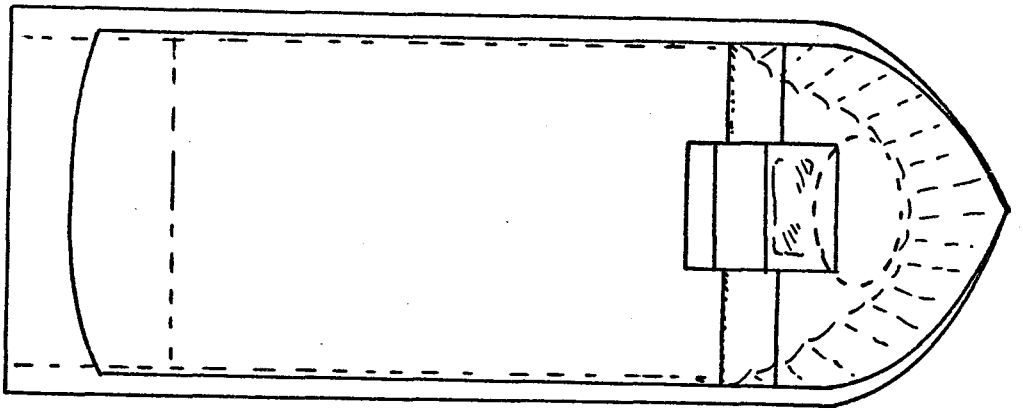

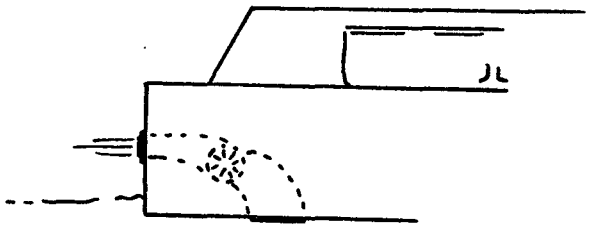

Jet Pump Propulsion

THE SIDEWALL CONFIGURATION

FIG.(8)

by a bag skirt (Fig. 8). The air cushions tend to be rather thin, compared to open plenum chambers, as their primary purpose is to break the viscous and form drag of their hulls. Most often, their propulsion is by marine screw or jet.

The sidewall vehicle's lift is generated like the open plenum chamber, but the vehicle is not totally air supported. Statically, some buoyancy forces (L_{b_y}) are involved and dynamically some planing forces (L_p) contribute to lift.

$$L = P_c A_c + L_b + L_{b_y} + L_p \qquad (12)$$

A fan thrust term is not included as cushion flow is usually almost negligible.

The drag analysis for CAB vehicles is similar to that for plenum chambers, but momentum drag forces are very low due to very low cushion flows and due to the relatively moderate speeds of these vehicles. The water drags of the immersed sidewalls and propulsion appendages are usually included in the wetting drag (Sec. III.3.4.2).

Sidewall vehicles are efficient up to about 40 knots when water drag on the immersed walls cause drags equivalent to that of the skirted edge-jets. In operation, there is virtually no spray, control is positive, and there are no apparent stability problems. Sidewinds cause no special corrections, however, CAB vehicles are subject to

damage from floating debris and shallow water. Their marketability was hindered by the industry's desire for fully amphibious vehicles.

II.4 The Edge-Jet Vehicle

The edge-jet principle incorporates a high speed curtain of air around the edge or periphery of the cushion. The cushion air must push the curtain aside before exiting, and hence is better contained than in a plenum chamber. An inward angle (θ) on the curtain enhances the cushion enclosing effect as greater horizontal momentum is available to balance the cushion pressure reaction on the curtain (Fig. 9).

$$P_c h = M_j \cos\theta + M_g \tag{13}$$

M_j is the jet momentum per unit length of periphery, and is given by the Bernoulli equation as

$$M_j = \left[\frac{2}{\rho}\left(P_j - \frac{P_c}{2}\right)\right]^{1/2} \tag{14}$$

if the static pressure of the jet is assumed to be $\frac{1}{2}P_c$. M_g is the momentum of the jet at ground contact.

But $$M_j = \rho V_j^2 t \tag{15}$$

where t = width of jet (Fig. 9)

and if M_j is assumed equal to M_g for equation (13), and (3) is substituted into (1),

$$\frac{P_c}{P_j} = \frac{2(t/h)(1 + \cos\theta)}{1 + (t/h)(1 + \cos\theta)} \tag{16}$$

where θ = angle of inward inclination of jet

Total lift of the edge-jet vehicles is provided by cushion pressure, and by the jet reaction on the surface. As centrifugal fans are usually employed, a fan thrust is not included.

$$L = P_c A_c + (\rho V_j^2 + \tfrac{1}{2}P_c)St + L_b \tag{17}$$

Nozzle power is given by

$$P_N = P_j Q_1$$

$$= P_c^{3/2} \frac{hs}{1 + \cos\theta} \left[\frac{2}{\rho} \left(1 + \frac{\chi}{2} \right) \cdot \left(2\chi \right)^{-\frac{1}{2}} \right]^{\frac{1}{2}} \tag{18}$$

where $\chi = (t/h)(1 + \cos\theta)$

If suitable values are given for the vehicle parameters for the edge-jet and for the plenum chamber, a ratio of nozzle powers works out to 0.7 in favour of the edge-jet. The edge-jet is clearly the superior concept for achieving a given daylight clearance, at least in the laboratory[2].

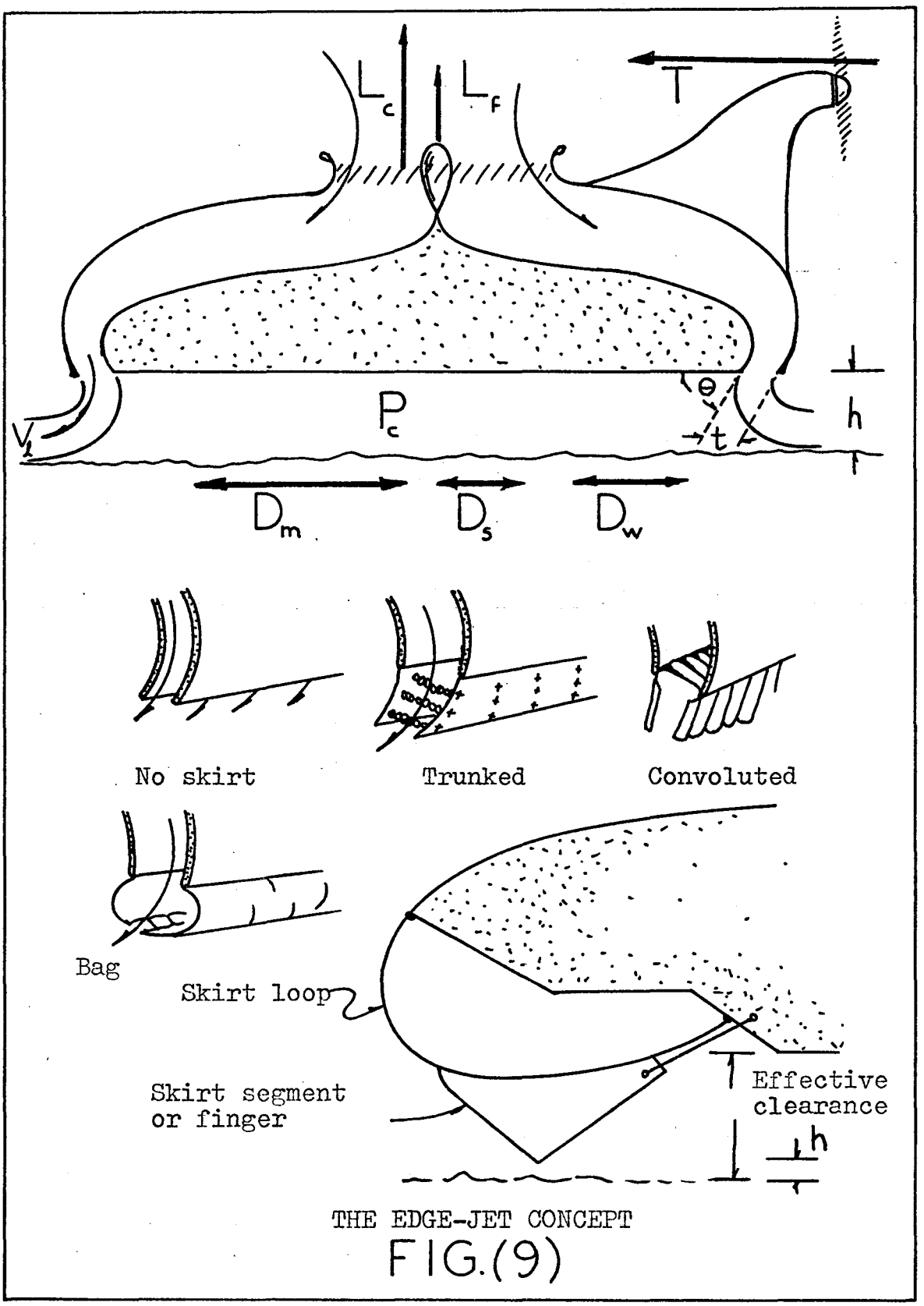

THE EDGE-JET CONCEPT

FIG.(9)

The advent of skirts for edge-jets greatly increases the hard structure clearance, and the analysis above still applies; but, with skirts, the actual daylight clearance is about half that without, due to the added duct losses.

Unfortunately, while the edge-jet promised superior performance, operational experience tempered the expectations. This statement is explained by G. H. Elsley [2] as follows:

> "...few if any craft have been built with a complete peripheral flexible nozzle because of the likelihood of damage resulting from the scooping action of the forward-facing rear nozzle. On early SRN-5 and 6 craft the flexible nozzle across the stern was replaced by an almost completely sealed bag. Thus in the hover condition this section of the craft operated as a plenum chamber machine with the outgoing air being supplied by the remaining peripheral jets. Effectively this meant that they split on surface contact, the inner section supplying the rear leakage. This is an inefficient mode of operation which is accentuated, on peripheral jet craft, by operation over uneven surfaces. In this condition local sections of the jet, at low clearance, split and cross flow to feed other sections temporarily operating at high clearance. Thus although over level

> ground the ideal peripheral jet craft requires less power than the plenum chamber craft, in practice this superiority largely disappears."

The Saunders-Roe SRN-6 and SRN-4 (see Chapter 1) have been the most successful ACV to date, and thousands of hours of experience have been gained with them. They are expensive to operate, and have proven to be financially feasible only on carefully chosen routes.

A form of skirt instability still affects skirted edge-jets, and, to date, four SRN vehicles have overturned on water at speed. The skirt is essentially round in cross-section, and if a wave is struck in a special way, viscous drag is established to create a negative lifting force to pull the vehicle into the wave. The sequence of events is very fast, and the vehicle violently decelerates in a "plough-in" [3]. If the vehicle is within a critical speed range, an overturning moment can result. Collapse of the foreward cushion causing the nose to drop, and the high thrust line of these vehicles aggravates the problem.

Typical drag forces on an edge-jet of large size are illustrated in Fig. 10. Similar curves would occur for smaller edge-jets, but because smaller edge-jets have comparatively higher cushion flows, they would have relatively greater momentum, wetting, and over wave drags. Fig. 10 shows a relationship between wetting and momentum

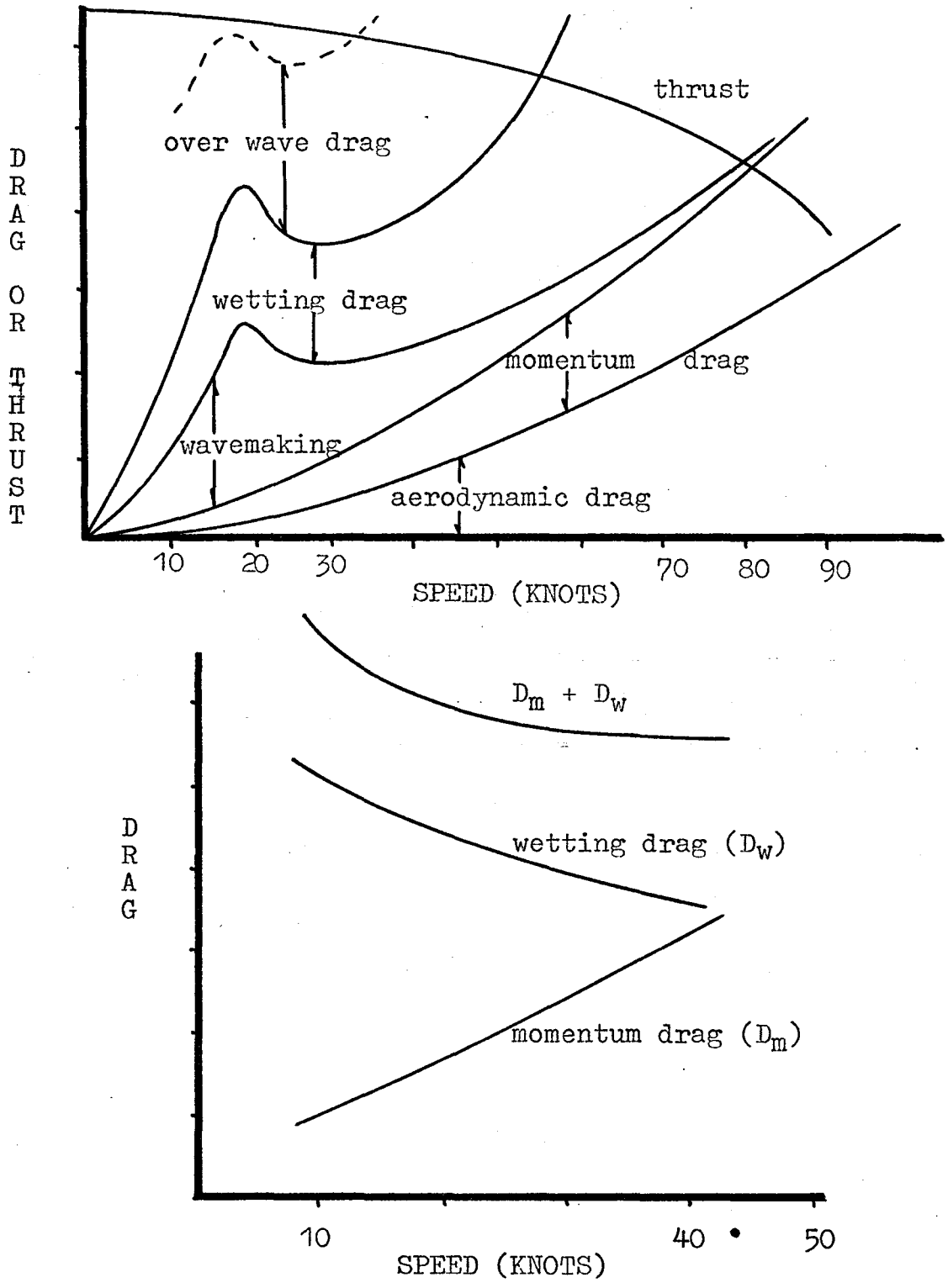

DRAG CURVES FOR EDGE-JET VEHICLES

FIG.(10)

drags for various clearances. The increasing wetting drag with decreasing clearance is caused by increasing masses of water spray being picked up by the high speed jet curtain, and striking the primary structure.

II.5 Tracked Air Cushion Vehicles

Wheeled vehicles became inefficient at about one hundred miles per hour. Air cushion suspensions, in comparison, are less efficient than wheels below one hundred miles per hour, but are more efficient and predictable for the range of speeds from one to five hundred miles per hour. To maintain control of the vehicle at these potential velocities, a guide system must be employed. Tracked ACV (TACV) can utilize the open plenum chamber concept, as the Bertain system does [10], the edge-jet principle, or some unique configuration (Fig. 11). Whatever system is used, the different ranges of speeds and operational surfaces are forcing higher ranges of pressures over smaller pad areas with very low clearances. Eventually, the analyses will be sufficiently different to warrant TACV being classified as a separate form of ACV.

Fig. 12 illustrates a quite different form of cushion suspension based on a vacuum chamber rather than on a pressure chamber [11]. Atmospheric pressure lifts the car from below until an equilibrium is established.

It is believed that the thrust cushion concept,

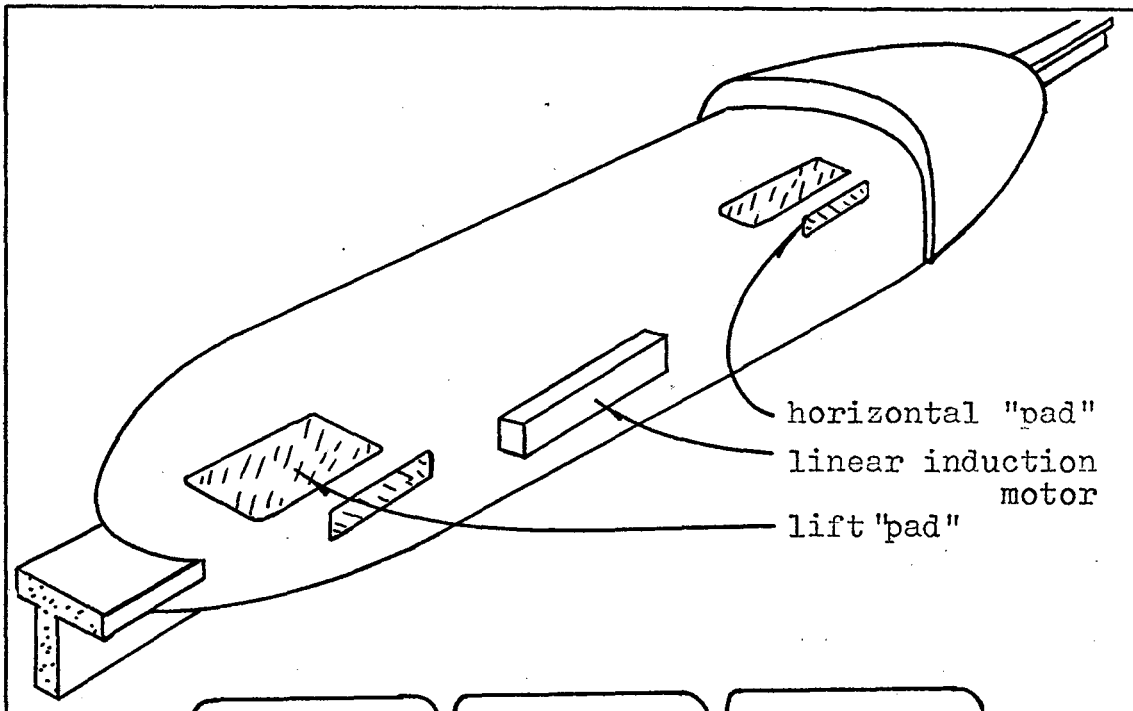

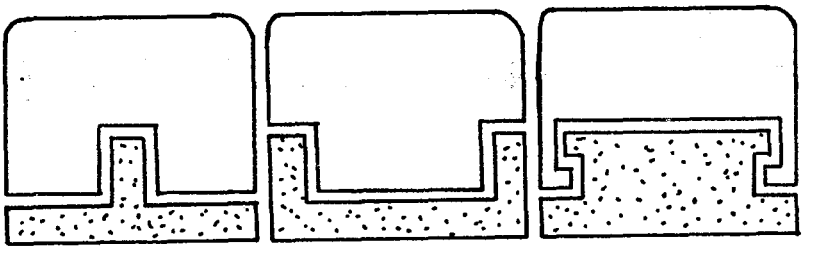

suggested track designs

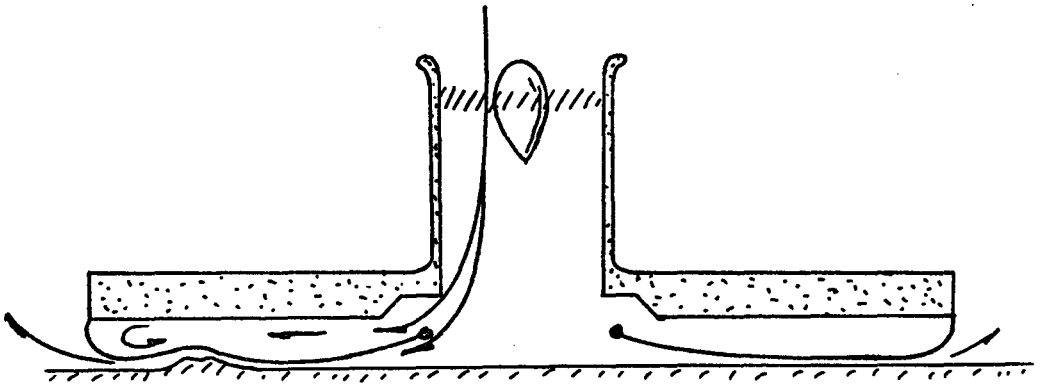

"Invasilift" concept

TRACKED AIR CUSHION VEHICLES

FIG.(11)

with its forward air intake and air flow in the direction of travel, would lend itself to very large TACV. These vehicles could move heavy payloads over hundreds of miles of tundra at high speed or provide very fast intercity travel. The track would be quite superficial compared to railways or year round roads.

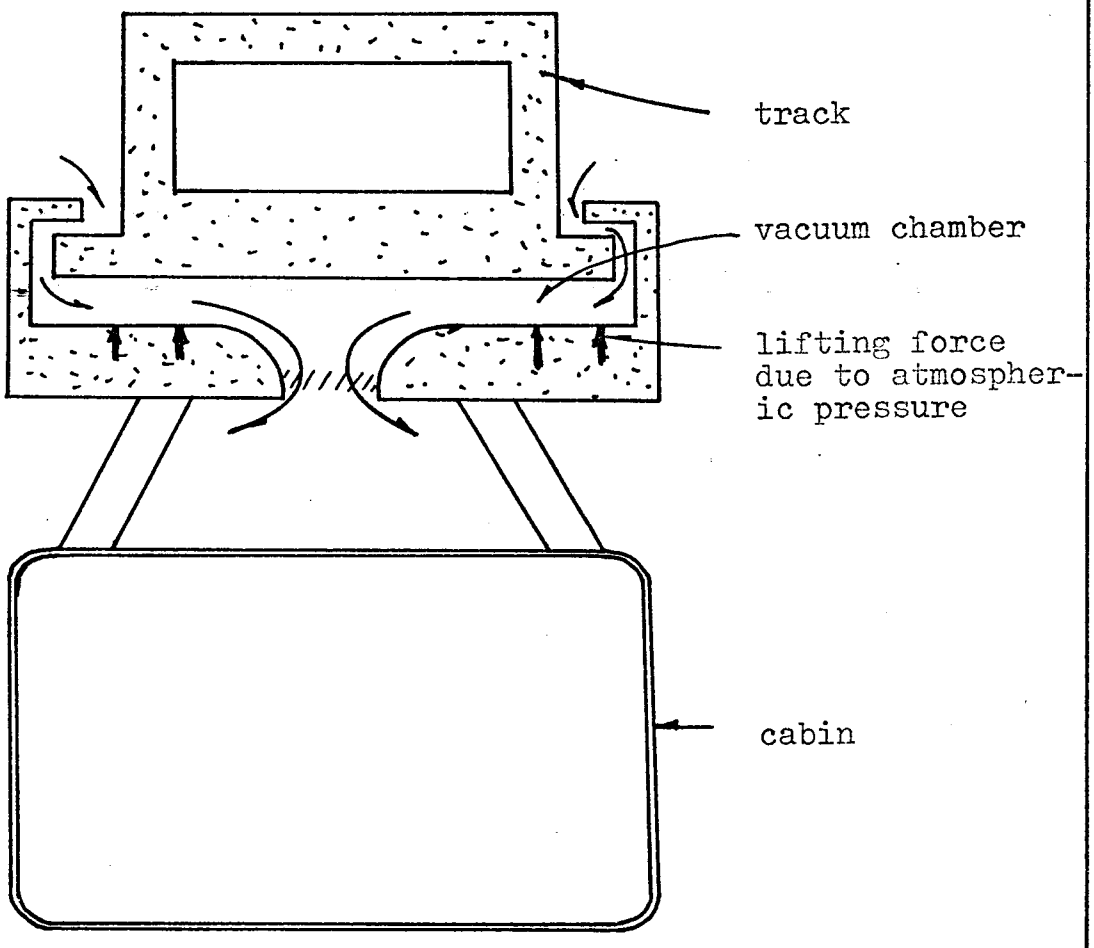

THE DYNAVAC VEHICLE

FIG.(12)

CHAPTER III

THE THRUST-CUSHION CONCEPT

III.1 Introduction

Thrust-cushion vehicles have fully integrated lift and thrust systems; that is, one fan assembly provides the functions of both lift and thrust.

As appealing as this aspect is to the builders and operators, it creates complications for the researcher; for example, as thrust cannot be fully separated from lift, the changes in thrust with vehicle speed are very difficult to measure, as are the vehicle drag components. The deceptively simple configuration is actually an efficient solution for complicated tasks, and the design parameters are all functions of each other. Further research complications arise from the vehicle's ability to operate partially or wholly as: a trimaran boat, a surface penetrating ACV with some buoyancy support, a surface touching ACV with some hydro-dynamic support, or as a fully air supported ACV operating much like an open plenum chamber at low speed and as a ram wing at high speed.

III.2 An Approximate Analysis of the Thrust-Lift Principle for Design

In the descriptions of the previous concepts, the lift and thrust systems received separate examination. In the thrust-cushion concept, however, the lift system is inherent in the thrust system, and the following analysis became an analysis of thrust. A single chambered thrust-cushion model was used.

III.2.1 Assumptions for the Theoretical Analysis

(1) All air flow is inviscid.

(2) Cushion pressure is constant over the cushion plan area, and is determined by the vehicle gross weight divided by the effective cushion area.

(3) Air loss along the sidewalls is linear; that is, an equal amount of air is lost through each square foot of daylight opening.

(4) Input air power is constant.

(5) Negligible flow occurs under the bow plate.

(6) Thrust forces occur as the air flow exits under the sidewalls or under the stern plate.

(7) Fan area equals main duct area.

III.2.2 General Discussion

Input pressure, supplied by the engine and by the freestream air, provides a flow of air against the constant cushion pressure in the main ducts. The flow of air that

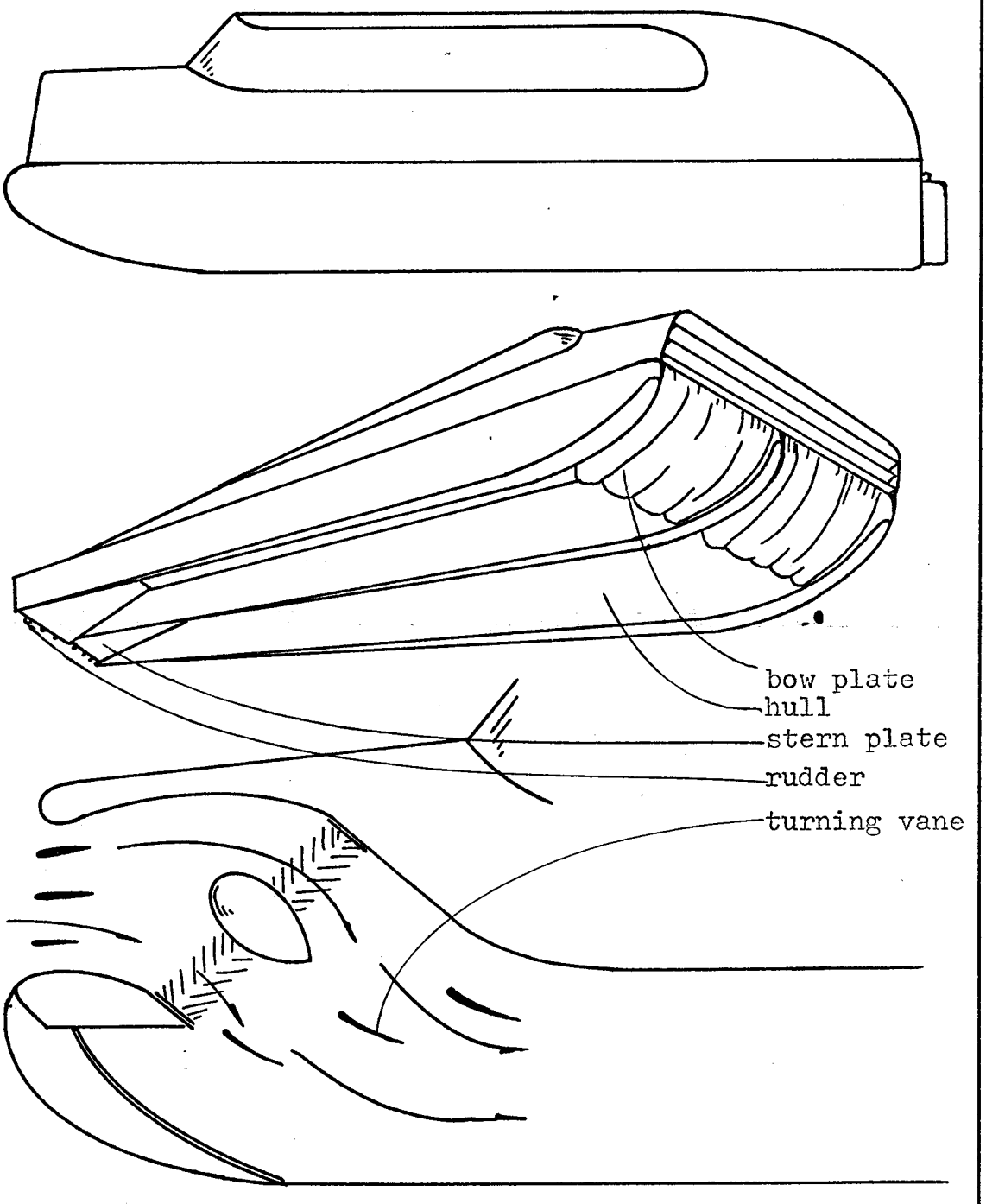

THE THRUST-CUSHION VEHICLE

FIG.(13)

enters the vehicle is first turned 45° downward from the horizontal, toward the surface as the flow passes through the fans (Fig. 13). Next the air is turned 45° again, this time by a set of turning vanes below the fans, so that the input air flow enters the main ducts in a rectangular-shaped volume with streamlines that are parallel to the main duct walls. When the daylight clearance is effectively zero, the duct flow is essentially a flow through a rectangular duct with one moving wall -- the surface.

Once an effective daylight clearance is established, the duct flow is complicated by a flow sink along the outside hulls and the total flow is not parallel to the direction of motion. Given that the flow enters the duct in a rearward direction, the only force which causes the flow to spread is the cushion pressure force being released, and it acts normal to the daylight clearance opening. Constant cushion pressure is assumed so a constant velocity vector, V_{l_o}, perpendicular to the duct wall occurs as shown in Fig. 15. When the stern plate is completely closed, that is, touching the surface, flow under the hulls would equal input flow and no air flow would occur under the stern plate (Fig. 14). For this analysis, it must be assumed that an equal flow of air occurs through each square foot of daylight clearance, and that thrust is provided as the flow exits under the stern plate and from the rearward component under the hulls.

FLOW COMPONENT VECTORS

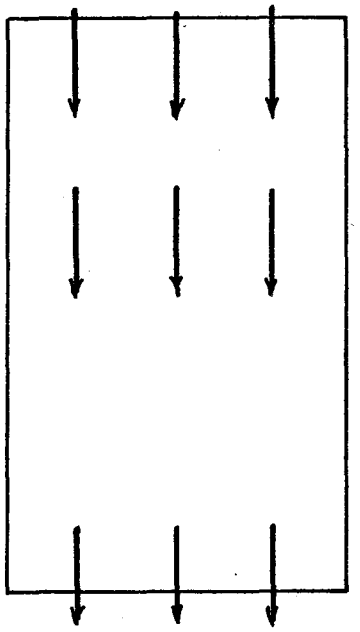

no daylight clearance

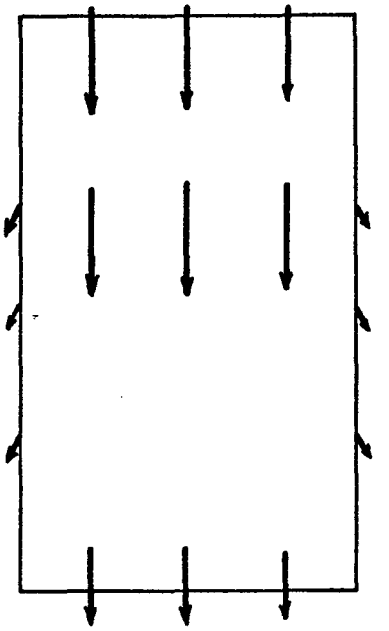

small daylight clearance

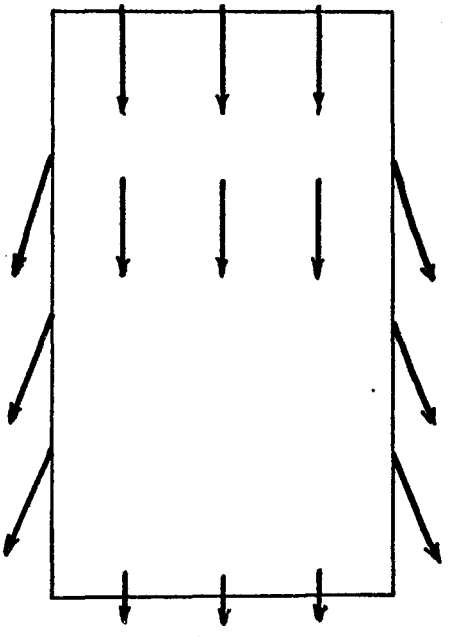

large daylight clearance

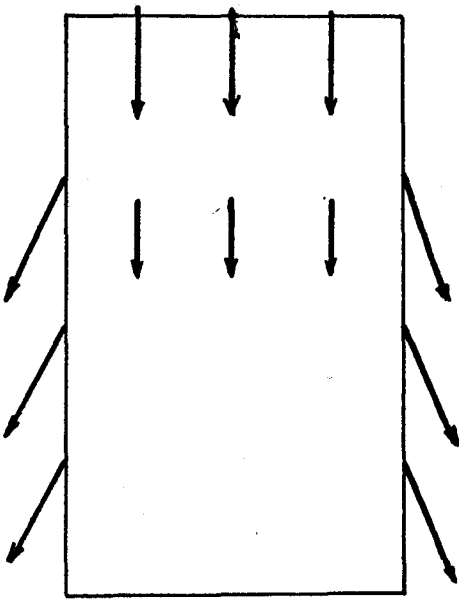

maximum daylight clearance

FLOW COMPONENTS FOR THRUST ANALYSIS

FIG.(14)

Experimentally, the air flow under the hulls did in fact appear to be equal over each unit area, and the cushion pressure was essentially constant over the plan area (Fig. 30).

Considering again the closed stern plate situation, input air flow would all escape under the sidewalls. However the sidewall escape air would still have the rearward velocity vector component it had while in the main duct, and this air flow can still provide usable thrust (Fig. 15). The component of escape air velocity, V_{l_o}, which is perpendicular to the sidewall, is, of course, a total loss.

III.2.3. Thrust Lost Perpendicular to Vehicle Due to Sidewall Escape Air

As stated in Sec. III.2.2, the input air flow (Q_f) equals the air flow exiting under the hulls and under the stern plate; that is,

$$Q_f = Q_l + Q_s \tag{19}$$

The cushion pressure, on exposure to the atmosphere, over the daylight clearance area gives rise to a velocity vector, V_{l_o}, which according to the Bernoulli energy equation is, approximately,

$$V_{l_o} = \sqrt{\frac{2P_c}{\rho}} \tag{6}$$

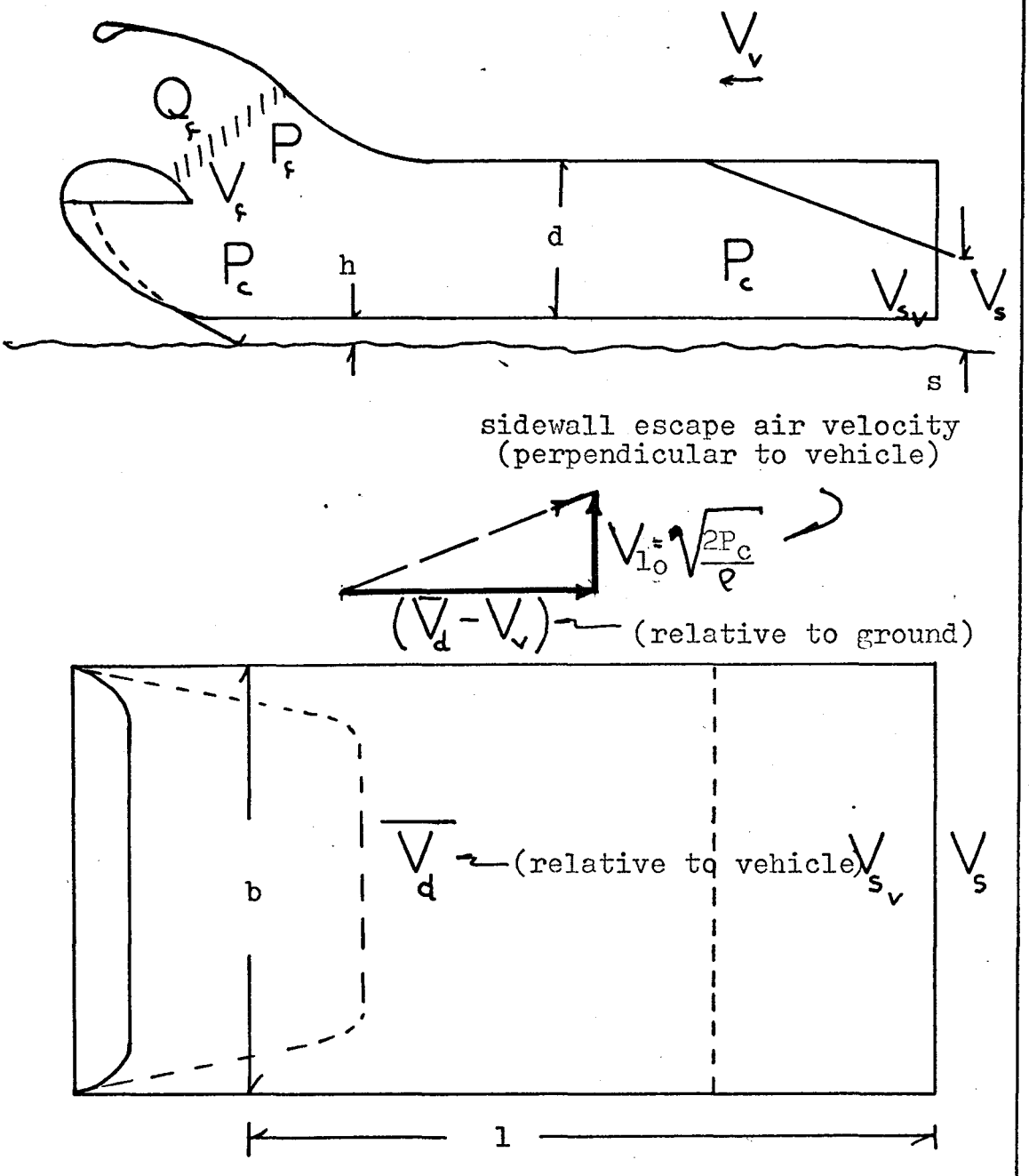

THE THRUST-CUSHION CONCEPT

FIG.(15)

The flow Q_1 with the velocity V_{1_o}, perpendicular to the vehicle sidewalls, causes a thrust T_{1_o} which is useless to the vehicle during level operation; that is, the thrust $T_{1_o}/2$ on one side balances an identical thrust on the other side (Fig. 14). T_{1_o} becomes useful only in control when more flow exits on one side than on the other (see Sec. III.3.4). T_{1_o}, relative to the ground, is then

$$T_{1_o} = Q_1(V_1 - 0)$$

$$= K_1 A_1 V_1^2 \qquad (20)$$

where K_1 = 0.75, an approximation based on a "V" upper edge and a rough flat lower edge to the exit area,

and A_1 = 21h = sidewall daylight clearance exit area,

and $(V_1 - 0)$ = the velocity change in the direction perpendicular to the duct flow.

Substituting and simplifying,

$$T_{1_o} = 31hP_c \qquad (20a)$$

III.2.4 Useful Thrust Parallel to Vehicle Due to Sidewall Escape Air

The flow Q_1 exits at some rearward angle dependent on the cushion pressure, but can be assumed to retain its initial rearward velocity component ($\overline{Vd}$) which the

total flow had within the main ducts. The sidewall escape air Q_l can then supply a thrust useful to vehicle propulsion at the same time it produces the thrust T_{lo}. This useful thrust T_{lr} relative to the ground is given by

$$T_{lr} = K_l A_l V_l (\overline{V_d} - V_v) \tag{21}$$

The same discharge coefficient K_l is used for T_{lo} and T_{lr} as the same quantity of air produces both. The separate thrust components stem from the two velocity vectors inherent in this flow as shown in Fig. 15.

The quantity V_d is the duct velocity relative to the duct at any point in the duct; however, it is not constant as a flow sink occurs along the duct walls. The duct velocity decreases down the length of the duct when constant duct area is assumed. The sidewall air loss is assumed to be linear along the length of the sidewall and $\overline{V_d}$ is taken as the average duct velocity, or the duct velocity at the midpoint between the duct entrance and a point just before the stern plate.

That is

$$\overline{V_d} = \frac{\frac{Q_f}{A_d} + \frac{Q_f - Q_l}{A_d}}{2}$$

$$= \frac{Q_f - \frac{1}{2}Q_l}{A_d}$$

and $$\overline{V_d} = \frac{Q_f - .751h\left(\frac{2P_c}{\rho}\right)^{1/2}}{bd} \qquad (22)$$

Therefore $$T_{l_r} = 1.5\rho 1h\left(\frac{2P_c}{\rho}\right)^{1/2}\left[\frac{Q_f - .751h\left(\frac{2P_c}{\rho}\right)^{1/2}}{bd} - V_v\right] \qquad (21a)$$

For the sake of this analysis, the duct air with its rearward velocity can be described as being pushed out from beneath the sidewalls, essentially unaltered, by the pressure release. This means that $\overline{V_d}$ can be the duct air velocity vector with the ducts, or it can be the rearward velocity vector component of the sidewall escape air.

III.2.5 Thrust Due to Flow Under the Stern Plate

The quantity Q_s is the flow of air which passes under the stern plate. While under the stern plate, the flow Q_s is accelerated from its velocity just before the stern plate V_{d_s}, to a velocity V_s due to the release of the energy stored as cushion pressure.

As before $$Q_s = Q_f - Q_l$$
$$= Q_f - 1.51h\left(\frac{2P_c}{\rho}\right)^{1/2} \qquad (19)$$

Therefore by continuity of flow, the duct velocity just at the duct exit is

$$V_{d_s} = \frac{Q_f - Q_l}{A_d}$$

$$= \frac{Q_f - 1.51h\left(\frac{2P_c}{\rho}\right)^{1/2}}{bd} \qquad (23)$$

where A_d = duct area,

b = duct width,

and d = duct height

By the Bernoulli energy equation taken inside and outside the duct,

$$V_s = \left(V_{d_s}^2 + \frac{2P_c}{\rho}\right)^{1/2} \qquad (24)$$

Therefore the thrust derived from the flow under the stern plate, relative to the ground, is

$$T_s = \rho Q_s(V_s - V_v) \qquad (25)$$

and substituting the above into equation (25),

$$T_s = \rho\left[Q_f - 1.51h\left(\frac{2P_c}{\rho}\right)^{1/2}\right] X$$

$$\left\{\left(\left[\frac{Q_f - 1.51h\left(\frac{2P_c}{\rho}\right)^{1/2}}{bd}\right]^2 + \frac{2P_c}{\rho}\right)^{1/2} - V_v\right\} \qquad (25a)$$

Note that the stern plate setting s does not appear in this equation.

III.2.6 An Examination of the Thrust Parameters

Thrust useful to the vehicle for propulsion T_u is generated by T_{l_r} and T_s; that is,

$$T_u = T_{l_r} + T_s \tag{26}$$

Examination of T_{l_r}, T_s, and the vehicle controls, reveals that

$$T_u = f_1(Q_f, l, h, P_c, b, d, V_v, s, AP)$$

For a particular vehicle, l, b, and d would be set in the original design. The assumption was already made that the input power AP was constant. However, the consequences of setting constant input power and constant cushion pressure are not yet clear. The flow through the fan Q_f will also be constant as shown below.

$$AP = Q_f P_t = K_1$$

But $$P_t = \tfrac{1}{2}\rho V_f^2 + P_c$$

Therefore $$A_f V_f(\tfrac{1}{2}\rho V_f^2 + P_c) = K_1$$

But ρ, A_f and P_c are assumed constant.

Therefore $$V_f(V_f^2 + K_2) = K_3,$$

or $$V_f(\frac{V_f^2}{K_2} + 1) = K_3.$$

hence $$\frac{V_f^3}{K_2} + V_f = K_3$$

that is $$V_f^3 + V_f K_2 = K_4$$

This statement can only be true if $V_f K_2$ gets smaller as V_f^3 gets larger. This is impossible so V_f and hence Q_f will be constant.

Therefore $$T_u = f_2(h, s, V_v) \quad \text{(Fig. 16)}$$

The relationship between the daylight clearance h and the stern plate setting s is perhaps a key in understanding the thrust-cushion concept. In practice, when the driver changes the stern plate setting, the vehicle assumes a new daylight clearance. This implies that h is a function of the stern place setting. To prove that h = f(s), consider the intake power to be divided between the power in the flow exiting under the sidewalls, and the power in the flow exiting at the stern plate. Let the vehicle be stationary. The air power of the sidewall flow could be considered in two components: the power the exit flow had just inside the duct, and the power required to push that flow out perpendicular to the duct walls.

Therefore $$AP = \frac{\rho}{2} \overline{V_d}^2 Q_1 + \frac{\rho}{2} V_{1_o}{}^2 Q_1 + \frac{\rho}{2} V_s{}^2 Q_s \qquad (27)$$

Equation (27) can be rearranged in terms of V_s^2 and an

examination of the factors reveals that

$$V_s = f_3(h)$$

The stern plate setting s has not appeared in any of the previous equations, however

$$Q_s = Q_f - Q_l \tag{19}$$

and by continuity of mass

$$Q_s = A_s V_s$$

$$= sbV_s \tag{28}$$

Combining equations (19) and (30) produces

$$V_s = \frac{Q_f - Q_l}{sb}$$

or

$$= \frac{Q_f - 1.51h\left(\frac{2P_c}{\rho}\right)^{1/2}}{sb} \tag{29}$$

A value for h in the power equation (27) will determine the value for V_s. Substitution of these values for h and V_s into equation (29) will determine the value for s. The stern plate setting is a function of daylight clearance so at one throttle setting,

$$T_u = f_3(s, V_v)$$

Theoretically, an attempt by the driver to force the stern plate to act as a nozzle will only cause the craft to assume a higher daylight clearance. Experimentally, however, the air velocities leaving the stern plate were in the order of two times the duct velocities when an approximate ratio value of 1.4 was predicted by equation (24). The stern plate seems to act, to some degree, as a nozzle.

III.2.7 Thrust Useful for Vehicle Propulsion (T_u)

Useful thrust from the total input power is given by

$$T_u = T_{lr} + T_s$$

$$= 1.5\rho lh\left(\frac{2P_c}{\rho}\right)^{1/2}\left[\frac{Q_f - .75lh\left(\frac{2P_c}{\rho}\right)^{1/2}}{bd} - V_v\right]$$

$$+ \rho\left[Q_f - 1.5lh\left(\frac{2P_c}{\rho}\right)^{1/2}\right]\left\{\left(\left[\frac{Q_f - 1.5lh\left(\frac{2P_c}{\rho}\right)^{1/2}}{bd}\right]^2 + \frac{2P_c}{\rho}\right)^{1/2} - V_v\right\}$$

For the following graphs of this chapter, a hypothetical vehicle with the following design values was used.

Total input air power (constant) = 160 X 550 ft-lb/sec

Cushion dimensions = l X b = 25 ft X 10 ft

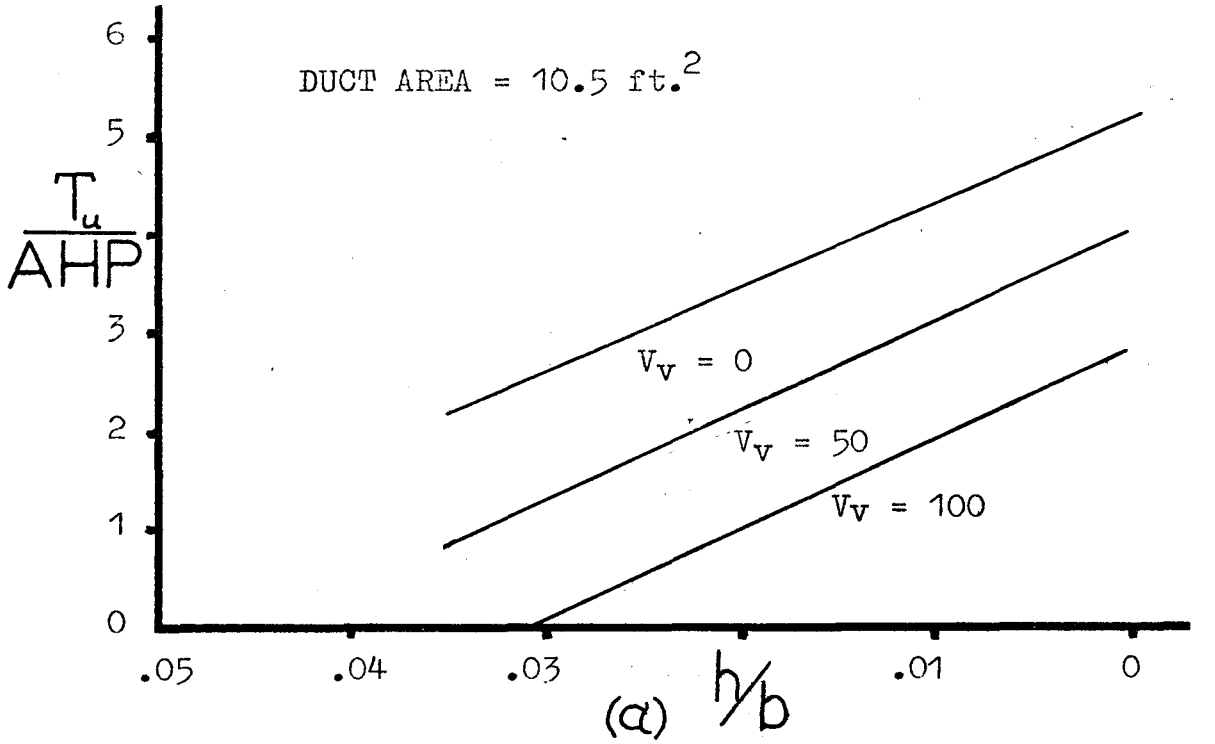

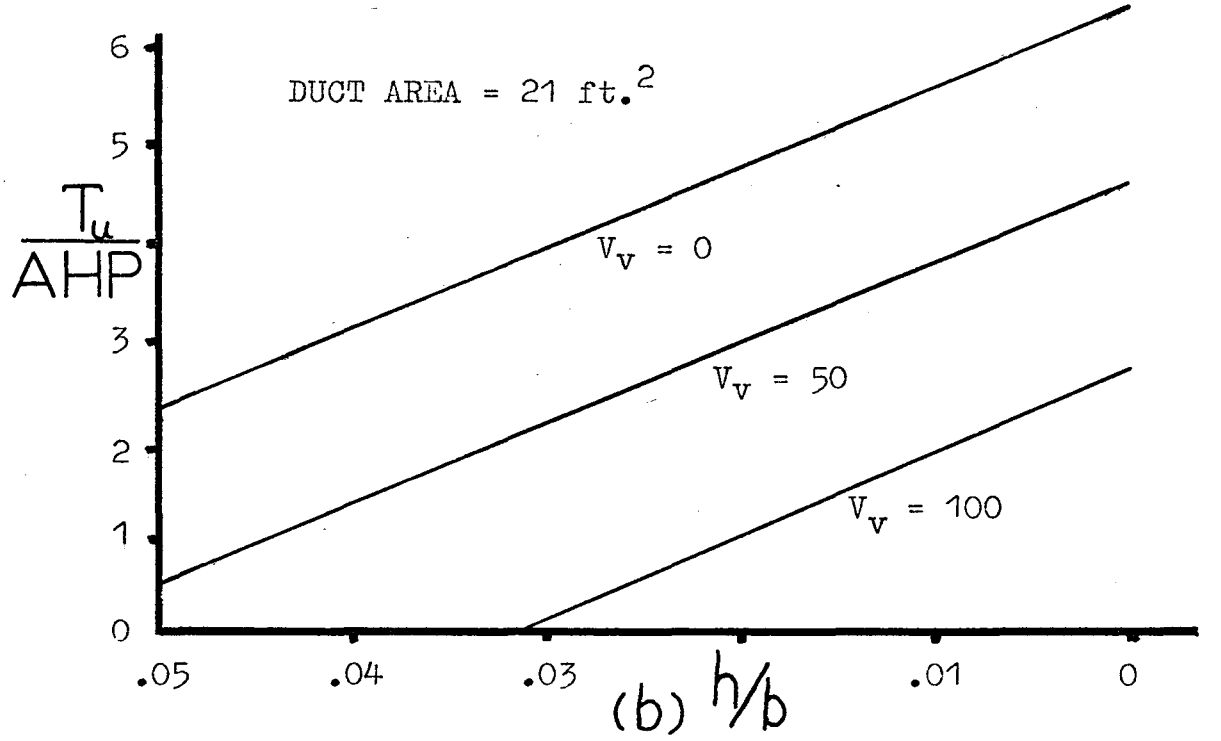

THEORETICAL USEFUL THRUST VERSUS DAYLIGHT CLEARANCE

FIG.(16)

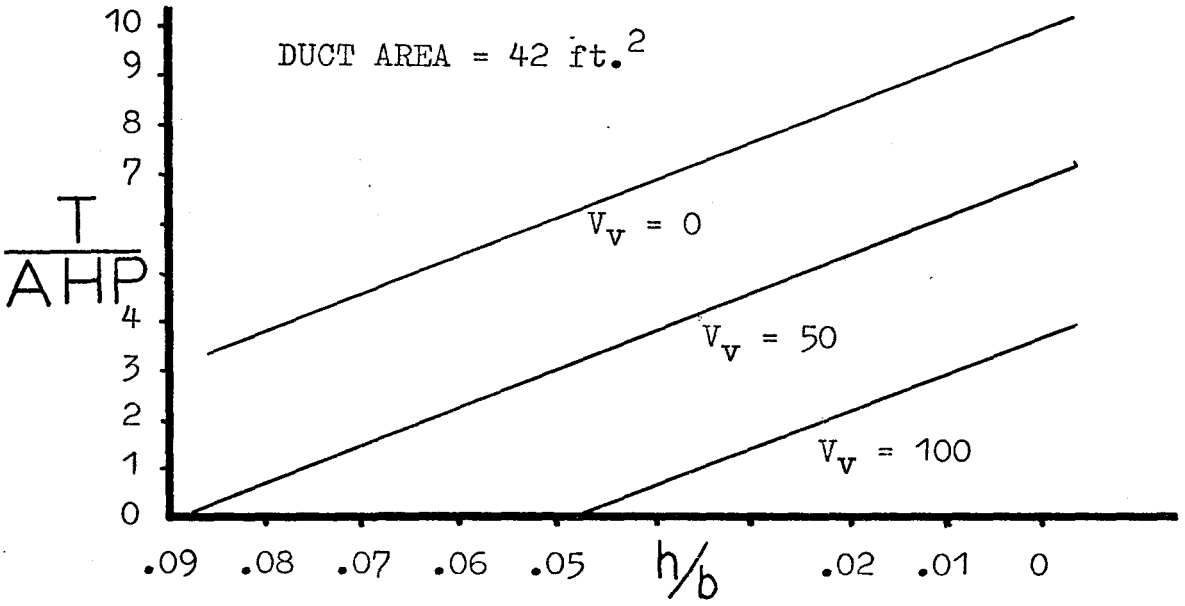

THEORETICAL USEFUL THRUST VERSUS DAYLIGHT CLEARANCE

(a)

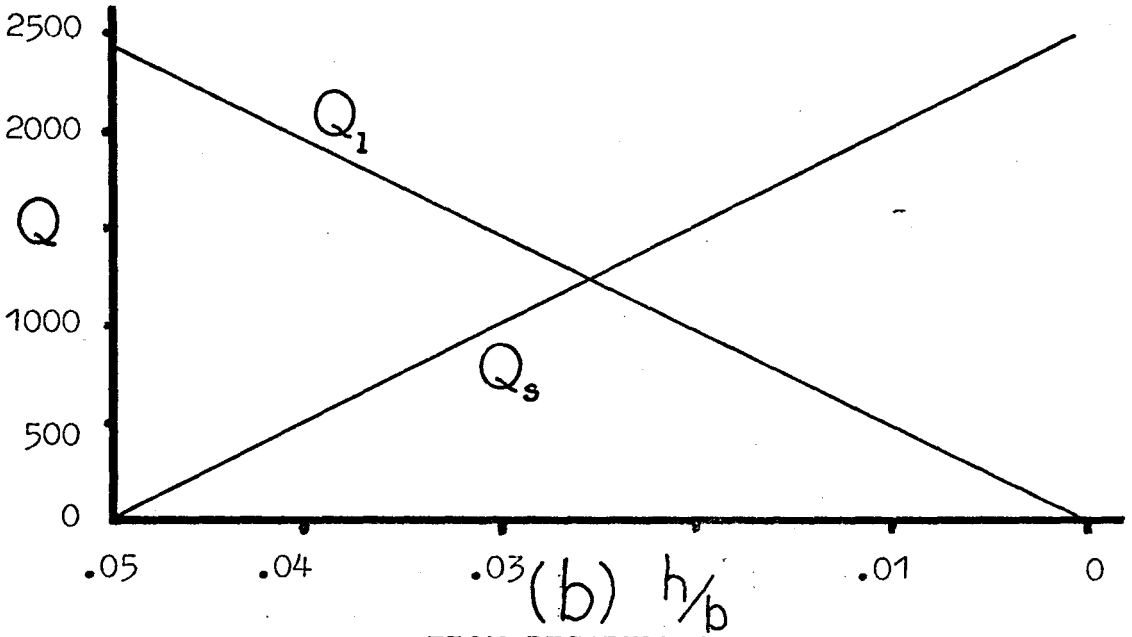

FLOW DISTRIBUTION

FIG.(17)

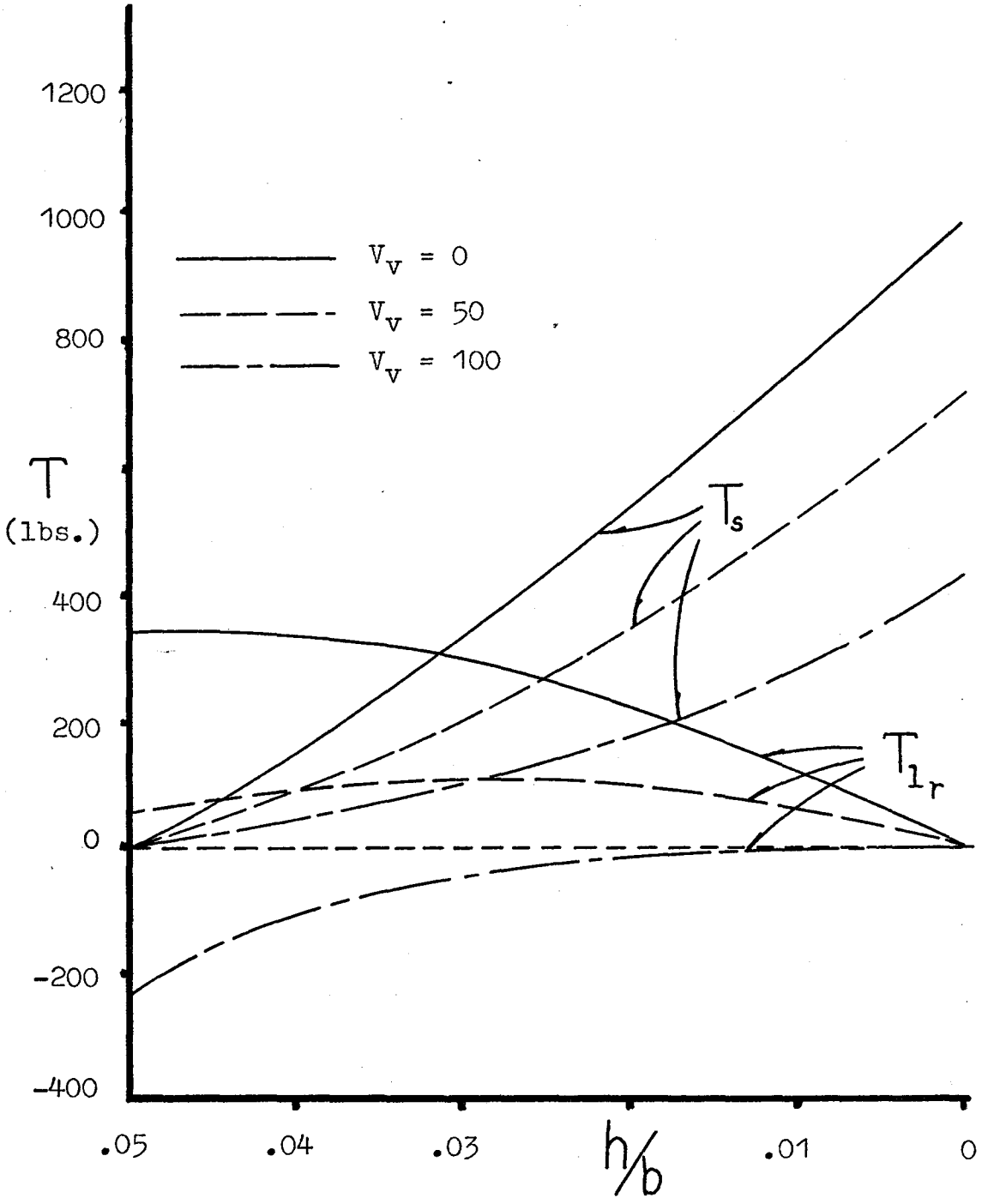

USEFUL THRUST COMPONENTS VERSUS DAYLIGHT CLEARANCE

FIG.(18)

Duct height	=	$d = 3$ ft
Cushion pressure	=	$P_c = 20$ lb/ft^2
Intake area = duct area	=	$A_c = 21$ ft^2
Air density	=	$\rho = .0024$ lb$_m$/ft^3

Intake velocity is therefore 116 feet per second and intake flow is 2440 cubic feet per second. The cushion width was taken as 10 feet for purposes of calculating P_c; however, the available duct area for duct flow is 7 feet due to the presence of the three hulls.

Fig. 16a shows the thrusts developed in the hypothetical vehicle, but with a fan area equal to duct area equal to 10.5 square feet. The graphs of Fig. 16b are for the same vehicle with the same input air horsepower, but with a duct area of 21 square feet; and finally, the graphs of Fig. 17a are for the vehicle with a duct area of 42 square feet.

The duct area has a substantial effect on useful thrust as illustrated in the graphs mentioned above. The thrust increase is due to the large increase in flow possible with the lower velocity heads, as shown in Fig. 19. The reason for the increased thrust with duct area is as follows: the theoretical thrust efficiency of a propeller increases as the velocity change through the propeller decreases; that is

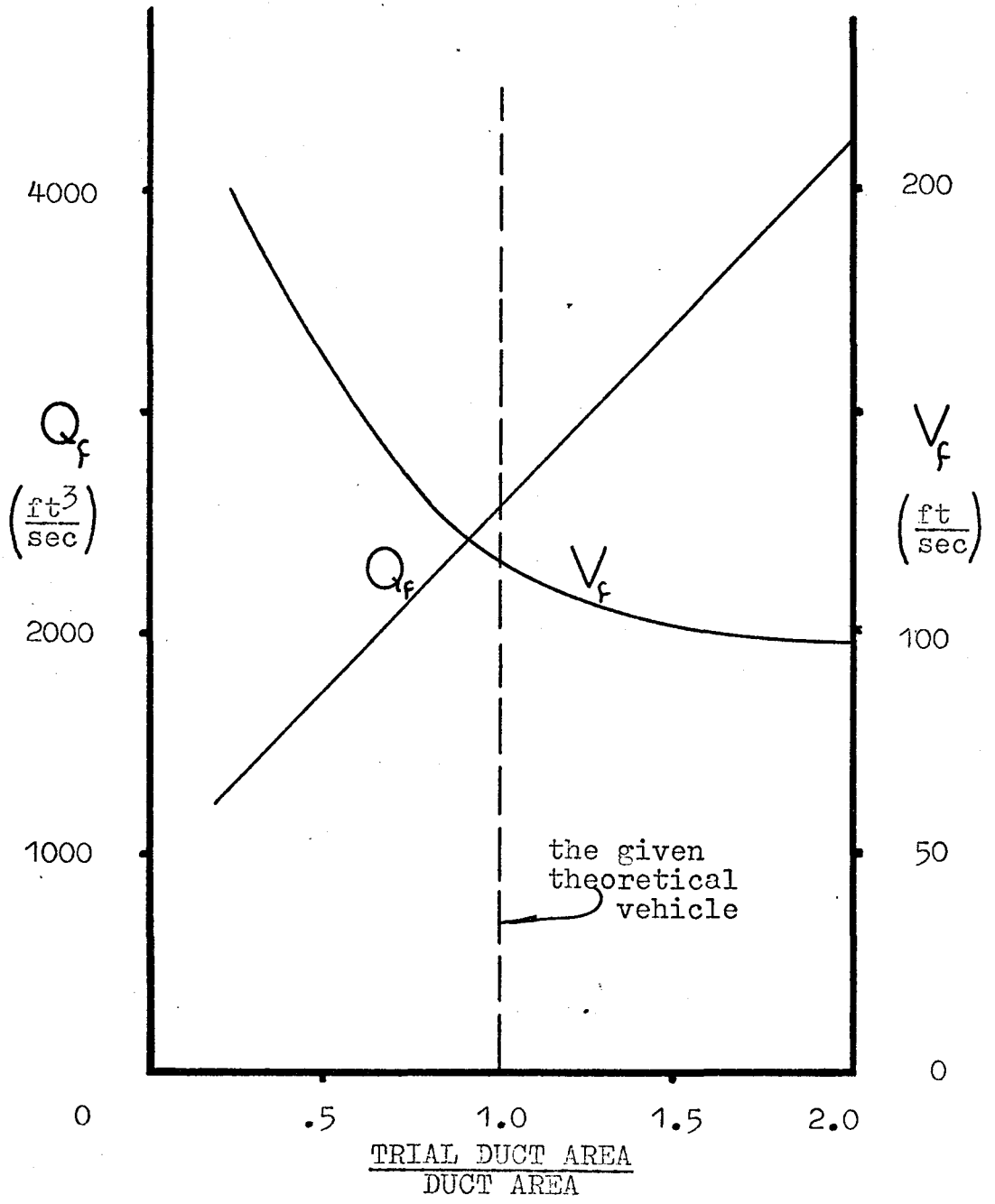

EFFECT OF DUCT AREA ON FAN FLOW AND FAN VELOCITY

FIG.(19)

$$\eta_P = \frac{\text{useful work}}{\text{power input}} = \frac{\rho Q(V_E - V_F)V_F}{\rho \frac{Q}{2}(V_E^2 - V_F^2)} \qquad (30)$$

where V_F = the freestream velocity

V_E = the propeller slipstream velocity

V = the velocity through the propeller

Assuming $V = \frac{V_E + V_F}{2}$

then $\eta_P = \frac{V_F}{V}$ (30a)

In the case of the thrust-cushion, because the cushion pressure is set at 20 pounds per square foot, and because input air power is constant at 160, a low dynamic pressure (velocity) will allow a high flow. The fan air velocity versus duct area is shown in Fig. 19. For the momentum generated, the higher flows overcome the less desirable lower velocity changes. However, as shown in Fig. 18, the useful thrust due to sidewall escape air T_{l_r} can become negative as the velocity change between the duct air and the vehicle velocity becomes negative (Equation 26). The operational effect of this would be to limit daylight clearance potential at speed.

The graphs of Fig. 16 and 17 show predicted useful thrusts, but the theoretical thrusts are deceptively low. This is due to the constant input power assumption.

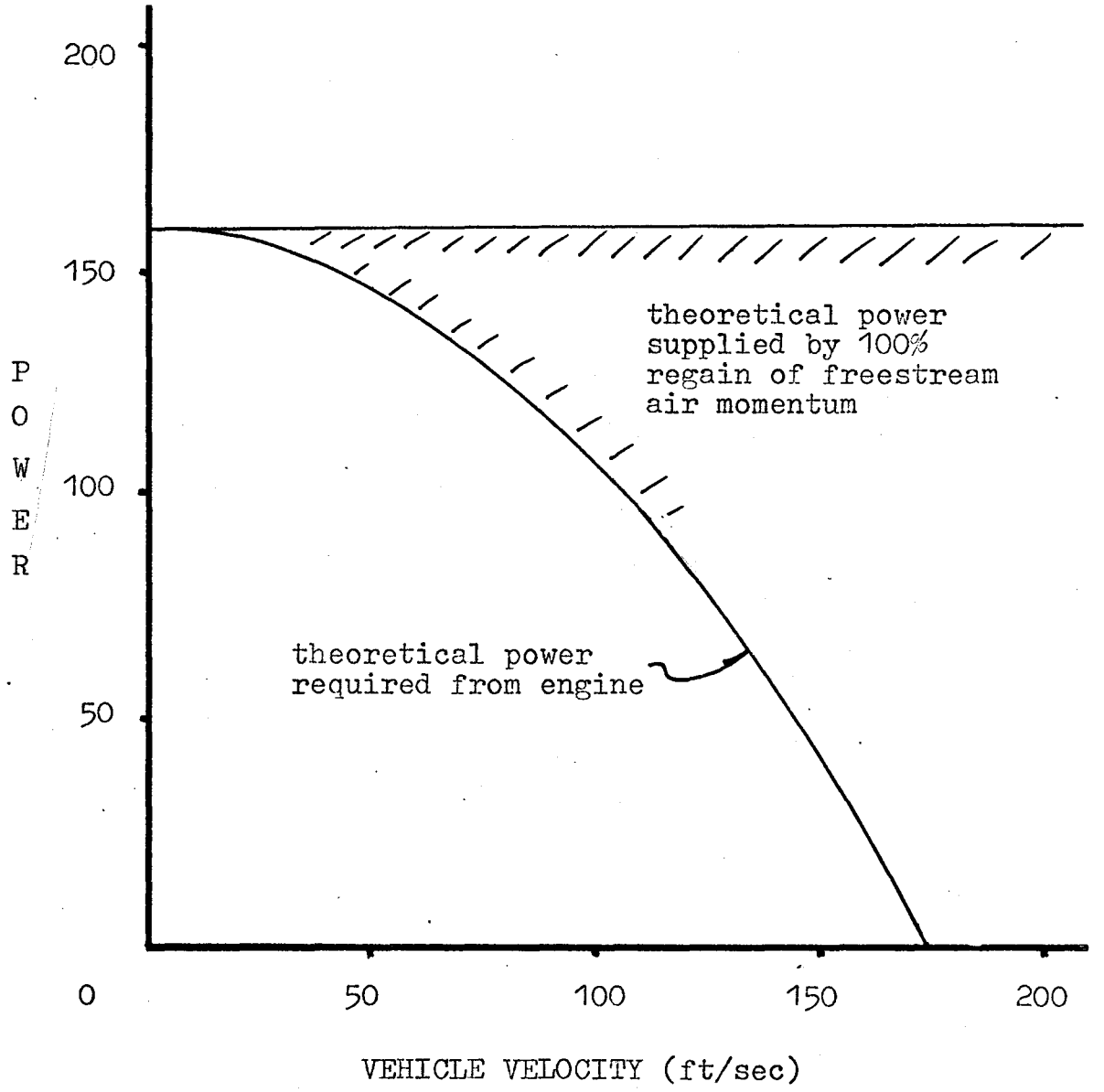

THEORETICAL ENGINE POWER REQUIREMENTS

FIG. (20)

As the vehicle gains speed the freestream air momentum begins to unload the fan. At 50 feet per second, the engine supplies 91 percent of its static power, and at 100 feet per second, the engine supplies only 63 percent of the total power (Fig. 20). In a more sophisticated mathematical model, constant engine power should be assumed so that the freestream air power can allow an increase in thrust at speed as would occur in practice.

III.3.1 Thrust Control and Braking

Thrust is the primary function of input power with secondary control provided by the trading of thrust for daylight clearance.

In practice, an initial power will be required to lift the vehicle by providing the cushion pressure as determined by the vehicle's gross weight. All additional input power is applied toward mass flow for thrust and daylight clearance. As explained in Section III.2, thrust at a given input duct flow stems from two components: the stern plate thrust and the edge-flow thrust. If the input air flow were totally converted to stern plate flow, (zero effective daylight clearance), then maximum thrust would result. As daylight clearance increases, the total thrust is reduced as the edge-flow thrust is not as effective as stern plate thrust, and it reduces more quickly with vehicle speed.

Because thrust is present as soon as lift is generated, the vehicle cannot maintain a static hover without drag brakes or some means of reverse thrust. It is difficult to envisage a real need for a static hover, but positive braking ability will be required for slowing, for emergencies, and for descending slopes. Drag brakes which can be differentially operated will be helpful, and reverse thrust can be achieved by lifting the bow plates or by tilting the vehicle rearward. Of course, touching down on the surface will allow controllable braking without severe decelerations as the hulls will skid or plane on the surface.

III.3.2 Lift and Daylight Clearance Control

Lift is provided by the presence of duct pressure. As soon as the duct pressure is equal to the vehicle weight divided by the effective cushion area, the vehicle becomes fully air supported. Ideally, this could happen with no duct flow, and does happen over water when the stern plate is closed. The stern plates provide the restriction to duct flow to allow the pressure to accumulate. Additional input power provides more air flow as duct pressure cannot increase above lift-off pressure. The vehicle will lift clear of the surface until the exit air, leaving under the hulls and under the stern plate, reaches an equilibrium with the input air. The stern plate

setting determines the portion of input air flow that will exit under the hulls and what portion will exit under the stern plates once the vehicle is fully air supported. The quantity of air that exits under the hulls will determine the daylight clearance. Daylight clearance, then, is a function of air flow.

At one throttle setting, the stern plate affords immediate control over the degree of air support, the daylight clearance, and to some degree the thrust. However, control of each one will affect the others; for example, while the driver has immediate control of the daylight clearance, altering the clearance will change the thrust. The original thrust will have to be restored with the throttle.

III.3.3 Pitch Control (Longitudinal Trim)

Pitch control is achieved by installing the bow plates on a movable track so that the bow plate hingeline can be moved forward or rearward with respect to the vehicle. This action causes the centre of lift to shift relative to the centre of gravity. The vehicle tilts forward when the bow plate is moved rearward.

Pitch control affects five aspects of thrust-cushion vehicle control.

First, a vehicle can be "fine-trimmed" after loading to account for small imbalances, longitudinally and

laterally. Lateral, or roll, trim is possible through differential use of the movable bow plates.

Secondly, a vehicle can be trimmed for static hover or slow speed work. As stated in Section III. 3.1, thrust will always be generated with lift. A rearward tilt, or nose-up trim, would cause a rearward thrust component which will allow the craft to hover statically, at least during part-throttle operations.

Thirdly, for operations over water, a nose-down pitch trim can aid crossing the "hump" (Fig. 41). The slight nose-up attitude present even after the hump can be trimmed out.

Fourthly, high speed operation will undoubtedly cause trim changes as lift forces generate over the vehicle, and these can be balanced.

Fifthly, and perhaps the most important aspect of pitch control, is the effect pitch control has on the vehicle centre of turning. With a level vehicle, the craft will rotate about the centre of pressure which proved best for slow speed operation with the Hövair II. With a nose-down trim, the vehicle tended to rotate about the front of the cushion area for better high speed manoeuvering. Nose-up trim caused the centre of turning to move aft and yaw control response was somewhat slower.

III.3.4 Roll Control

Roll control is the control of the vehicle's attitude on the transverse axis. On the thrust-cushion vehicle, it is effected through differential use of the stern plates. The third, and central hull causes the formation of two ducts under the vehicle. If one stern plate is raised, air flow in that duct exits under the stern plate, and daylight clearance on that side drops. In the extreme, the pressure drops as well and the hull (inside to the corner) contacts the surface. If, at the same time, the other stern plate is closed, the air flow passes under the outside hull and daylight clearance is increased on that side. An overall tilt or roll results in the direction of the open stern plate.

As the thrust is greater from the open stern plate than from the closed one, a yaw moment results to turn the craft away from the direction of roll, but this slight effect is easily corrected with rudders. At the same time, the horizontal component of the lift vector causes a drift in the direction of roll.

Roll control will allow the vehicle to maintain its compass heading on its track; that is, the hulls will be parallel to the direction of travel. Current ACV depend on a yaw angle to allow a transverse component of thrust to hold the vehicle on track during crosswind or sideslope operations. An undesirable reduction in effective

thrust results, as well as an increase in drag.

Primarily, roll control plays a key role in overall vehicle manoeuverability. Trying to turn an ACV at speed without roll control results in tedious, skidding operations with large turning radii. Even very small roll angles shorten the turning radii significantly. On water, very tight turns are possible by allowing the inside hull to "key into" the water surface.

As mentioned in Section III.3.3, roll trim is possible through differential use of the movable bow plates.

III.3.5 Yaw Control

Yaw control is the control of the vehicle heading with respect to the vehicle track. On the thrust-cushion vehicle, as with most ACV , yaw control is attained with air rudders. These are located in the stream of high speed air exiting from the stern plate, in the case of the thrust-cushion vehicle.

Use of yaw control with roll control allows coordinated turns with no side-slipping, and the hulls run parallel to the vehicle track.

During submerged hull operations on water, the air rudders also act as water rudders for positive control at slow speeds. Each rudder is spring-mounted so that, if struck, it will swing up and out of the way.

III.3.6 Stability

Basically, the thrust-cushion configuration is that of a trimaran boat. At rest, or at speed, it is one of the most stable of the marine configurations, as it can tolerate substantial off-centre loadings. Because the hulls tend to be tall and thin, wave passage causes relatively small pitch and roll angles as compared to single, wide-hulled craft. When necessary, the vehicle can be easily towed. At speed, the hard sidewalls provide positive corrections for sudden disruptive forces such as those experienced in waves. Though not yet established, the ratio of sidewall height to beam should be not as critical as the maximum one-sixth ratio demanded for skirted vehicles. The necessity of "hard-structure" near the surface for stability at high speed has been established and all the projected high-speed, transoceanic vehicles have hard-structure next to, or in the surface to provide immediate restoring forces (Sec. I.3).

The necessity of absolutely clearing a wave is overcome by the trimaran's ability to slice through the tops of the waves. Because the bow and stern plates are spring-loaded, a wave or wave top can pass through the ducts with a minimum of resistance. Vertical motions are then reduced by this slicing action.

A secondary beneficial effect is obtained from the spring-loaded stern plates. When a wave passes into the

cushion area, a sudden reduction in cushion air volume occurs. The cushion pressure then increases, and tries to suddenly lift the vehicle higher. A vertical acceseration impulse is experienced by the passengers as a "hard bump" [12]. However, when the cushion pressure increases in the thrust cushion vehicle, the stern plate setting increases momentarily, and the effect of the wave passage becomes a burst of thrust. The thrust-cushion becomes, in effect, a one-way dash-pot.

As mentioned in Section II.4.4, skirted edge-jets of the Saunders-Roe type, can experience "plough-in" and overturn, mainly because the vehicle's thrust line is substantially above the vehicle's drag line [3]. The thrust-cushion vehicles have a thrust centre-line very close to the drag centre-line and the vehicle has a relatively low centre of gravity. It appears that severe moments due to drag or thrust changes cannot occur, at least on the longitudinal axis. If the driver makes a major error in control so that the vehicle ends up sideways to its track, with the leading hull forced into the surface, roll-over could occur. On water, careful hydrodynamic design of the lower surface of the hulls will ensure a smooth planing action. On land, the low centre of gravity and wide beam will temper the overturning tendency, but obstacles could damage the sidewalls.

III.4 Drag Analysis

III.4.1 Analysis Procedure

As mentioned in Sec. III.1, the integrated lift and thrust systems of the thrust-cushion configuration make it impossible to measure drag forces directly as is the current practice with all but the ram wing, WIG, and channel wing concepts. Actual drag component forces will have to be calculated from experimental data taken from a series of controlled experiments. However, the currently accepted drag components of ACV can be described, and their effect upon the thrust-cushion can be postulated.

III.4.2 Internal Drags

Internal drags are all of those drags stemming from the passage of ingested air from intake to exit. Two aspects of internal drag are usually considered; namely, duct efficiency, and momentum drag.

III.4.2.1 Duct Efficiency

Pressure losses due to internal duct flow are calculated under the heading "internal aerodynamics", and are presented as duct efficiencies. Present duct and skirt systems are so complicated aerodynamically that duct efficiently is calculated from measurements taken from either full-size craft or scale models. Duct efficiency for a

given mass flow is usually given by

$$\eta_{duct} = \frac{\text{exit air power}}{\text{input power}} \qquad (31)$$

which would include the conversion of mechanical power to air power. Some calculations (prominent in the 1960's) based duct efficiency on input air power. Exit air power is referred to as nozzle power in the case of edge-jets.

For separated lift and thrust ACV, the lift system power requirements were readily calculated as forward motion was assumed to have negligible effect on lift power (an assumption criticized by E. J. Andrews [13]). As lift power requirements vary to the cube of the air velocity and duct efficiency varies to the square of air velocity, the trend now is to minimize duct air velocities and flow by keeping daylight clearance to a minimum [5]. Higher surface contact drags and higher skirt wear factors are traded for lower lift power requirements.

Based on Equation 31, the duct efficiency of the largest and most developed ACV, the SRN-4, is stated as 0.49, while smaller edge-jet and plenum chamber types range between 0.30 and 0.45. The captured air bubble ACV (CAB) has the least lift power per ton requirements of the current ACV due to their very low mass flows.

For the thrust-cushion configuration, the mass flow for both lift and thrust enters two large ducts which are parallel to the direction of travel.

Theoretically, there can be up to 100 per cent regain of the lift power when there is no air loss along the hulls. The Hovair II and the various thrust-cushion models indicated efficiencies between 0.55 and 0.68 (based on Equation 31) for static operation with no effective daylight clearance. Air power ratios for intake and exit were from 0.77 to 0.83.

III.4.2.2 Momentum Drag (D_m)

The mass of air that is ingested into an ACV lift system must be accelerated from rest to the relative air speed V_r between the prevailing wind and the vehicle. If the intake air is expelled equally in all directions, then the momentum energy gained by the air on ingestion is lost to the vehicle.

The drag force will be in the direction of the relative wind and will act on the intake lip of the lift fan duct. The moment due to the momentum drag force has to be considered in the physical location of the intake lip.

The momentum drag is given by

$$D_m = \rho Q V_r \qquad (32)$$

For ACV that expel lift air equally in all directions, the drag force of this air momentum change must be continually overcome by thrust power.

Momentum drag can be reduced through lower duct air

flows (lower daylight clearance), or by attempts to regain some of the momentum energy given to the air flow; that is, by expelling more air in the rearward direction. Unfortunately, in skirted edge-jets, attempts to expel more air to the rearward causes cushion crossflows which affect cushion stability. Saunders-Roe had hoped for a ten percent regain of this momentum energy but this has been unattainable.

The thrust-cushion, the WIG, the channel wing, and the ram wing have no momentum drag when the craft is moving in the direction of the prevailing wind. These vehicles can be visualized as riding on their own slipstream, and the slipstream is pressurized below the structure to form the cushion. In the thrust-cushion, the free-stream air momentum adds to the duct air energy to reduce engine power requirements (Fig. 18), or adds to the thrust.

When the wind vector is at some angle to the direction of vehicle travel, a momentum drag will occur perpendicular to the thrust-cushion, WIG, channel-wing, or ram-wing equal to

$$D_{m_p} = \rho Q_f V_{w_p} \qquad (33)$$

where V_{w_p} is the wind component perpendicular to the direction of the vehicle's sidewalls. This force D_{m_p} would be considered as part of a sidewind force and would be equalized by a roll angle in the case of the thrust-cushion.

III.4.3 External Drag

External drag encompasses all those drags caused by the vehicle's passage through the air and over the operational surface. This involves profile drag, trim drag, wave-making drag and cushion-shear drag. Drags caused by structural contact are dealt with in Sec. III.4.4.

III.4.3.1 Profile Drag (D_p)

Profile drag is determined by skin friction drag due to the viscosity of the air, and by form drag due to the pressure distribution caused by the vehicle's passage. Because of the overwhelming effect of the form drag, friction drag is usually neglected.

Form drag is traditionally given by

$$D_p = C_d \frac{\rho}{2} S V_r^2 \qquad (34)$$

where C_d is the constant drag coefficient and S is the frontal area.

Ideally, the drag coefficient should be calculated with models having working lift systems as the lift fan affects the pressure distribution around the vehicle, but wind tunnel tests to determine C_d have all been conducted with solid models. The skirted edge-jets had C_d values ranging from 0.25 to 0.60. If the vehicle has some yaw angle to the relative wind, then the C_d can approach 1.0.

The profile drags for the thrust cushion vehicles should be lower than skirted edge-jets or open plenum chambers for four reasons. The first is that it tends to be a more streamlined design. The second is that the air velocity over the vehicle is equal to the vehicle speed as the fan system ingests the bow wave and high speed propellor slipstream. ACV with external thrust fans have air velocities over the vehicle which are higher than the vehicle's speed. The third is due to the effect of the lift air intake on form drag. The present skirted edge-jets have intakes located toward the rear of the vehicle and the effect would be to aggravate the reduced pressure region behind the vehicle. The thrust-cushion's intake is at the very front of the vehicle to reduce the bow wave and the stern exit air would aid the flow of air over the stern. The fourth is the fact that the thrust-cushion will operate a greater percentage of the time with a lower yaw angle to the wind due to its ability to roll on its longitudinal axis.

III.4.3.2 Trim Drag (D_t)

If the vehicle floor is not parallel to the operational surface, a horizontal component of lift force will result. This force can be a drag or a thrust depending on the inclination (β) of the vehicle.

$$D_t = A_c P_c \sin\beta \qquad (35)$$

III.4.3.3 Wavemaking Drag (D_w)

Trim drag is very similar to wavemaking drag. The wavemaking drag results from adverse trim angles caused by a depression in the water surface beneath the supporting air cushion. Statically, the ACV sits in a depression in the surface as does any floating body. As the ACV moves forward, the depression follows it; but with more speed the water does not have a chance to deform due to its inertia. The craft, as it picks up speed, begins to climb up and out of the depression, As it climbs up, a longitudinal trim angle forms equal to the average slope of the depression. The nose-up trim results in a "trim-drag". Once on top of the depression and ahead of it, the trim angle reduces toward zero and wavemaking drag is much reduced. The drag occurring at maximum nose-up trim is called the "hump drag". Wavemaking drag is given by

$$D_w = \frac{2P_c^2 A_c}{l \rho_w g}\left(1 - \cos\frac{gl}{V_v^2}\right)$$

$$= \text{mean wave slope under pressure distribution} \qquad (36)$$

where ρ_w = the density of the water

g = gravity constant

This relationship is given in Fig. 21, and ρ_w, g, and w were considered constant. The pressure distribution was assumed to be rectangular.

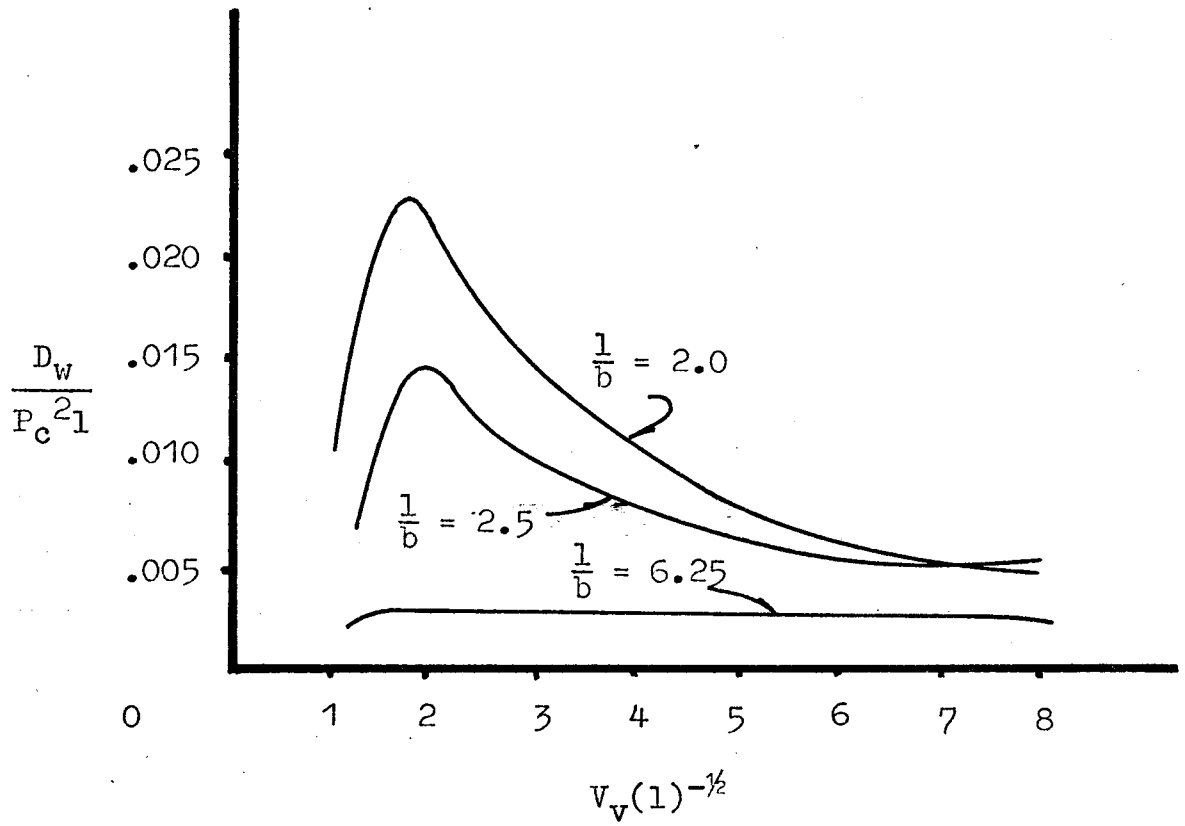

WAVEMAKING DRAG COEFFICIENT VERSUS LENGTH/SPEED RATIO

FIG.(21)

The wavemaking drag will affect the thrust-cushion as it will any other fully air-supported ACV, but the ability of the thrust-cushion to obtain some buoyancy and planing support through the critical hump speed will temper this peak drag somewhat. Also the trim angle is readily adjustable and a nose-down trim would not substantially increase drag or reduce stability while the "hump" is negotiated.

III.4.3.4 Cushion Shear Drag (D_S)

Plenum chamber and edge-jet ACV all suffer a cushion shear force as the vehicle's cushion is swept over the operational surface. The aerodynamics of cushion shear are very complicated over an irregular surface, and usually either some experimental estimate is made for D_S, or it is combined with some other drag, usually wetting drag, or overland drag (Sec. III.4.4.1; III.4.4.2). M. Bertain of Bertain et Cie has stated that cushion shear from his open plenum chambers can be thirty percent of total drag when operating under the worst shear drag conditions.

If, however, the cushion air has an overall rearward component as is the case with thrust-cushions, WIG, and channel-wings, the relative velocity of the cushion air to the surface is reduced and it is possible to have no cushion shear at the surface at all (Fig. 22). Perhaps optimum cruise conditions for the thrust-cushion include

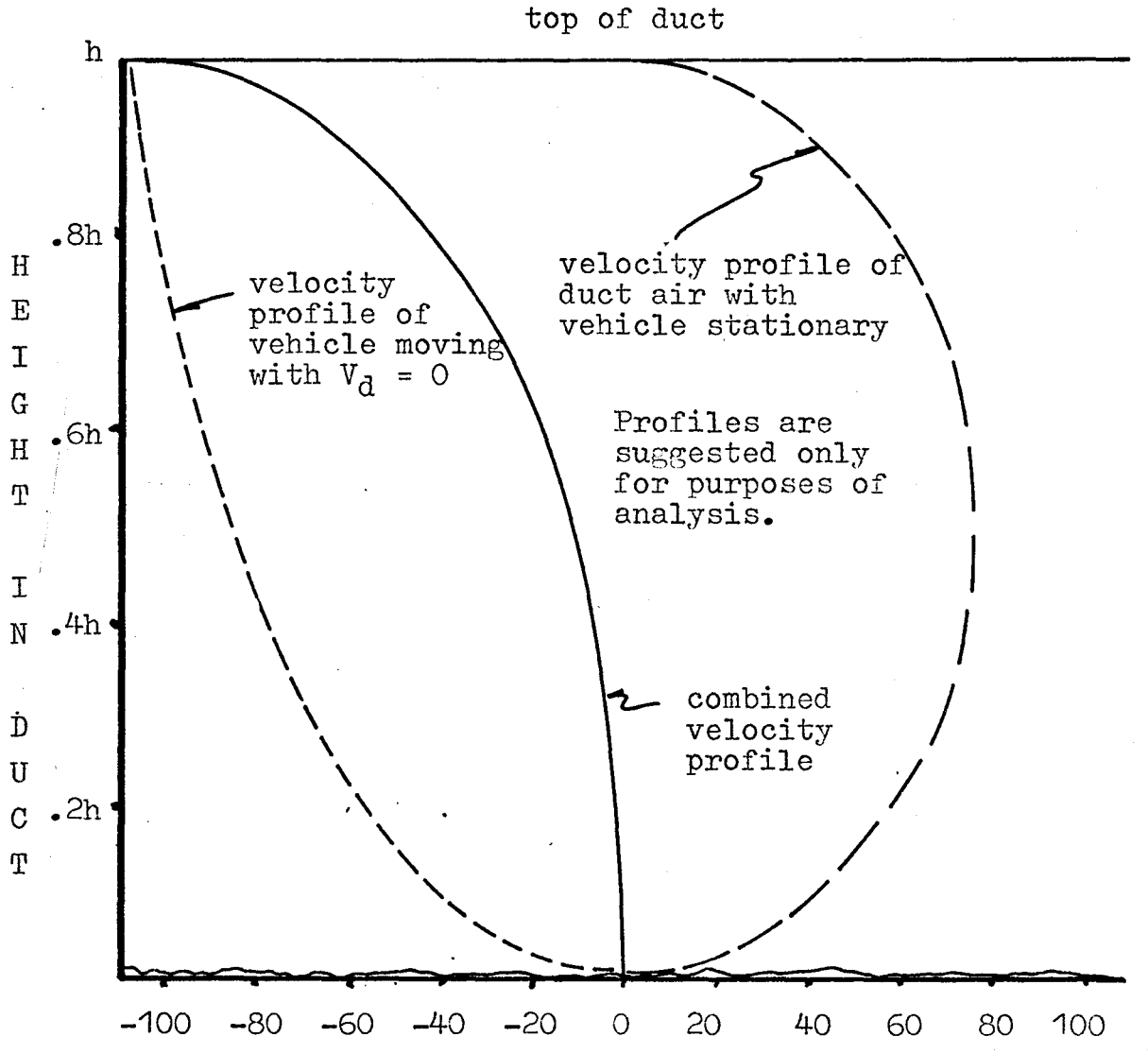

DUCT AIR VELOCITY (RELATIVE TO GROUND) VERSUS HEIGHT IN DUCT

FIG.(22)

a vehicle speed equal to the duct air speed. A minimum air velocity under the hulls also results in minimized spray.

III.4.4 Surface Contact Drag

III.4.4.1 Ground and Snow Contact

Overland contact drags will have to be empirically calculated for each vehicle and each terrain. However, if no surface dislocations occur, the coefficient of friction should be independent of speed and approximate drags could be calculated for simulated contact frequencies and intensities.

Surface friction can be reduced by minimizing the contact areas, and by using low friction materials where contact will take place. Any transverse barriers will have to be designed to prevent snagging and, if possible, be spring loaded to ensure small forces holding them in place.

III.4.4.2 Wetting Drag (D_e)

As an ACV operates over water, spray is generated under the cushion and some of it lands on the vehicle itself. This mass of water can be considerable, and it must be accelerated to the vehicle speed. The energy needed to accelerate this mass of water is lost as wetting drag. The drag varies greatly with the type of ACV and the skirt de-

sign. A skirted edge-jet with segmented fingers is affected worst as the high speed nozzle air generates large quantities of spray. One formula is given by Stanton-Jones[14] for skirted craft as

$$D_e = 2 \times 10^{-6} P_c S_c \frac{1}{h} V_v \qquad (37)$$

where S_c is the cushion perimeter length.

Another approach to wetting drag is to measure the acutal drag over calm water and subtract the drag components listed above. This form of wetting drag would include some contact drag as well as the drag of any projections in the surface of the water. On sidewall craft it would include the drag of immersed hulls. Fig. 23 shows the effect of daylight clearance and speed on wetting drag of skirted ACV as obtained by the subtraction method.

In comparison, the thrust-cushion should have a small wetting drag as air velocities near the surface are relatively small (Sec. III.3.3.4). However, spray will be generated by the piercing action of the hulls into wave tops. The hulls will have to be designed to keep hard structure out of the path of the primary spray patterns. Spray generated under the stern plate should not have an opportunity to land on hard structure.

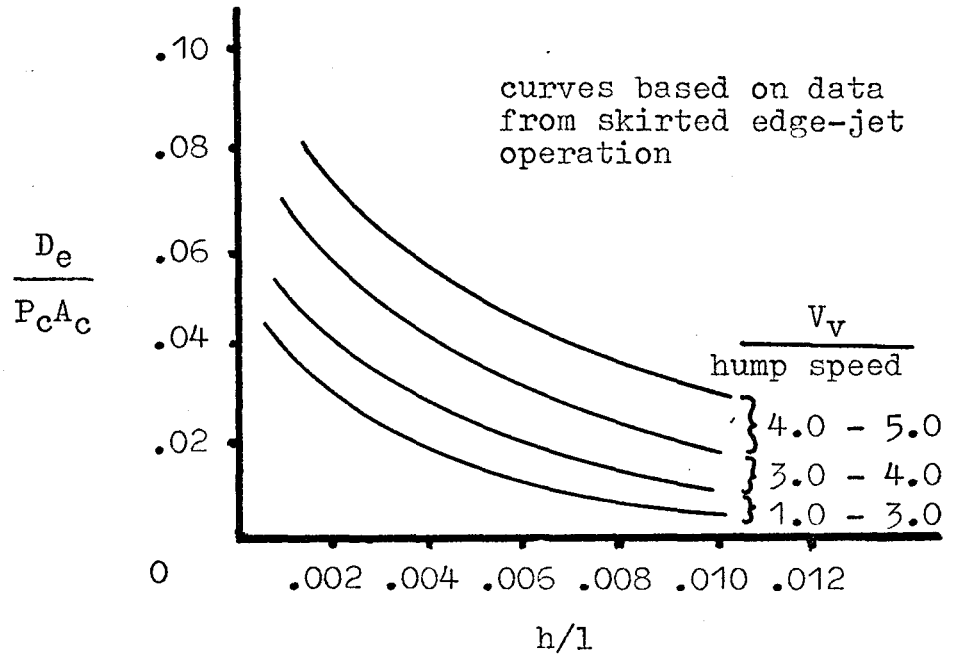

WETTING DRAG VERSUS DAYLIGHT CLEARANCE AND SPEED

FIG.(23)

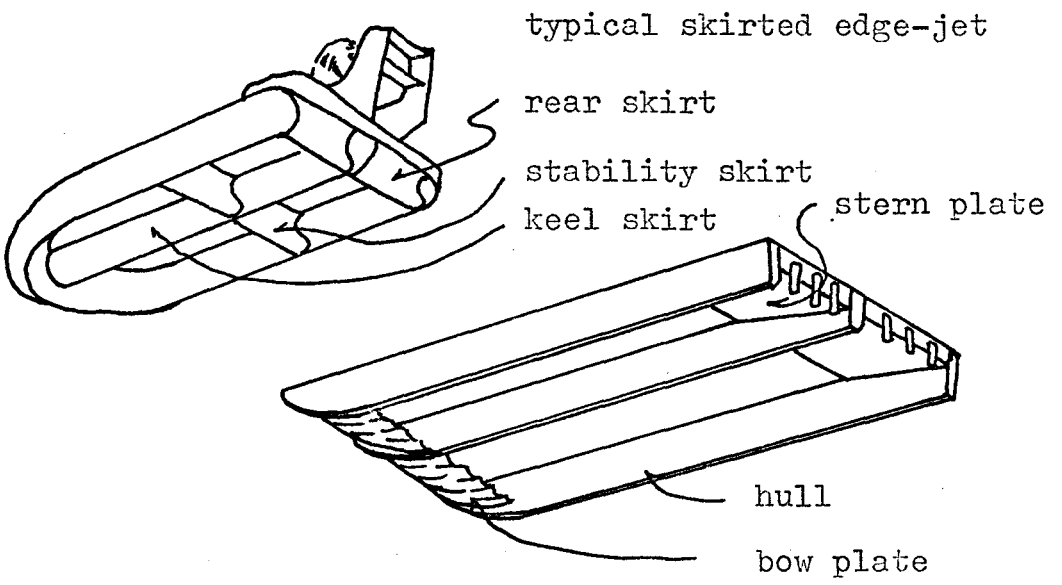

WATER PENETRATION DRAG CONSIDERATIONS

FIG.(24)

III.4.4.3 Water Penetration Drag (D_d)

Water penetration by any vehicle at speeds above approximately forty knots involve very substantial loadings and drags. The drag takes the form of friction drag and pressure drag.

Frictional drag, drag due to the viscosity of water on the wetted area, is given by

$$D_{df} = C_f \frac{\rho_w}{2} S V_v^2 \qquad (38)$$

where C_f is a function of the flow Reynolds number and is given by

$$C_f = 0.4631(\log R_n)^{-2.6} \qquad [15] \qquad (39)$$

Pressure drag is quite variable with design, but the maximum pressures in pounds per square inch for high speed planing craft can be calculated by

$$P_p = (2.151 V_v^2 + 1.267 V_v \, l + 16.8841)\ 144.55 \qquad (40)$$

Once P_p is calculated, the pressure drag would be calculated as the horizontal and longitudinal component of the pressure forces.

However, Equation (40) was intended for high speed planing craft dependent on hydrodynamic support. Also, when the lower surfaces are flexible and the contact areas are variable, as is the case with skirted ACV , the theoretical calculations of D_d become unreliable.

Usually D_d is calculated by simply measuring a particular wave state drag and subtracting from it the calm water drag. Each vehicle design would have its own particular D_d curves for speed and cushion pressure. However, for undetermined reasons, the prediction of drag due to waves for skirted edge-jets seems to have been badly underestimated. The SRN-4 was expected to have a block service speed of 70 to 80 knots. The average block speed, in service, was just under 40 knots, and the discrepancy was attributed to wave impacts. Fig.24 illustrates a skirted edge-jet lower surface. The skirts are flexible but substantial forces are still required to cause them to deflect.

Because the transverse bow and stern plates require only small downward forces to hold them in place on the thrust-cushion, form drag from them would be negligible and viscous drag can be minimized by minimizing the contact area. The hulls will require careful hydrodynamic design to reduce the piercing forces.

When the thrust-cushion is operating at zero effective daylight clearance, viscous drag should be lessened by a thin film of air exiting under the hulls. Testing will have to determine the extent of this "anti-friction" potential.

CHAPTER IV

THE EXPERIMENTAL ANALYSIS

IV.1 The Purpose and the Approach

The major purposes of the experimental program were as follows:

(i) to make some measure of duct efficiency both statically and dynamically.

(ii) to determine plan view pressure distributions at the surface and at the floor level both statically and dynamically.

(iii) to determine the thrust per input air horsepower of the tethered model (described in Sec. IV.4) over various surfaces at various daylight clearances.

(iv) to measure the speeds attained by the model at various gross weights per input air horsepower at different daylight clearances.

A three-step program which involved instrument calibration, static model tests for parts (i) and (ii), and tethered model tests, was carried out. When possible, the separate drag components or groups of components (Sec. III.3) were determined. The various daylight clearances were set by different stern plate openings.

IV.1.1 Discussion of the Experimental Intents

Because the dynamic model (Fig.32) was on loan from Hovair Ltd., a minimum of handling and alterations was desirable. Also, the model was relatively heavy for its cushion area when the test equipment was added, so a static model program was designed around an aluminum duplicate of the test model's duct system (Fig.26). The test duct eased the demands on the model, and, because of its light weight, permitted a wider range of cushion pressures.

An instrument package was built during the calibration program, and was used as a unit in the static and tethered models. The critical element of the instrument package was the Scanivalve described below. The test program was designed to allow ample familiarity with the valve before attempts were made to measure the complicated aerodynamics of the moving model.

The original plan was to carry out a more extensive program of testing on various surfaces such as asphalt, gravel, grass, water, ice and snow, at various daylight clearances, but the program had to be reduced because of a lack of time.

The Scanivalve proved to be an intricate and temperamental instrument which required constant adjustment and care, even after the long instrument calibration program. Two breakdowns of the tethered model's drive

chain, and one signal generator failure, caused substantial delays in testing. As a result, tethered model tests were carried out over grass surfaces only. Also, the pressure distributions for the floor and surface level became approximately floor and surface levels as they were taken by static head traverses one-half inch from each level.

IV. 2 Description and Calibration of the Instruments

The instrument package was centred around the Scanivalve 48D3S/N453 . This instrument was capable of taking forty-eight pressure readings in succession, in approximately four seconds. The individual pressures were exposed to the pressure transducer (SN437±.2psi) by means of a lapped-plate assembly. A signal generator (SCANCO POC A3) delivered a refined signal to the transducer. The transducer was deformed by the pressure unbalancing the bridge, and the carrier signal was altered. The modified signal was then returned to the signal generator where the modification was amplified and sent to the recorder. The recorder used throughout the test program was a single channel, portable Sanborn 300. It is possible to feed the signal generator output onto a magnetic tape, transfer this to a special one-half inch tape, and then have the readings punched directly onto data cards. This was not attempted as the equipment required constant monitoring and checking with the visual tape output.

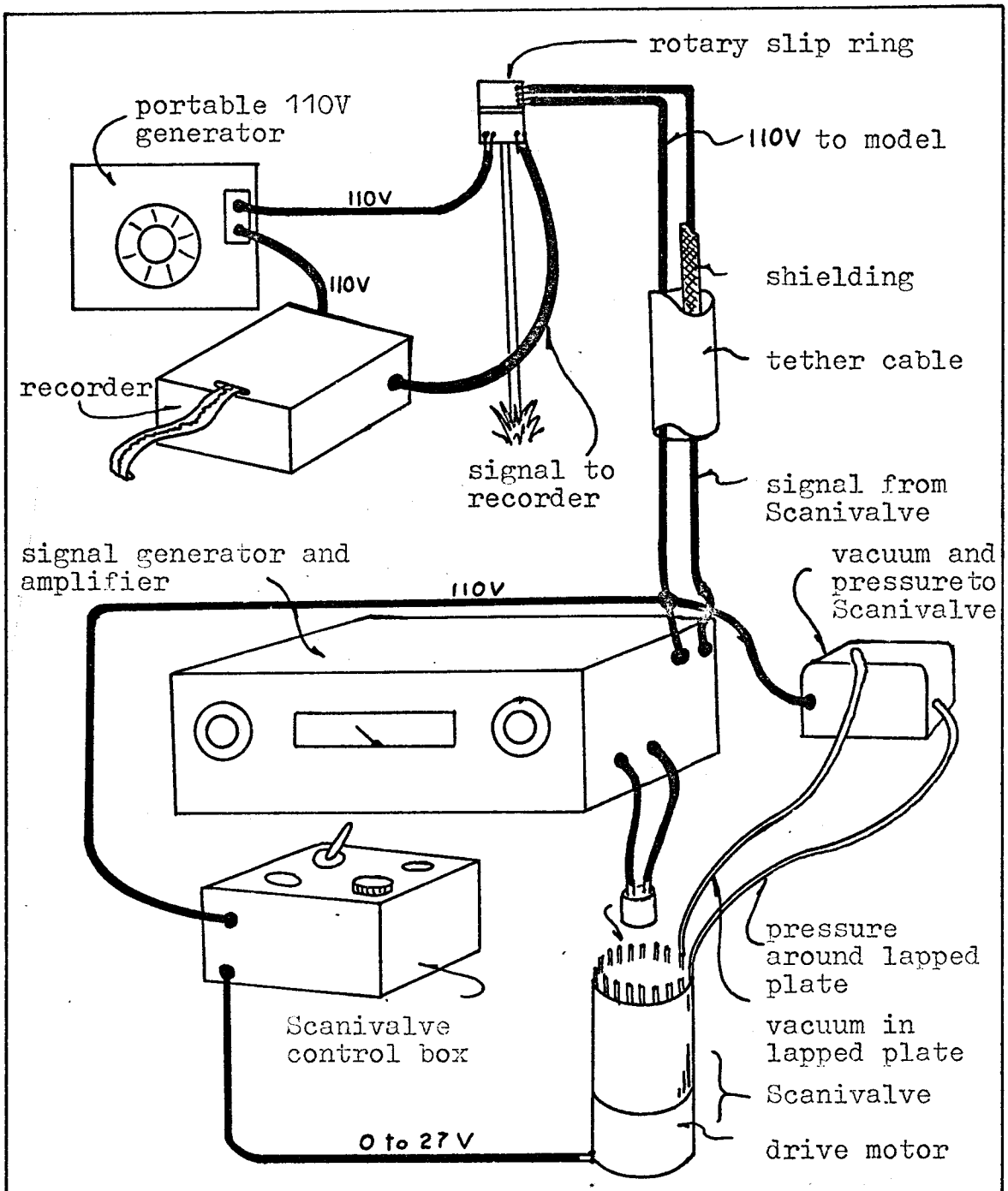

INSTRUMENT LAYOUT

FIG.(25)

The Scanivalve was attached to a forty-eight tube water manometer bank to test for output linearity and variability. The proper head of water (increments from zero to two inches) had to be carefully injected into each tube so that an air "buffer" remained between the water and the valve. Unfortunately, each time a tube was exposed to the transducer, a quantity of air was released from that tube as the lapped plate proceeded to the next tube. The carefully injected water gradually sank to the bend of each tube, and the pressure source was ruined. Longer tubes resulted in some of the water "plugs" breaking down and draining to the bottom.

A new water manometer bank was made with long individual tubes running horizontally from a large water reservoir. The Scanivalve could then be run with accurate pressure sources until the water reached the end of the horizontal section.

The instruments gave acceptable linear output from zero to two inches of water with two percent variation from one peak to its corresponding peak. However, the valve could only run for four minutes at a time. Use of the valve on the static model for longer periods of time caused the buildup of residual pressures around the lapped plate which superimposed the lower one-third of the range. It was necessary to attach a vacuum system (12 inches of water was sufficient) to the lapped-plate chamber to clear this out.

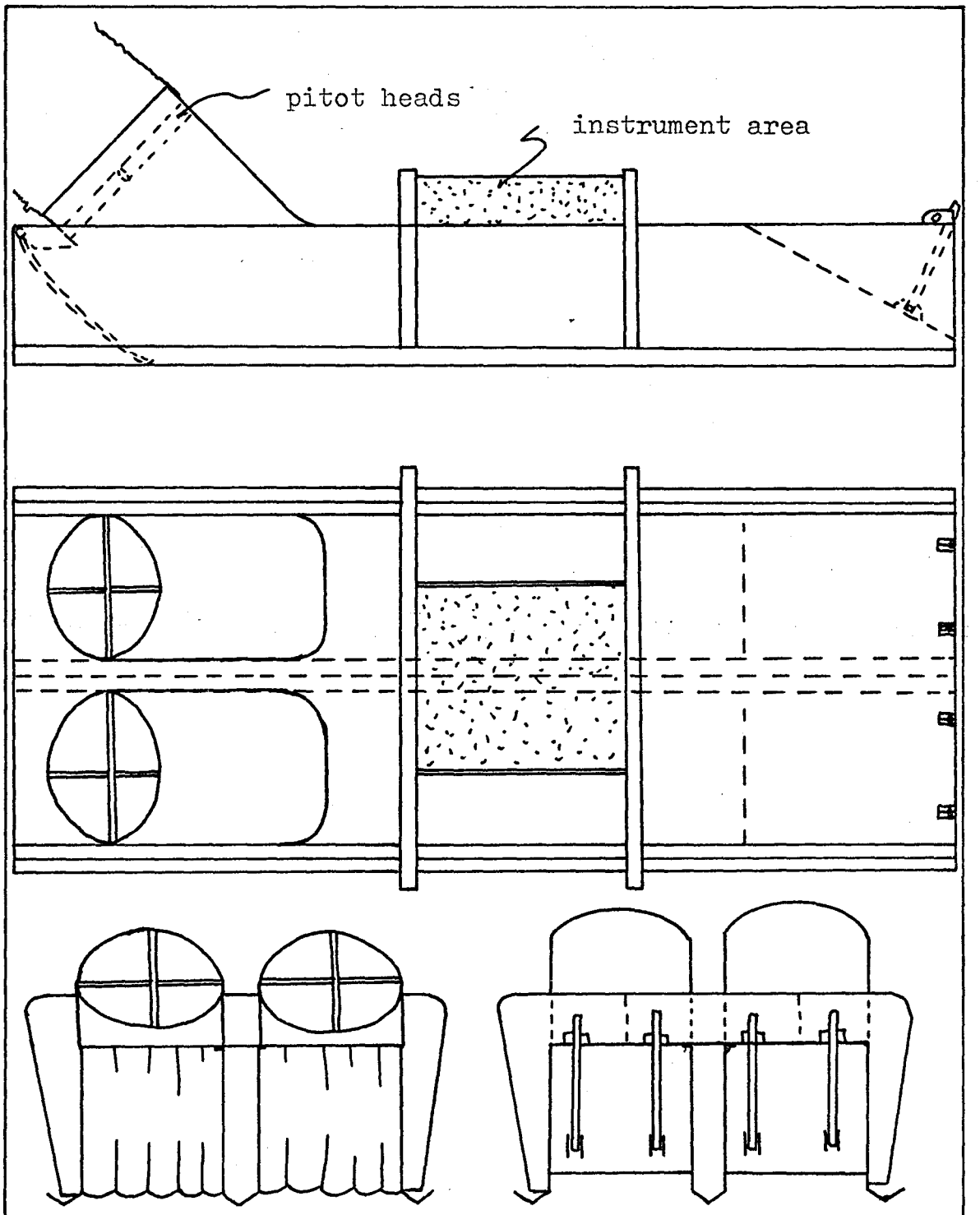

THE STATIC MODEL

FIG.(26)

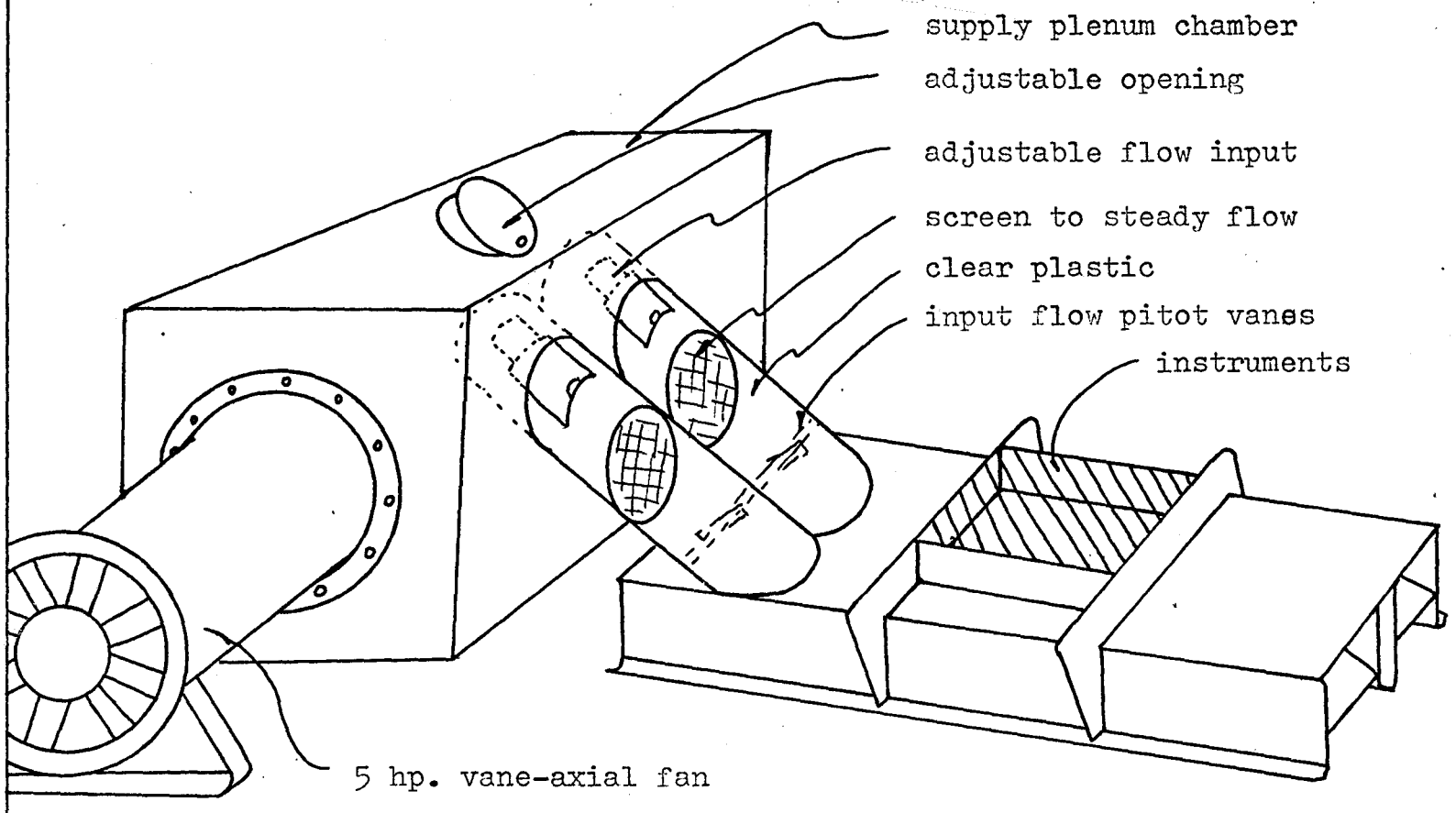

STATIC MODEL ARRANGEMENT

FIG.(27)

This vacuum system was used for all further testing. It became clear that each test run and instrument setting was going to produce a unique output range on the tape. The instrument package would have to include at least two test heads to provide a predictable high and low reading to calibrate each set of readings for each plate rotation. All further tests contained one one-inch and one two-inch head of water. Unfortunately, a deterioration of output quality occurred in proceeding from the water manometer to the static model (three to six percent variation), to the tethered model assembly (eight to fourteen percent variation on both the total and static heads). Perhaps much of the variation, at least on the tethered model, was die to the variability of the air flow itself. The measures for input air horsepower, taken directly below the fans, were particularly bad.

IV. 3. The Static Model

IV.3.1 The Equipment Arrangement

An aluminum duplicate of the duct system of the tethered model (Fig. 27) had air supplied to it from a 3' X 4' X 2' closed plenum box which was supplied in turn by a five horsepower vane-axial fan system. The plenum box had two portholes with covers which could be adjusted to alter the static pressure within the chamber. The model

air intakes were positioned ninety degrees to the vane-axial fan in an attempt to supply the model with the steadier static head energy. The model intake ducts had adjustable openings to control the flow to the model and each duct had a fine screen cover to help steady the flow (Fig. 27).

IV.3.2 Input Air Power Results

Each static model intake duct was fitted with two streamline bars containing static and total head measuring tubes. The bars were positioned as they would appear in the tethered model.

The first tests were designed to measure the input air power of the static model in preparation for air power measurement of the tethered model. Initially, forty of the available Scanivalve lines were installed for a twenty point pitot traverse of one duct. The duct was divided into five equal annular areas, each of which contained four static and four total head sources. The data collected above was to provide an accurate base upon which alternate air horsepower measurements could be compared.

Subsequent air power measurements based upon ten, and finally six, pitot point traverses gave essentially the same results as the twenty point traverse. Stern plate setting had no measurable effect on input air power. Fig. 28 gives the static and total heads in inches of water for the static model. Input air horsepower averaged to 1.12 as

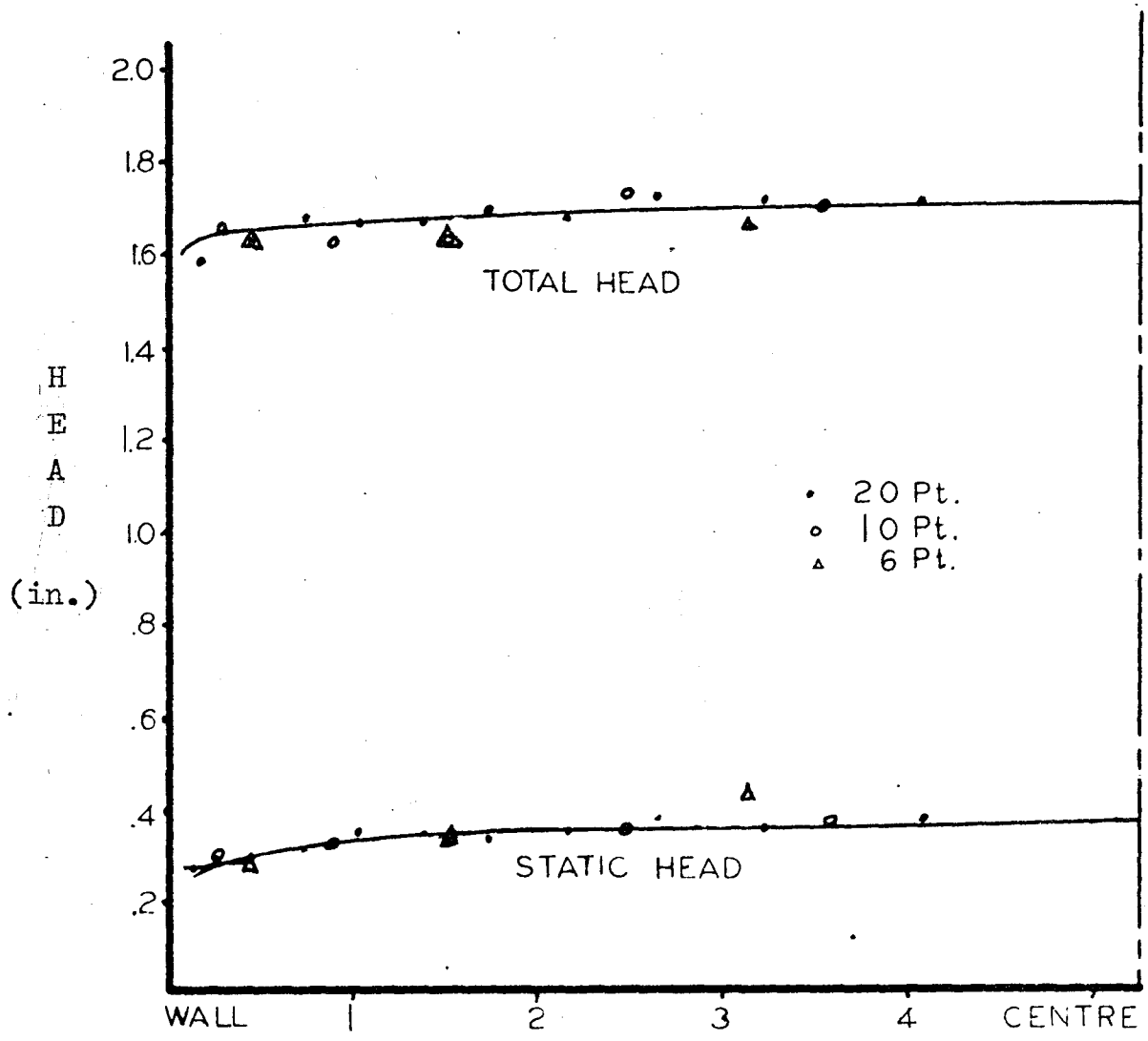

STATIC MODEL INLET DUCT HEADS

FIG. (28)

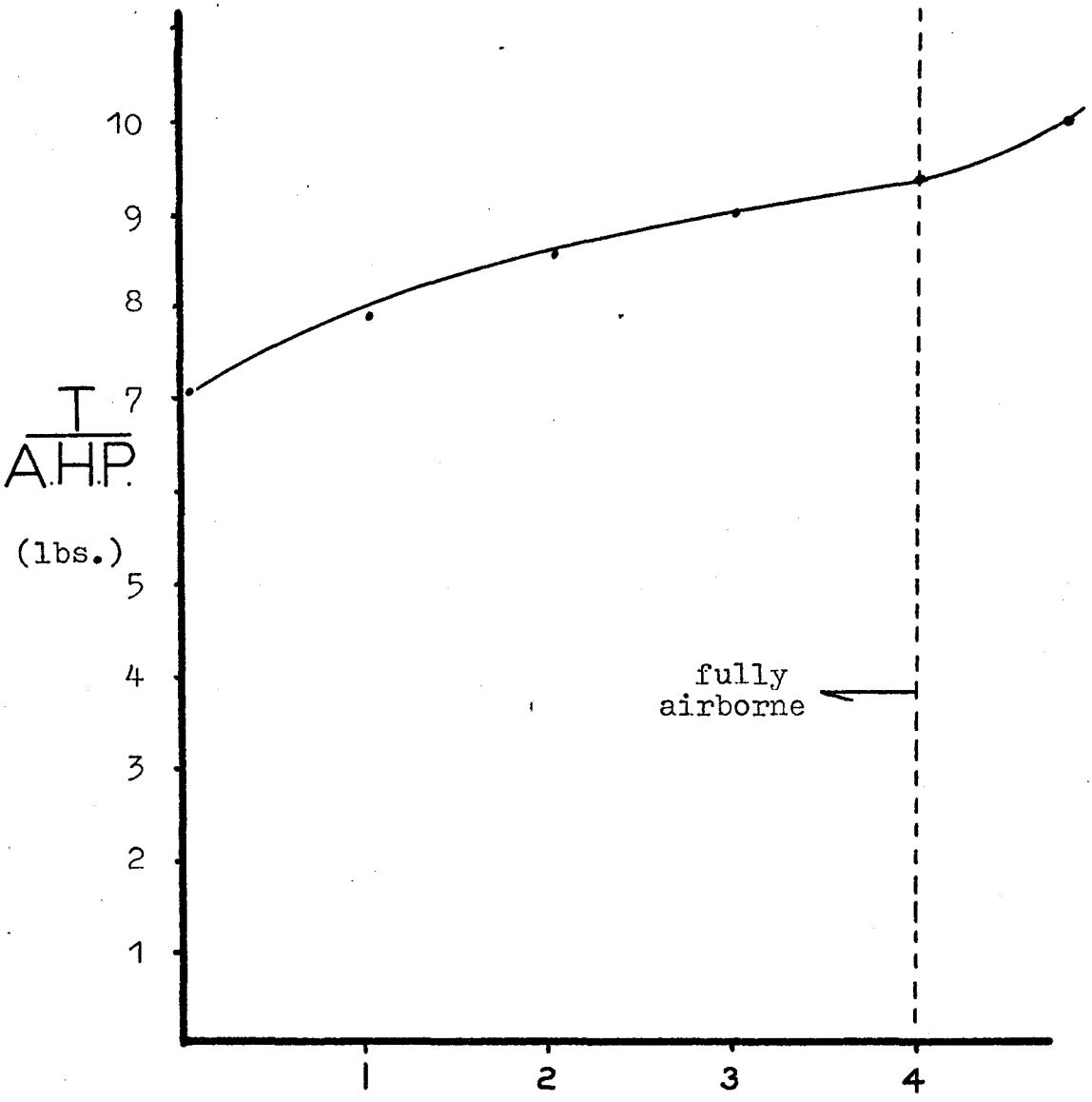

THRUST VERSUS STERN PLATE SETTING -- STATIC MODEL

FIG.(29)

the total for both ducts.

IV.3.3 Planform Static Pressure Patterns

Planform static pressure traverses were taken one-half inch above the surface, (smooth cement), and one-half inch below the upper duct wall of the model with a hand-held probe.

The weight of the model was a constant fifty-four pounds for these tests, and the air horsepower entering the model was 1.12 for all the tests as measured by the ten point pitot traverse described in Sec. IV.3.2.

Note that the static pressures were virtually constant over the plan area up to the centre of each outside hull and for about one-half of the stern plate projected area (Fig. 30 and 31). The static pressure distribution was only slightly affected by the stern plate settings. It is interesting to note the pressure pattern beyond the rear edge of the stern plate. Also, the indicated cushion pressures seem low as the weight divided by the cushion pad area is 3.74 lbs/sq.ft. However, lift is contributed by the pressure pattern extending under the hulls, under the bow plate and beyond the stern plates. Also, the dynamic head is partially utilized for lift as the flow strikes the rear stern plates.

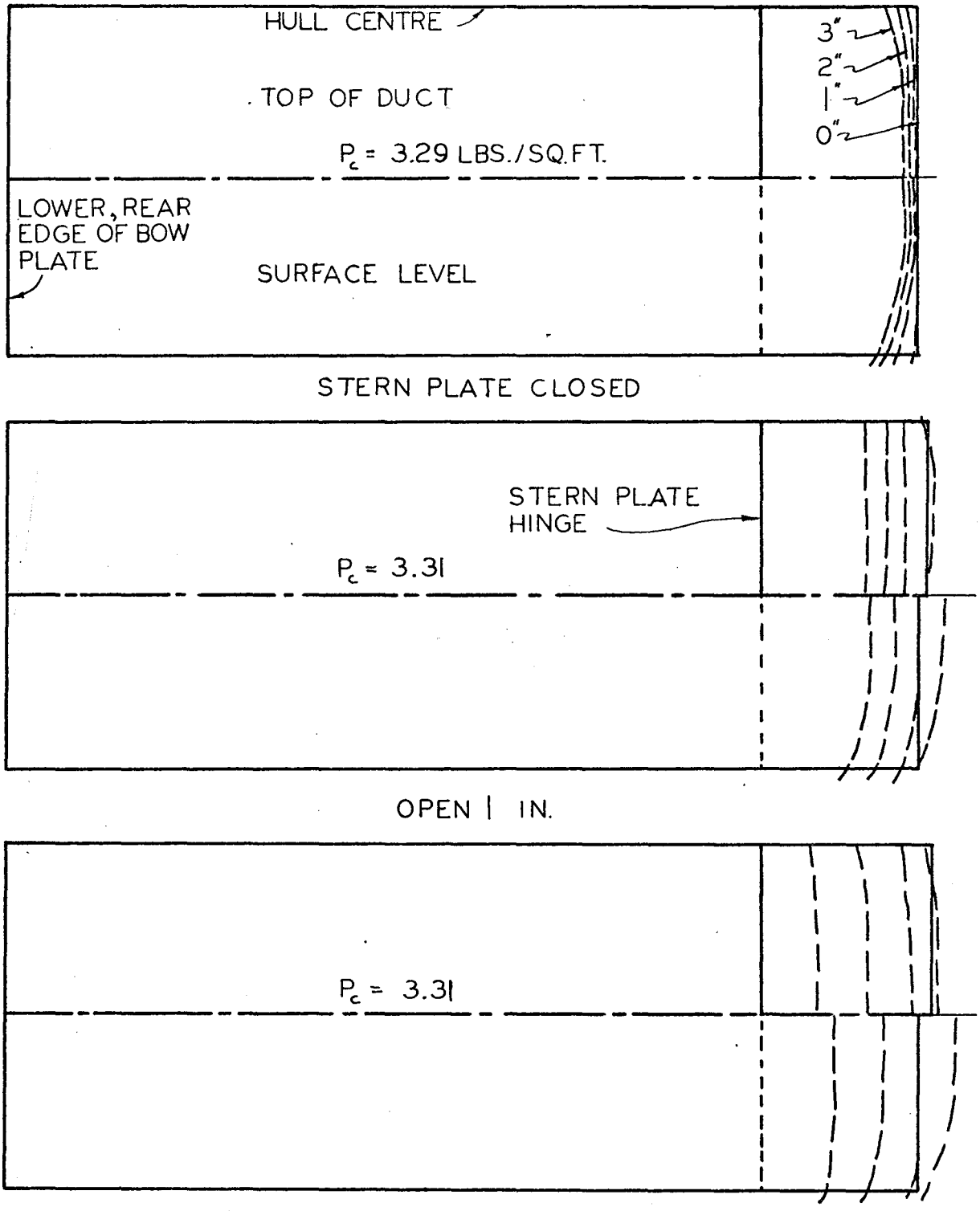

STATIC MODEL STATIC PRESSURE DISTRIBUTIONS

FIG. (30)

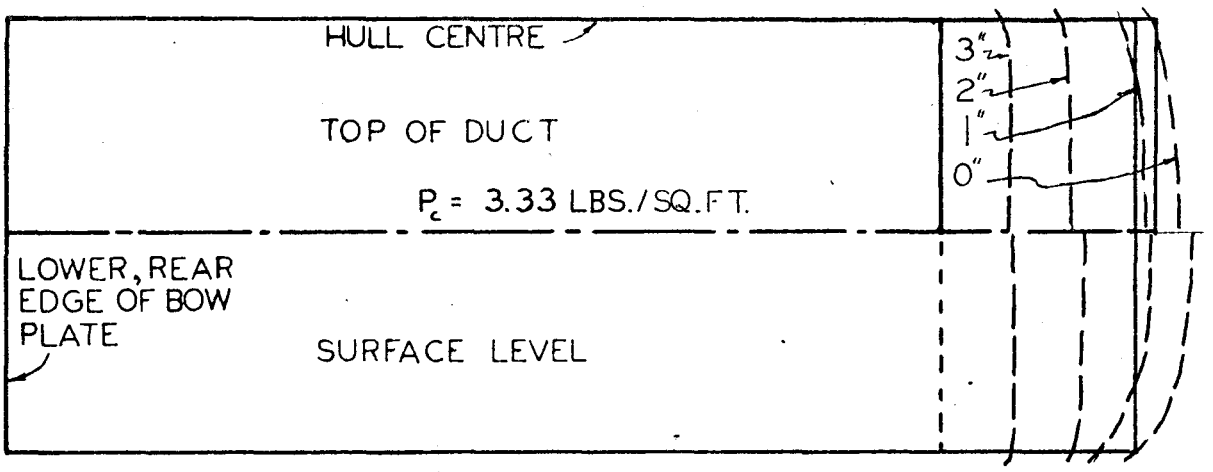

STERN PLATE OPEN 3 IN.

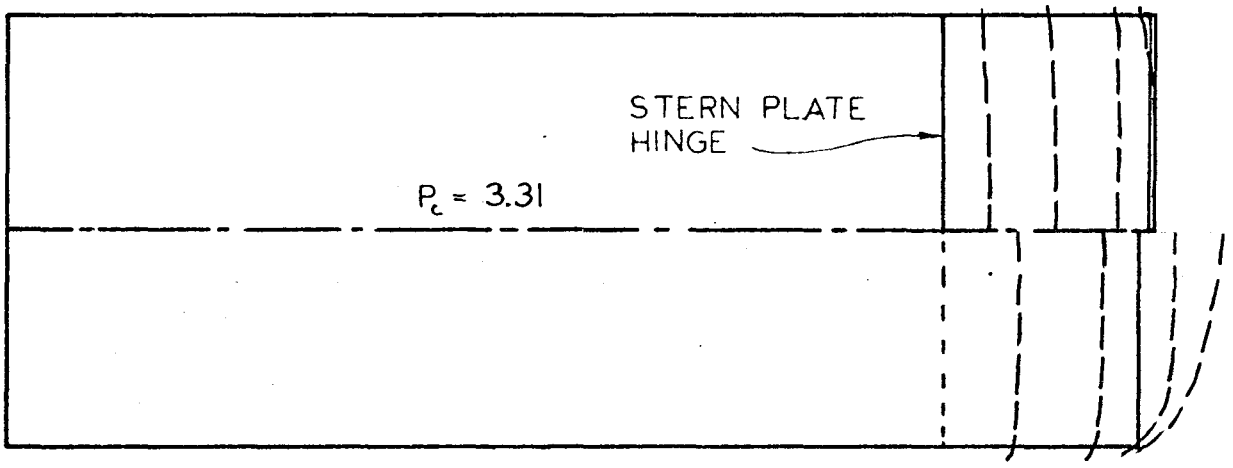

OPEN 4 IN.

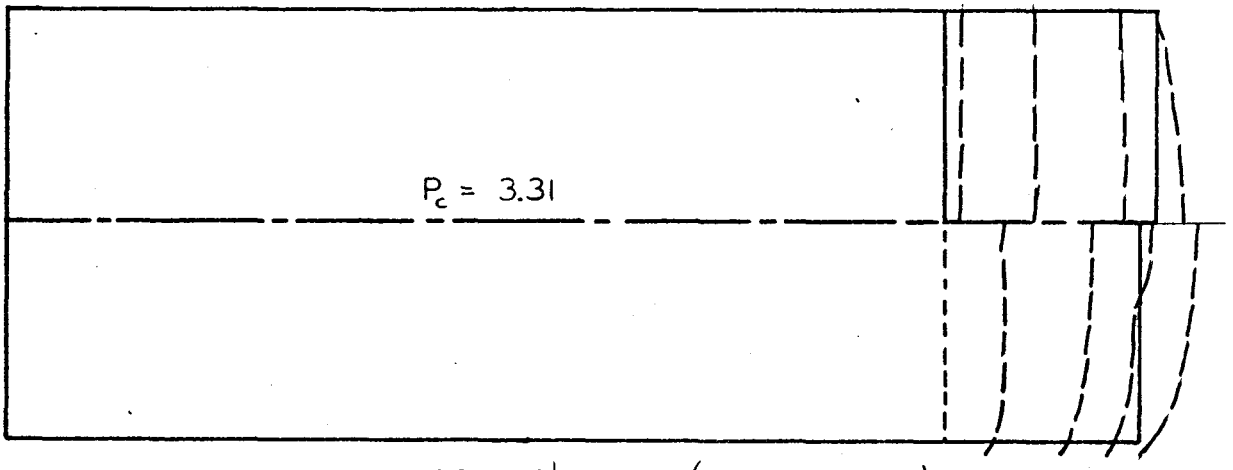

OPEN 4¼ IN. (JUST CLEAR)

STATIC MODEL STATIC PRESSURE DISTRIBUTIONS

FIG. (31)

IV.4 The Tethered Model

The model used for dynamic testing was an approximate one-inch-to-the-foot model of a cargo craft as envisaged by Hovair. The power was provided by a two-and-one-quarter horsepower, two-cycle gasoline engine located at the rear of the model. A five-sixteenth inch flexible shaft coupled the engine to a fan drive pulley at the front of the model. A one-inch "toothed" rubber belt made the final connection to the two ten-and-one-half inch diameter propellers. The fans were eleven-bladed radiator fans as used in the Austin America sedan.

The propellers proved to be quite suitable as tuff tests indicated no stalling or reverse flow even at rather high cushion pressures (6.35 psf). However, the flows just below the fans were somewhat erratic in direction which was probably the reason for the higher variability of the total head readings taken in that vicinity. The flow variability was surprising, (at lower static pressures as well), as the fans had eleven-blade flow pre-rotators immediately above them.

The axis of the fans were fixed at forty-five degrees to the horizontal, and three one-and-one-half inch turning vanes made the forty-five degree turn of the air column into the main ducts. The ratio of area of the duct at the fan to the main duct cross-sectional area was .940, so a slight divergence of flow occurred at the main duct

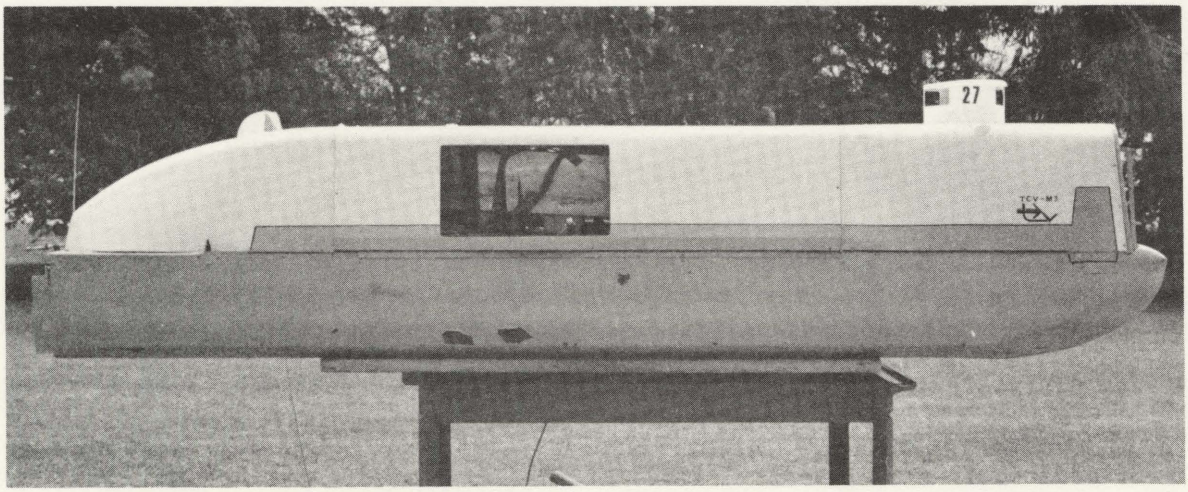

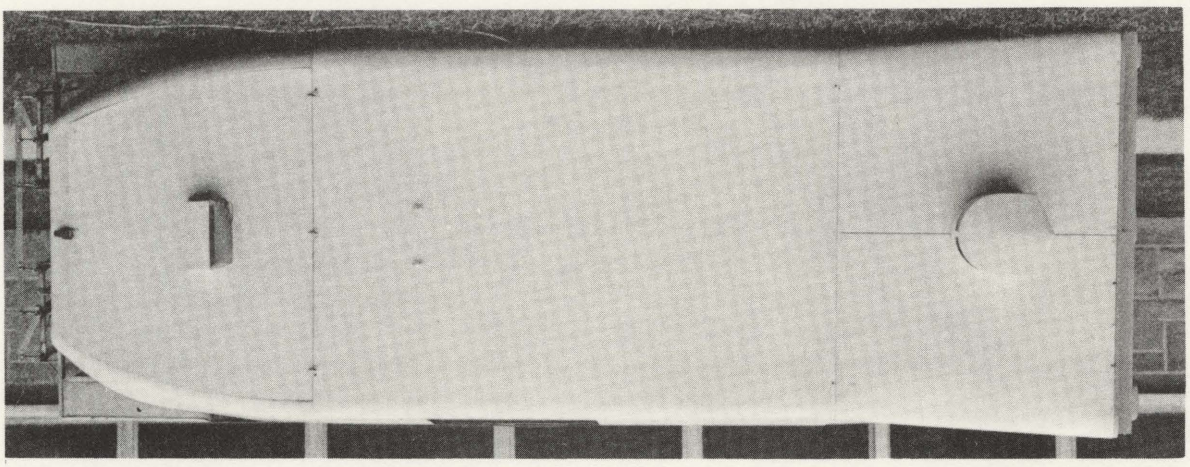

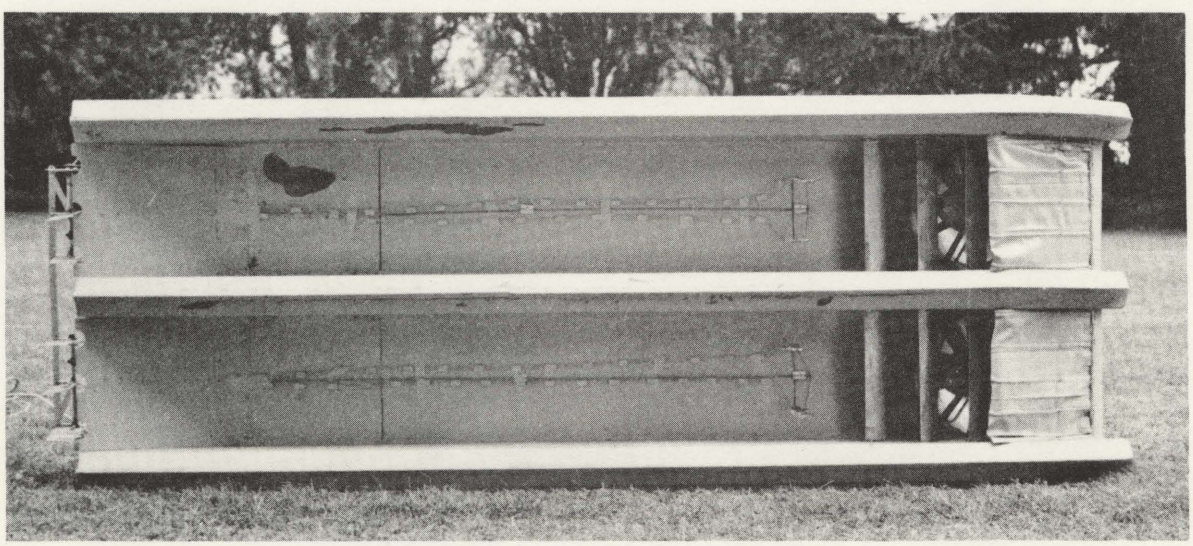

THE TETHERED MODEL

Figure 32

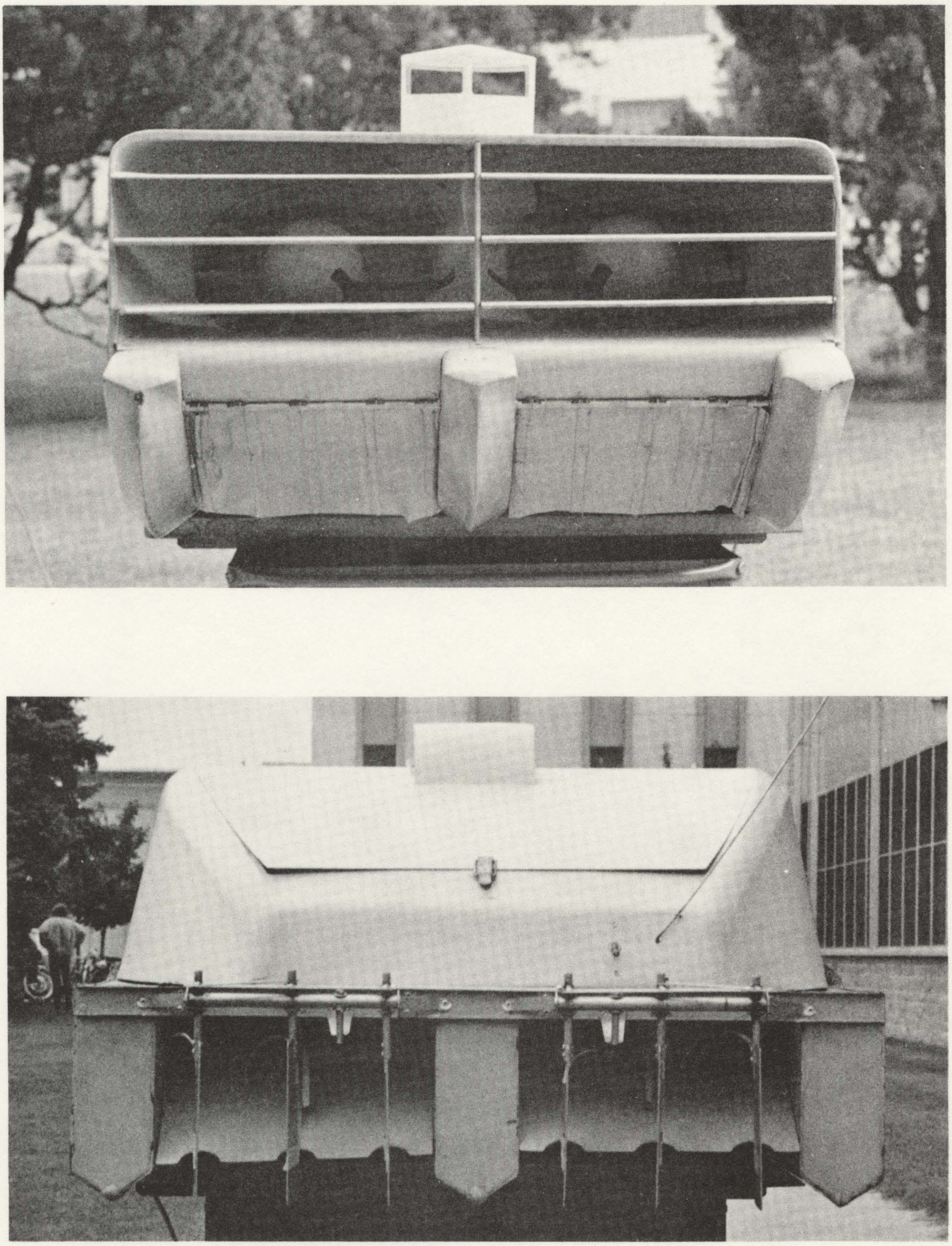

THE TETHERED MODEL

Figure 33

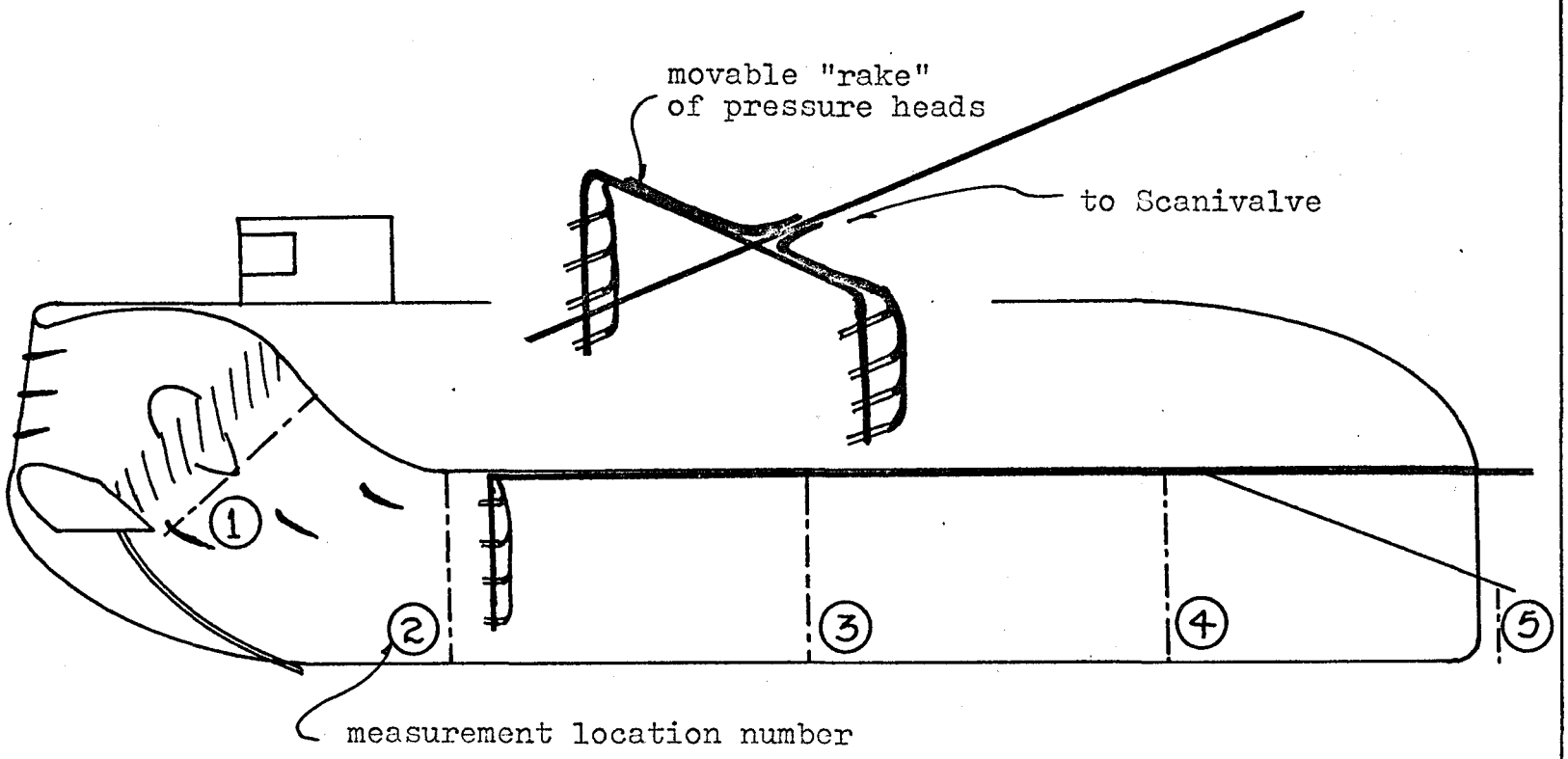

DUCT TRAVERSE LOCATIONS

FIG.(34)

entry. Tuft tests showed no rotation of the flow and the streamlines were parallel to the duct walls except near the bottom of the outside walls. The model weighed 69 pounds with the instrument package aboard.

The forty-eight pressure channels of the Scanivalve were utilized as follows. Each duct had twenty-three channels, twelve of which provided a six-point pitot traverse just below each fan. Eight channels provided a four-point pitot traverse in the main duct on a movable "rake" illustrated in Fig. 34. The remaining three channels provided one static and two dynamic head measurements in the jet sheet at the stern plate exit. The two channels not leading to the ducts were connected to a one-inch and a two-inch water head in the instrument package to calibrate each set of forty-six readings. The air flows in each duct were calculated as the sum of the flows in four equal area layers which ran the width of each duct.

IV.4.2 Static Tests on the Tethered Model

Static tests involved the determination of input air horsepower and static pressure distributions within the cushion area as well as static thrusts of the model.

The static pressure distributions were taken just over the surface and just under the floor of the upper duct wall of the model. These distributions are given in Fig. 38 and 39. As was the case with the static model, the pressure

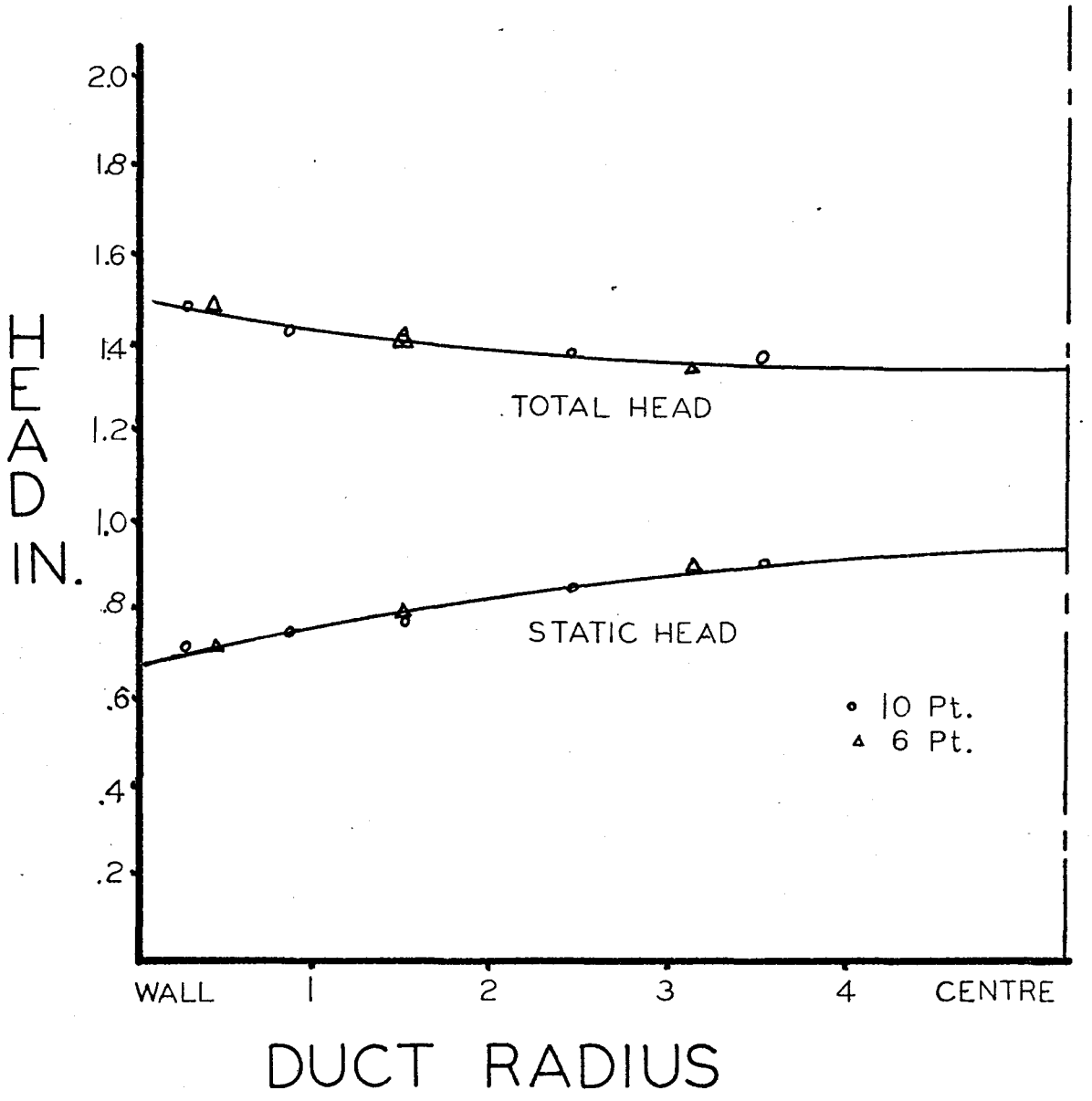

TETHERED MODEL INLET DUCT HEADS

FIG. (35)

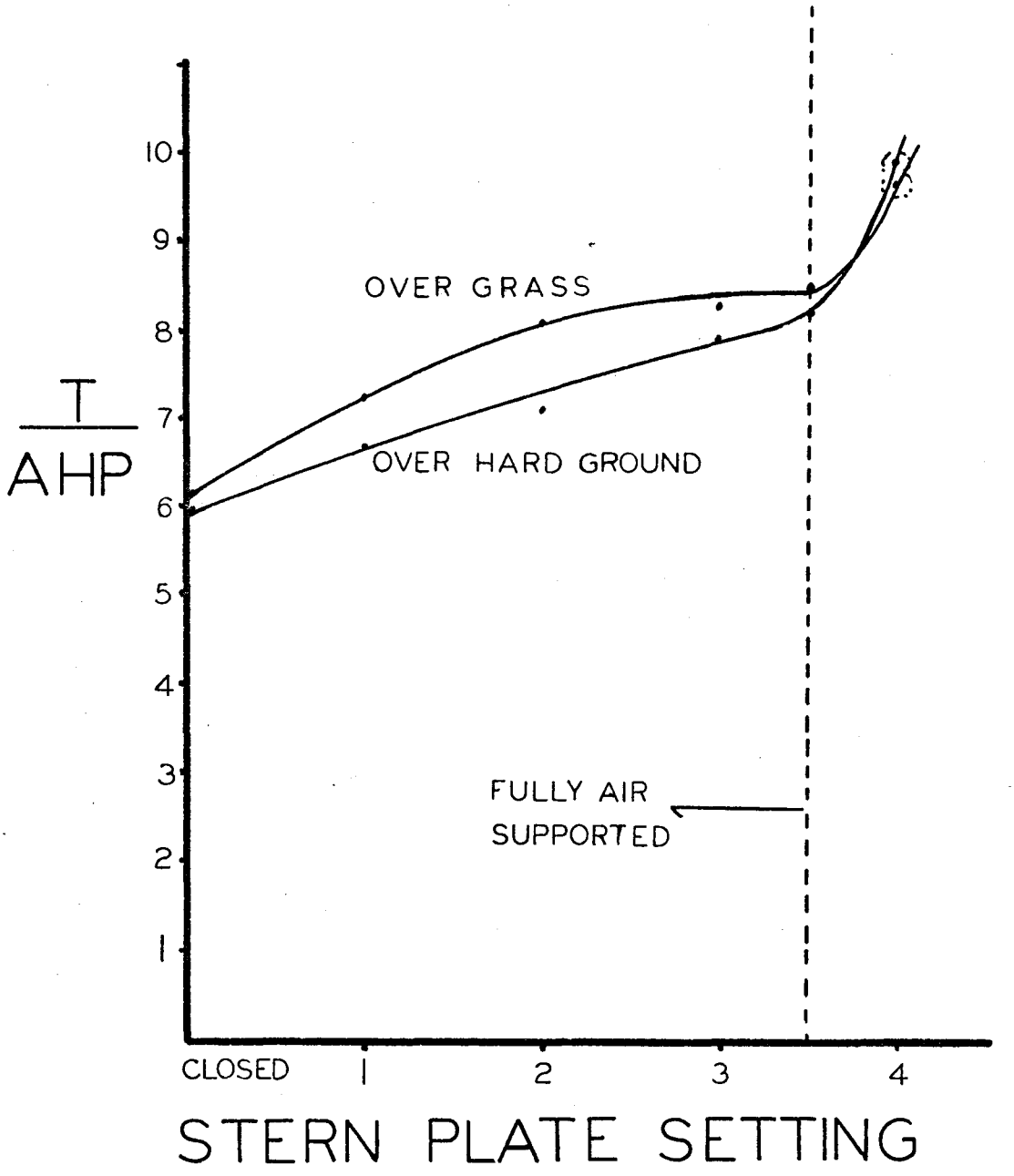

THRUST VERSUS STERN PLATE SETTING -- TETHERED MODEL

FIG. (36)

distributions extended beyond the geometric cushion pad area. The model weight was a constant 69 pounds and air horsepower input averaged 0.882 with little variation during these tests. As shown in Fig.38 and39, the static pressure over most of the cushion was constant at about 4.2 pounds per square foot. This measure seems low as the weight divided by the geometric cushion area gives an expected cushion pressure of 5.22 pounds per square foot. However, the discrepancy amounts to 13 pounds of lift form other sources. The static pressures extending from the stern plate, under the hulls, and under the bow plates would account for added lift. Also, the angle of the stern plate to the flow causes it to provide a lift component due to the dynamic head.

Fig.37 indicates the air horsepower remaining at each station for the stationary model. This graph simply gives some of the data calculations and cannot be used to reflect duct efficiency. The values fall off quickly as the flow at each station reduces. The remaining flow outside the duct is still contributing to thrust.

Overall thrust measures are given in Fig.36 as a function of stern plate setting over pavement and over grass. The values over grass tend to be somewhat higher, presumably because edge flow is reduced by the grass. The thrust values seem high for the system and perhaps some thrust augmentation results from the jet sheet exiting close to the

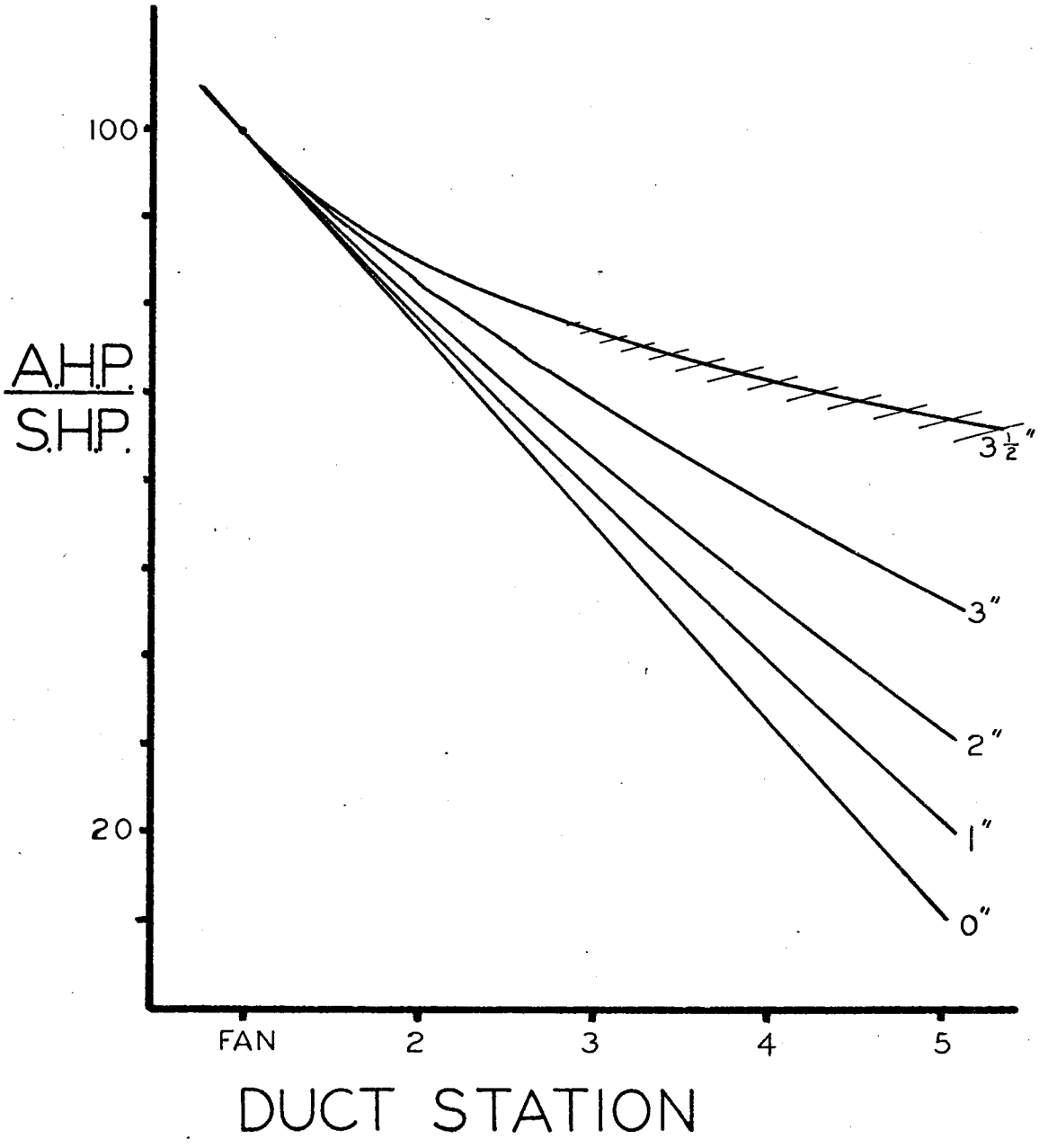

STATION DUCT AIR HORSEPOWER VERSUS STERN PLATE SETTING

FIG.(37)

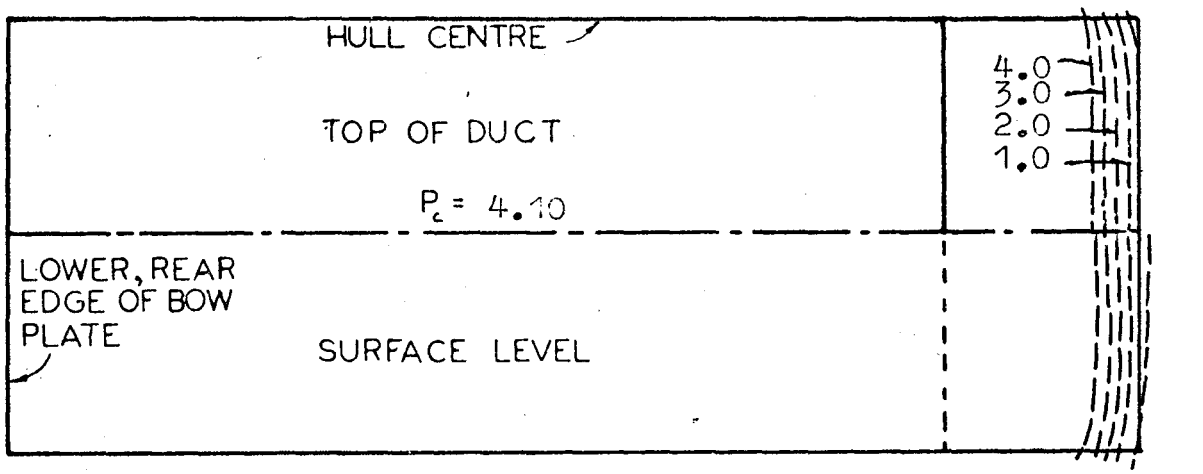

stern plate closed

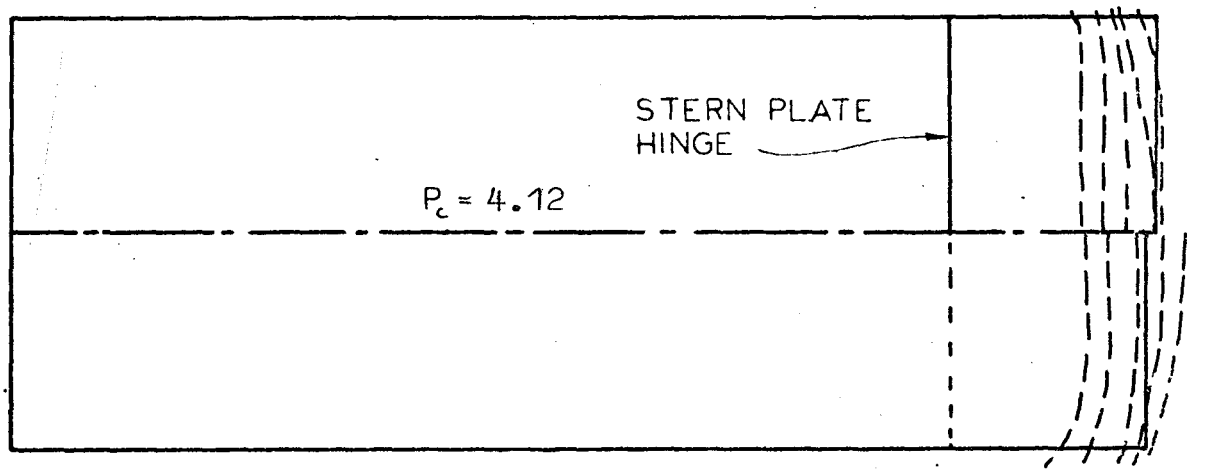

open 1"

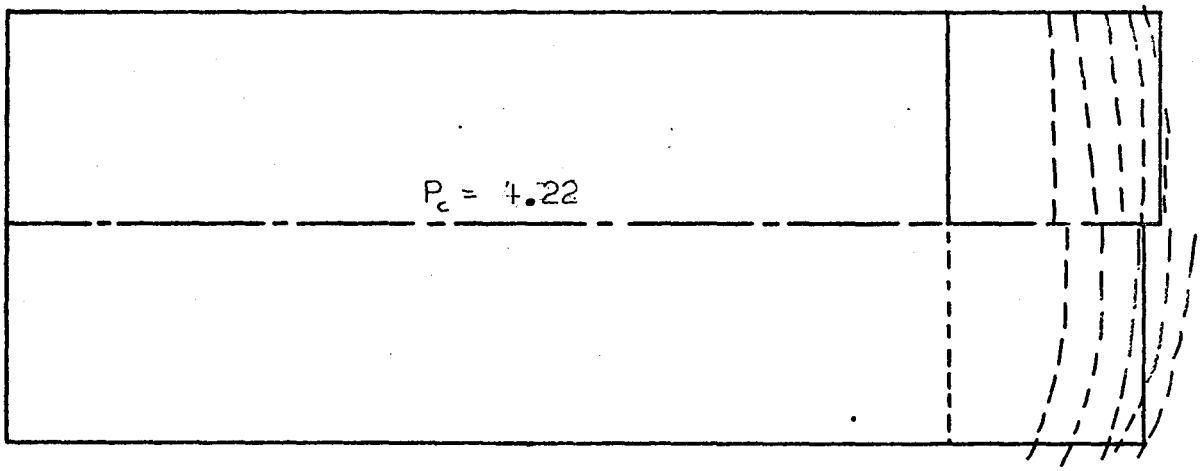

open 2"

TETHERED MODEL STATIC PRESSURE DISTRIBUTIONS

FIG.(38)

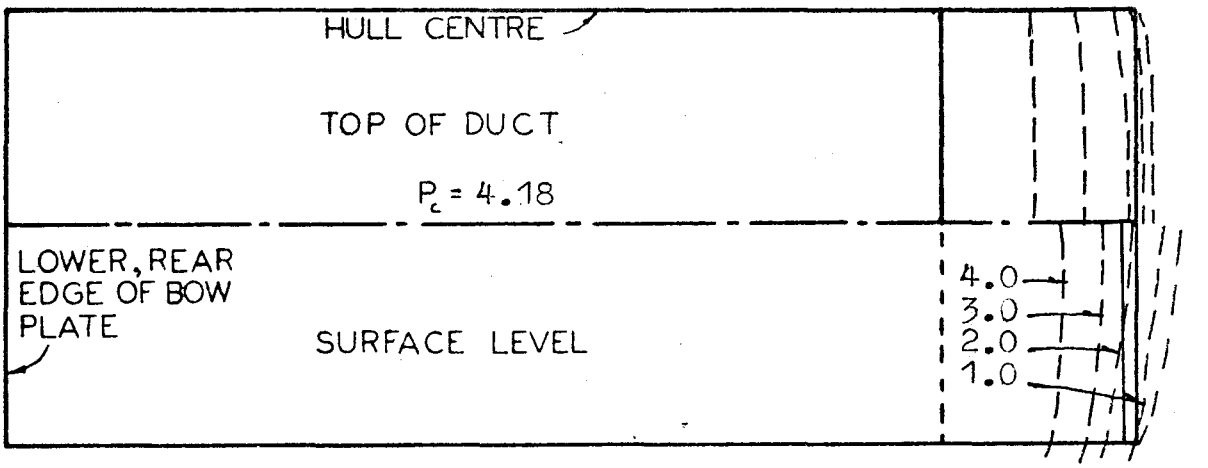

stern plate open 3"

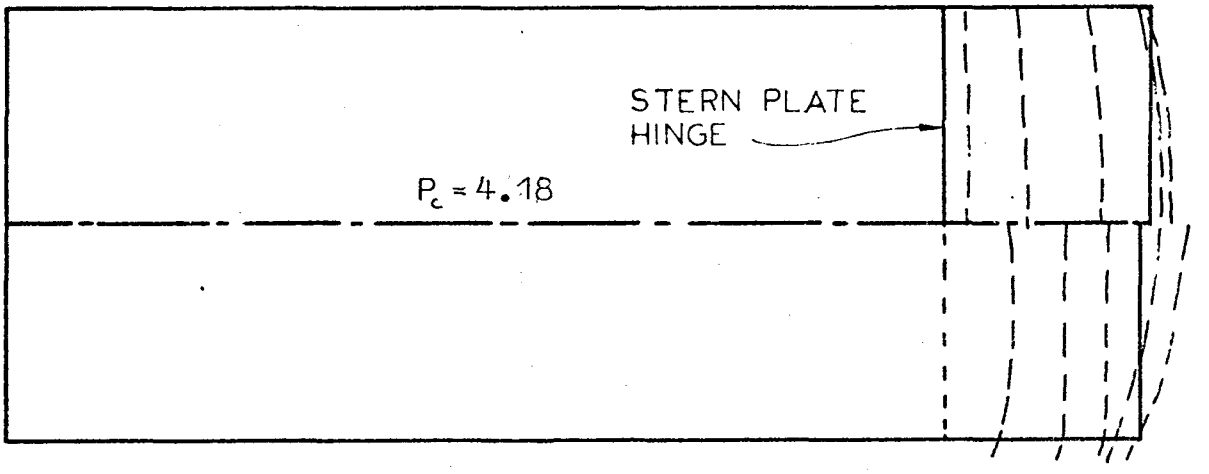

open 3½" (just clear)

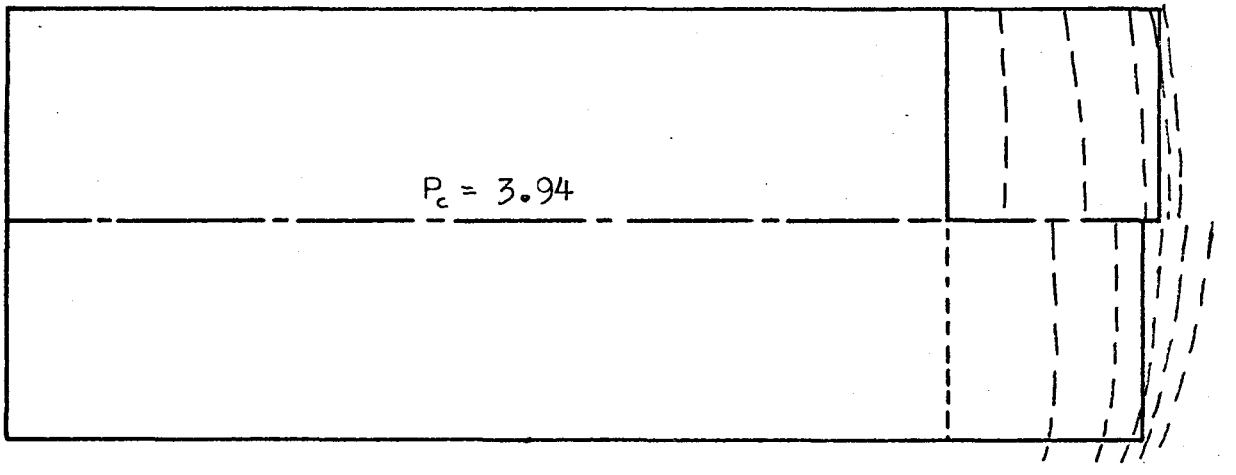

open 4" (not fully airborne)

FIG.(39)

surface.

IV.4.3 Dynamic Tests of the Tethered Model

While overall performance (that is, speed) could be calculated, individual components of drag could not. The best speed achieved was 28 feet/second; however, the speeds were adjusted to account for the air drag of the tethering cable as illustrated below.

In general $\quad drag = \frac{1}{2} C_d \rho V^2 S$

where $\quad C_d$ = drag coefficient = 1.2

and $\quad S$ = frontal area

Let d be the cable diameter and r be a variable distance from the centre outward along the tether.

Then $\quad ds = d \cdot dr$

and $\quad V = rw$

where $\quad w$ = angular velocity

Therefore cable drag $= \frac{1}{2} C_d \rho r^2 w^2 d \cdot dr$

$$= \frac{1}{2} C_d \rho w^2 d \cdot \int_0^R r^2 dr$$

$$= {}^3/_2 C_d \rho w^2 R^3 d \qquad (41)$$

where $\quad R$ = cable radius

For the model travelling at 25 feet/second on a 70 foot, ¼ inch cable, the cable drag would be 0.9 pounds. This force amounts to approximately 11% of the total model

thrust if the model is producing 8 pounds of thrust. In the absence of a drag versus speed curve for the thrust-cushion, an approximation of the square of the drag versus speed can be assumed. An increase in thrust of 11% would then create a 11 or 3.3% increase in speed. The model would then achieve (25 X 1.033 =) 26 feet/second without the cable. An average of model speeds achieved for each stern plate setting while operating over grass is given in Fig.40. It is interesting to note that over grass, the best stern plate setting occurs when the model is just airborne, that is, at minimum daylight clearance.

At speed, the input air flow of the model increased by an average 12% over the static air flow. Thrust at speed, when calculated using

$$T_{d_y} = \rho Q_s (V_s - V_v) \qquad (42)$$

dropped to an average 39% of the static thrust (Fig.40).

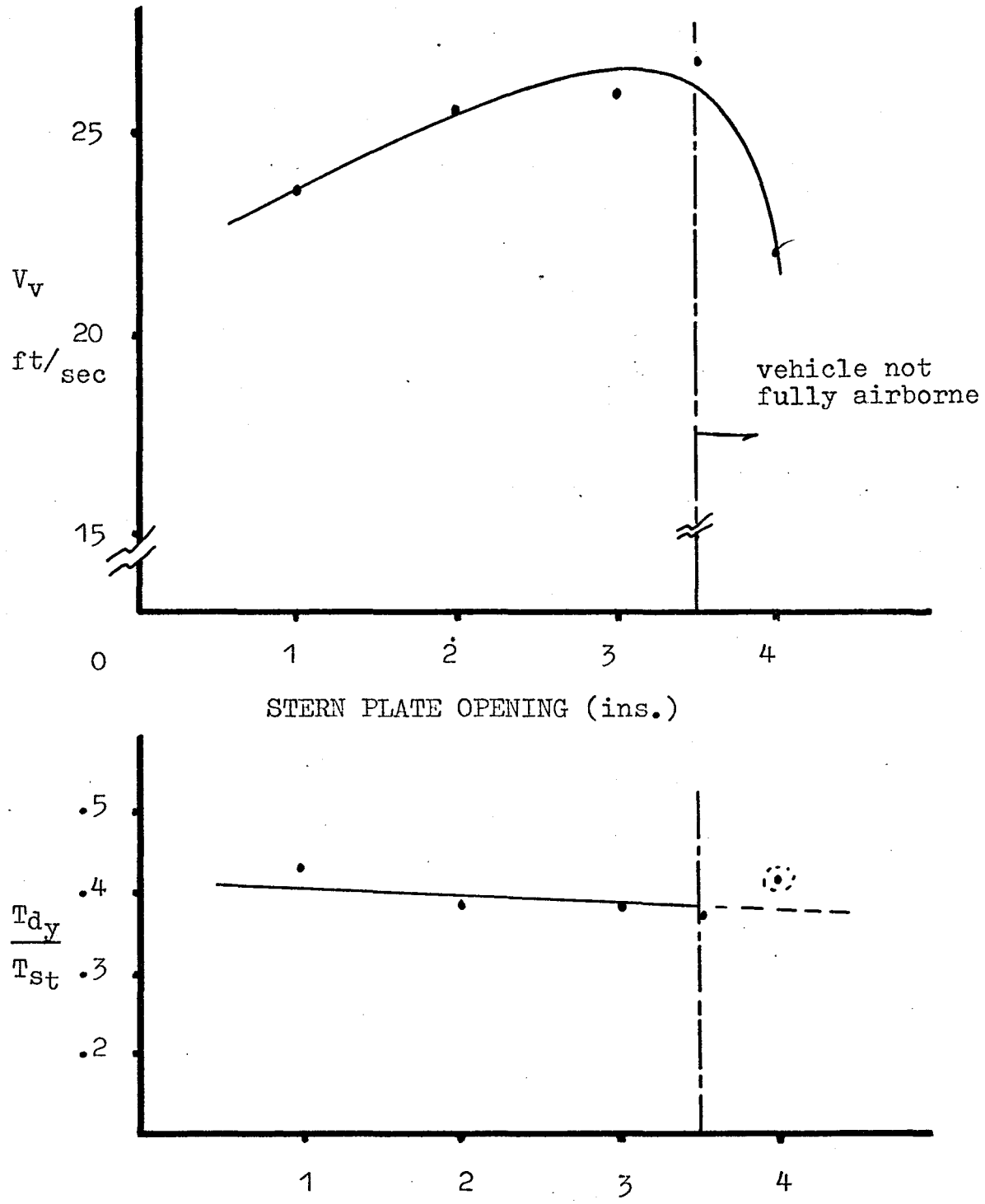
25
V_v
20
ft/sec
15
0
1
2
3
4
vehicle not
fully airborne
STERN PLATE OPENING (ins.)
.5
.4
$\frac{T_{d_y}}{T_{st}}$
.3
.2
1
2
3
4
TETHERED MODEL PERFORMANCE

FIG.(40)

CHAPTER V

COMPARISONS CONCLUSIONS AND RECOMMENDATIONS

V.1 Comparisons

The thrust-cushion's roll control, powerful yaw control, and ability to "key into" a water surface, are definite advantages that this vehicle has over other ACV because this provides for much more positive control. Comfort in a thrust-cushion vehicle is enhanced by the lack of noisy exposed fans, and the ability of the vehicle's cushion to suffer a sudden reduction in volume without, as is presently the case with hovercraft, imposing a vertical acceleration "bump" on the vehicle [12]. Safety is enhanced by the absence of fans operating in the plane of the passenger compartment. Also, the thrust centre-line is very close to the drag centre-line and both are relatively stable so that thrust or drag changes do not generate severely adverse moments on the vehicle.

The vehicle will be designed so that its lower surface will be as compatible as possible to the surface. On water, contact will be unavoidable and when it occurs, the effects should be minimized. Skirted vehicles, at least in the author's opinion, do not represent a satis-

factory solution for travel over water. The drag is relatively high, the vehicle stability and control is marginal, and cost factors are unreasonable.

Some support for the statement above comes from E. J. Andrews in his concluding remarks from a paper on the external aerodynamics of skirted edge-jets [13].

> "...these results confirm my opinion that the handling problems of amphibious hovercraft (skirted edge-jets), being as dependent as they are on aerodynamic and hydrodynamic effects, will not be solved by refinement in configuration design. The problems will be overcome by providing the vehicle with force and moment producing devices of sufficient magnitude, and under the command of the driver, that inherent characteristics are relatively reduced to impotence."

Mr. Andrews goes on the recommend the development of automatic systems to control the devices described above, to keep the control systems manageable by the pilot. Perhaps the presence of inherent control problems, and their correction by "devices of sufficient magnitude" under automatic control, represents an inefficient and undesirable basis for a form of transportation.

Questionable as yet, for the TCV, is the commercially exploitable extent of its amphibious capability. Snow travel is immediately possible, as the Hovair TCV III

proved, but sidewall design for ice and overland travel will no doubt require extensive field testing. The thrust-cushion patents include the use of skirt materials for sidewalls and perhaps for the relatively slower speeds over hard ground, skirts would be best. Slower speeds were suggested because the unpredictability of most terrains would slow any vehicle due to vehicle reaction times.

Performance comparisons of the TCV to other ACV can take the form of drag comparisons and vehicle efficiencies. Fig. 41 compares the drag co mponents of typical marine vehicles and ACV vehicles including the thrust-cushion. The thrust-cushion is well below the edge-jet for total drag and the ram wing is lowest, at least while airborne.

Recall that the thrust-cushion vehicle can operate as a trimaran best at low speed, as an immersed sidewall through the hump speed range, as a fully airborne ACV at higher speeds, and perhaps as a channel wing at very high speeds, to keep engine power usage to a minimum.

Fig. 42 illustrates the vehicle efficiencies of several types of transport. The diagonal line is the line which represents the technological limit as of 1950 (and has yet to be violated).

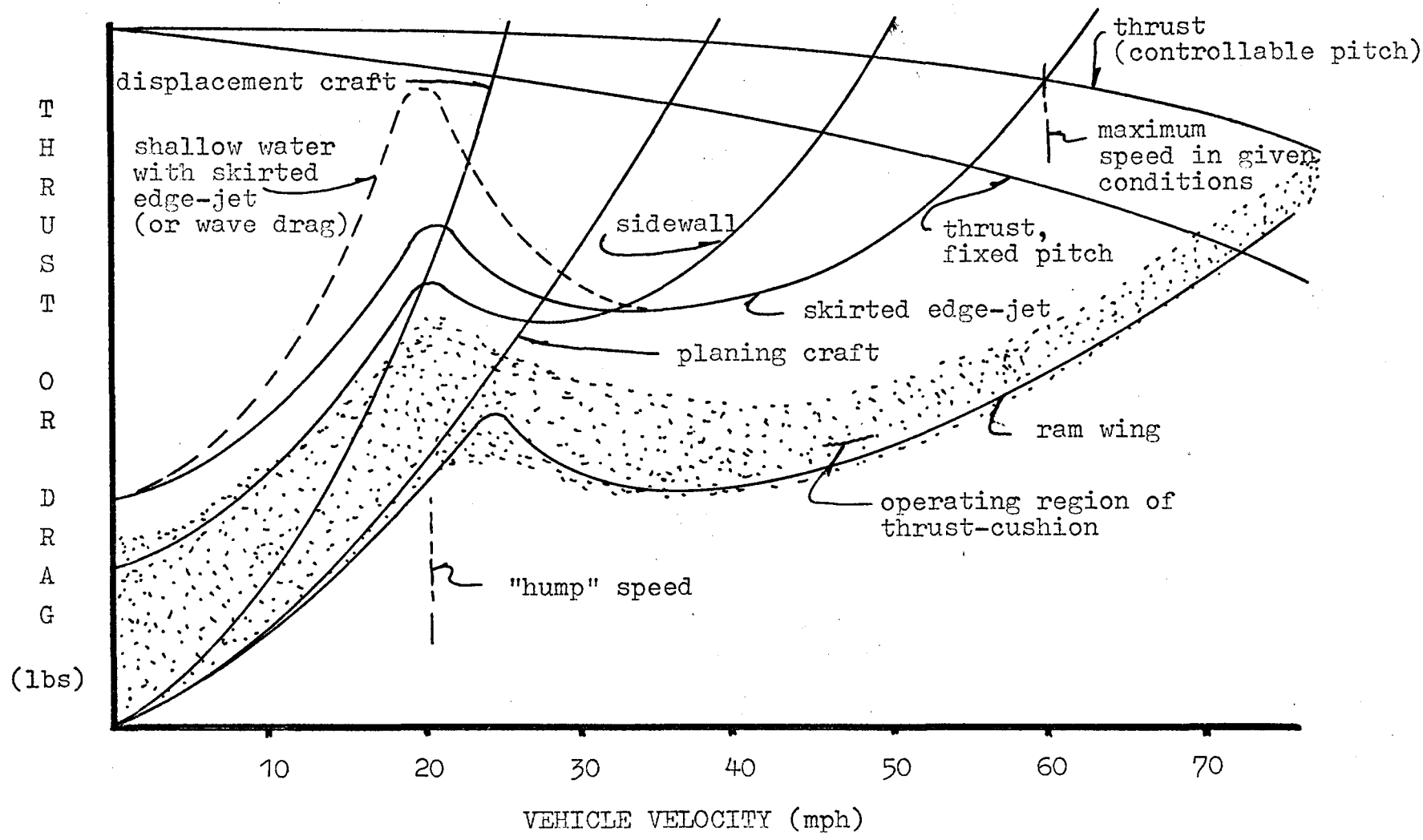

COMPARISON OF MARINE VEHICLE DRAGS

FIG.(4-1)

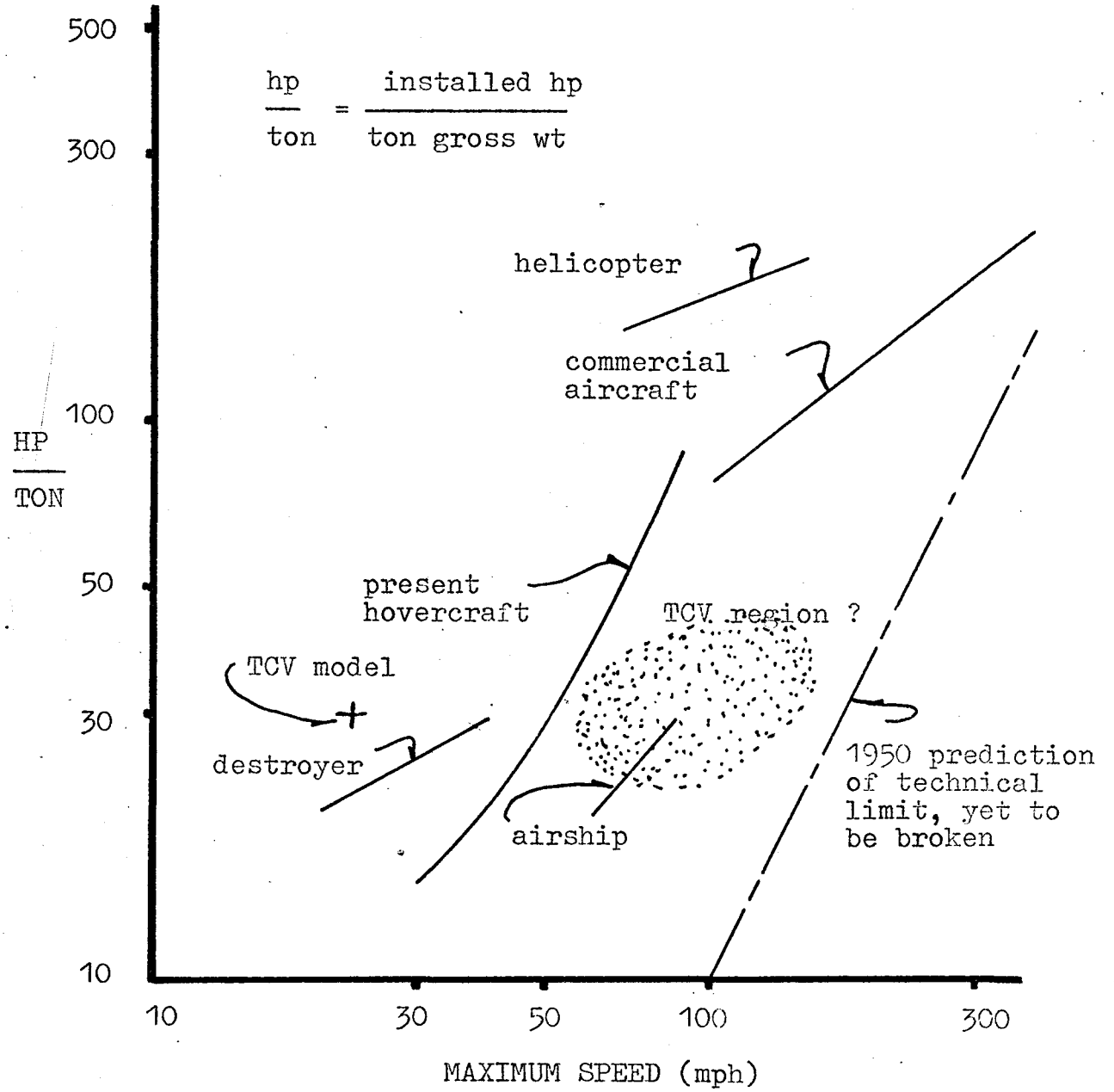

SPECIFIC POWER COMPARISONS

FIG.(42)

V.2 Conclusions

1. The seven foot model of the thrust-cushion configuration that was tested in this program, demonstrated 28 feet per second velocities using in the order of 30 horsepower per ton. This finding establishes the thrust-cushion as an efficient and potentially long-range form of ACV transport (Fig. 42). The relatively low drags (Fig. 41), with the absence of momentum drag, make the thrust-cushion a potentially high speed ACV, perhaps well-suited to tracked operations as well.

2. The ability of the thrust-cushion to adjust its exact ACV mode from a negligible, to a partial, to a fully air supported suspension makes it unique in the ACV industry. This ability allows the driver of the vehicle to determine, and to proceed at, the least power situation for a given speed. The best speeds always occurred with a very low daylight clearance in the fully air supported ACV mode.

3. Comparison of Fig. 16b with Fig's 29 and 36 show that thrust predictions based on momentum analysis fall short of the actual thrusts developed. The discrepancy can be interpreted as evidence of thrust augmentation factors. The first factor would involve thrusts generated by the intake area which can act as the ring of a ducted propeller. Careful inlet design can generate thrust

augmentation in the order of two times the momentum change through the fan. The second factor, which is strictly conjecture on the author's part, has to do with the thrust air being expelled in a thin jet sheet at the surface. A positive shear connection may be generated so that either a thrust augmentation occurs, or more simply, the shear force of the air flow on the ground can be added to the thrust. Further testing is required to investigate these conjectures.

4. The assumption was made, in the theoretical analysis section, that the cushion pressure was constant over the plan area. Actual pressures in the models substantiated this, but the values were about 17 percent low when compared to the calculated value given by model weight per cushion area. The cushion area was assumed to be the area from the rear edge of the bow plate to the rear edge of the stern plate, and between the outside hull centre lines. Perhaps the cushion area should include the entire beam. Further, the cushion pressure changed slightly with the stern plate setting. There is, perhaps, a lift component being generated by the dynamic head acting on the stern plate.

V.3 Recommendations

Because very little of the published work on ACV can apply directly to the thrust-cushion concept, extensive

research is warranted in all aspects of the TCV. Some suggested areas follow.

Equations for vehicle thrust were developed in this thesis, and some configuration refinements could be determined from a sensitivity analysis of these equations. However, more detailed equations encompassing all aspects of the flow, including any thrust augmentation factors, from intake to exit, with an appropriate set of constraint equations, should be developed and an optimization of the vehicle parameters undertaken. The above represents a substantial undertaking and will probably have to be investigated, theoretically and experimentally, in parts. The overall flow patterns and the stern plate analyses will require experimental data to test the assumptions and equations.

On the applied aerodynamics side is the intake plenum and fan design. Counter-rotating fans are specified by George Cocksedge of Hovair because they provide the required pressures at low tip speed, establish irrotational flow, and balance yawing forces generated from the asymmetrical thrusts of the inclined fans.

On water, the TCV sidewalls must provide vehicle buoyancy at low speeds, planing support at moderate speeds, and be able to pierce solid water at all speeds. Any water contact must be as smooth as possible. In the event of contact while the vehicle is moving sideways, a stable

skidding over the surface must result with an automatic gradual drift to a head-on situation. Careful hydrodynamic design, and experimentation is required.

The determination of vehicle loading factors for stress analysis is uncertain. Some knowledge is available from practice, but the extent to which it applies to the thrust-cushion is unknown. As soon as possible, TCV should be fitted with strain gauges, and the actual loading in various situations determined. The stress analysis is complicated by the shock absorbing sidewall design of the TCV.

Once several sizes of TCV have become available, a thorough model scaling study can be undertaken and some dependable dimensionless numbers arrived at.

V.4 Summary Statements for the Thrust-Cushion Concept

When the basic concept of the ACV became widely known about 1959, it was heralded as a transportation breakthrough, and world-wide utilization was expected in the near future. Unfortunately, while the ACV potential remains, a truly practical ACV has yet to be put into production. Each type of ACV has its own advantages and disadvantages and no one type has been able to establish wide acceptability. However, the skirted edge-jet has dominated the industry thus far, but the industry is declining. The thrust-cushion, in the author's opinion,

is the only ACV concept which is versatile enough to provide efficient service over a wide spectrum of speeds and surfaces to capture the ACV potential. At the same time it is simple in configuration, and has the potential to perform with quite acceptable operating costs.

This thesis has established the potential of the thrust-cushion, and the author strongly recommends further research including field studies of actual TCV vehicles.

APPENDIX I

A Torsion Analysis of the Thrust-Cushion Vehicle

For Torsion Loading

Assume that the vehicle and payload weights are evenly distributed over the lift area. Further, assume a static reaction of one-quarter craft weight at each corner of the lift area. For dynamic loading, assume one-half the craft weight at each corner.

The applied torsion couples are then:

(½ craft loaded weight)(length of lift area
= longitudinal torsion couple

(½ craft loaded weight)(width of lift area)
= transverse torsion couple

Neglect any torsion resistance of the hulls.

Torsion Shear Flow

The structure resisting torsion is as below:

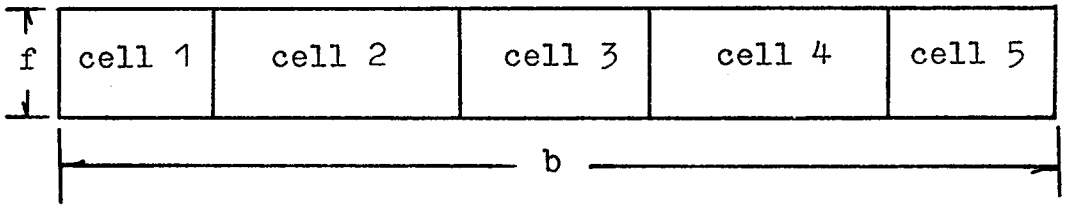

In General

$q_1 = \tau_1 t_1$ = shear load/inch on outside wall of cell.

$$\dot{T} = 2q_1A_1 + 2q_2A_2 + 2q_3A_3 + 2q_4A_4 + 2q_5A_5 \qquad (1)$$

for elastic continuity $\theta_1 = \theta_2 = \theta_3 = \theta_4 = \theta_5$

where $$\theta = \frac{q}{2AG}\oint\frac{ds}{t} \quad \text{or} \quad 2G\theta = \frac{q}{A}\oint\frac{ds}{t} \qquad (2)$$

let $$a_{10} = \oint\frac{ds}{t}$$ for outside wall of cell (1)

(clockwise stress flow positive)

$$\text{cell 1} \quad \frac{1}{A_1}\left[q_1a_{10} + (q_1 - q_2)a_{12}\right] = 2G\theta \qquad (3)$$

$$\text{cell 2} \quad \frac{1}{A_2}\left[(q_2 - q_1)a_{12} + q_2a_{20} + (q_2 - q_3)a_{23}\right] = 2G\theta \qquad (4)$$

$$\text{cell 3} \quad \frac{1}{A_3}\left[(q_3 - q_2)a_{23} + q_3a_{30} + (q_3 - q_4)a_{34}\right] = 2G\theta \qquad (5)$$

$$\text{cell 4} \quad \frac{1}{A_4}\left[(q_4 - q_3)a_{34} + q_4a_{40} + (q_4 - q_5)a_{45}\right] = 2G\theta \qquad (6)$$

$$\text{cell 5} \quad \frac{1}{A_5}\left[(q_5 - q_4)a_{45} + q_5a_{50}\right] = 2G\theta \qquad (7)$$

Solve the above for $q_1, \ldots\ldots q_5$ and θ

where $$G = \frac{E}{2(1 + \mu)}$$

and μ = 0.33 for aluminum

and G = 3,790,000 p.s.i. for aluminum.

and $$a_{tn} = \frac{\text{line length}}{\text{line thickness}}$$

The Thrust-Cushion Case

A program, not included, was set up to compute some trial configurations. Due to symmetrical structure, use three cells where top and bottom sheets are identical

and $q_1 = q_5$ and $q_2 = q_4$

Assume a safety factor on torque of 2.

$$\text{Torsion} = 2q_1fb + 2q_2f(\tfrac{b}{2} - 1.5b) + q_3fb \qquad (1)$$

$$2Gq_2 = ((q_1l_1 + l_2(q_1 - q_2))/(f \cdot b) \qquad (2)$$

$$2Gq_2 = ((q_2 - q_1)l_2 + q_2l_3 + (q_2 - q_3)l_2)/(f(\tfrac{b}{2} - 1.5b)) \qquad (3)$$

$$2Gq_4 = (2q_3l_2 - 2q_2l_2 + q_3l_4)/(fb) \qquad (4)$$

where f = floor thickness

b = floor width

$l_1 = 2bt_1 + f/t_2$

$l_2 = f/t_2$

$l_3 = 2(\frac{b}{2} - 1.5b)/t_1$

$l_4 = 2b/t_1$

where t_1 = floor material thickness

t_2 = web material thickness.

APPENDIX II

Dimensional Analysis Results

Variable nomenclature is that which was used in the text, and the dimensionaless groups are based on the thrust equations of Chapter III.

1. $$\frac{d}{\sqrt{AHP}}\sqrt[4]{\frac{P_c^3}{\rho}}$$

2. $$\frac{P_c V d^2}{AHP}$$

3. $$V\sqrt{\frac{\rho}{P_c}}$$

4. $$Vb\sqrt{\frac{V\rho}{AHP}}$$

5. $$\left(d\sqrt{\frac{P_c V}{AHP}}\right)^{\ell}\left(\frac{AHP}{V_v}\right)$$ where ℓ is unknown.

6. $$\frac{AHP}{V}\left(\frac{1}{1}\sqrt{\frac{T}{P_c}}\right)^{f}$$ where f is unknown.

APPENDIX III

Small Boat Hull Loading

Consideration of vertical and horizontal velocities of a boat hull, and the orbital velocities of water particles in a wave, produces the following equation [15]:

$$P_I = \frac{AV^2 + BV\sqrt{L} + CL}{D}$$

where P_I = maximum local impact pressures (psi)

V = speed (miles/hour)

L = waterline length at rest (feet)

$$D = \frac{2 \times 144}{\rho} = 144.55$$

A, B, and C are experimentally determined constants

where $A = 2.151$

$B = 1.267$

$C = 16.884$

The nomograph on the next page presents this formula. The determination of the area over which this pressure acts to allow calculation of the loading forces is entirely subjective.

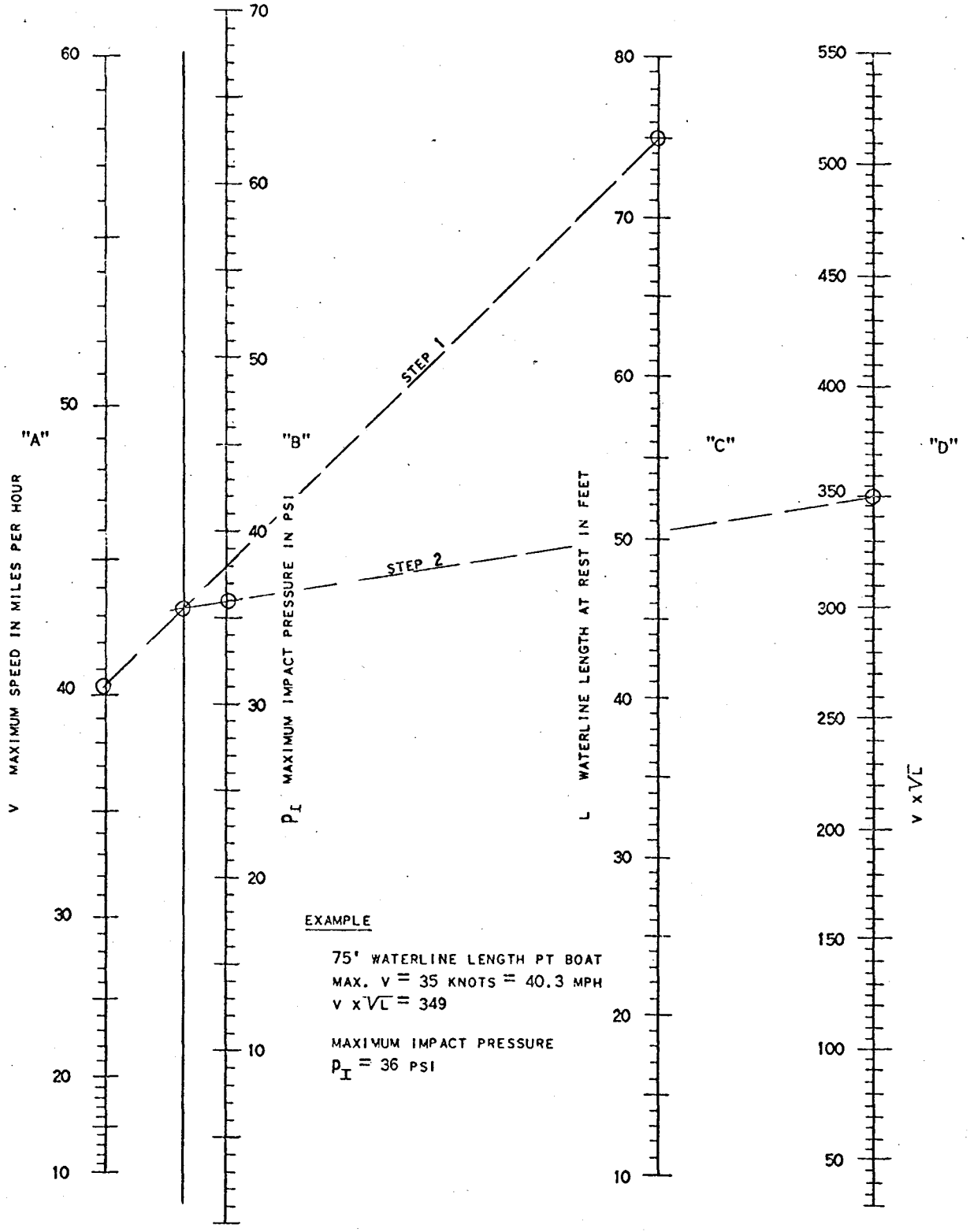

Fig. 2-14. Maximum bottom pressure for high speed planing boats

REFERENCES

1. Hayward, L., "The Development of the Hovercraft and its Possible Uses in Somerset",Hovering Craft and Hydrofoils, Kalerghi Publications, May 1967.
2. Elsley and Devereux, Hovercraft Design and Construction, David and Charles Newton Abbot, 1968.
3. Crago, W.A., "Problems Associated with the Use of Skirts on Hovercraft", Hovering Craft and Hydrofoils, Kalerghi Publications, 1968.
4. Coloquhoun, L.R., "Cross Channel Hovercraft Operations", A Paper Presented at Fourth Canadian Symposium on Air Cushion Technology.
5. Kordenbrock, J. V. and Horland, D. A., "Design Principles for Air Cushion Devices", Engineering Digest, Vol. 15, No. 6, June 30, 1969.
6. **Earl, T. D., "AGARDograph Ground Effect Machines" National Research Council, 94898, Jan. 1962**
7. "Bigger and Faster", Air Cushion Vehicles, Flight International Supplement, Nov. 17, 1966.
8. Chaplin, H. R., and Ford, A. G., "Some Design Principles of Ground Effect Machines", Department of the Navy. Report 2121A, April, 1966.

9. Keiller, I. L., "Hovercraft Research at Royal Aircraft Establishment, Bedford", Hovering Craft and Hydrofoils, Kalerghi Publications, Sept. 1967.

10. Bertin, J., "A Transport Philosophy for Developing Countries, "The Terraplane", Hovering Craft and Hydrofoils, Nov., 1967.

11. Barthalon, M. E., and Watson, P., "A Suspended Air Cushion Monorail", International Hovercraft Conference, Session 1, Paper 3, Southampton, 1968.

12. Cockerell, C., "The Place of Hovercraft -- Present and Future", Hovering Craft and Hydrofoild, Kalerghi Publications, Nov., 1967.

13. Andrews, E. J., "The External Aerodynamics of Hovercraft", A Lecture Given to the Rotocraft Section of the Society, Cranfield Institute of Technology, April 23, 1969.

14. Waters, David, "Light Hovercraft Design Handbook", Department of Transport Tchnology, Loughborough University of Technology, April, 1969.

15. Smith, R. M., "Applied Naval Architecture", American Elsevier Publishing Co., New York, 1967.

16. Gibbes and Cox, Marine Design Manual, McGraw-Hill Book Co., Toronto.